REPORT UAG-72

WORLD DATA CENTER A
for
Solar-Terrestrial Physics

ENERGY RELEASE IN SOLAR FLARES

Proceedings of the Workshop on Energy Release in Flares 26 February - 1 March 1979 Cambridge, Massachusetts U.S.A.

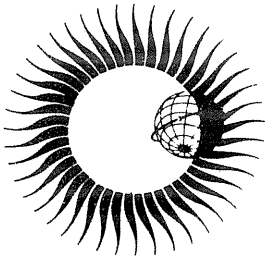

July 1979

WORLD DATA CENTER A
National Academy of Sciences
2101 Constitution Avenue, N.W.
Washington, D.C., U.S.A., 20418

World Data Center A consists of the Coordination Office

and seven Subcenters:

World Data Center A
Coordination Office
National Academy of Sciences
2101 Constitution Avenue, N.W.
Washington, D.C., U.S.A., 20418
[Telephone: (202) 389-6478]

Glaciology [Snow and Ice]:

World Data Center A: Glaciology
[Snow and Ice]
Inst. of Arctic & Alpine Research
University of Colorado
Boulder, Colorado, U.S.A. 80309
[Telephone: (303) 492-5171]

Meteorology (and Nuclear Radiation):

World Data Center A: Meteorology
National Climatic Center
Federal Building
Asheville, North Carolina, U.S.A. 28801
[Telephone: (704) 258-2850]

Oceanography:

World Data Center A: Oceanography
National Oceanic and Atmospheric
Administration
Washington, D.C., U.S.A. 20235
[Telephone: (202) 634-7249]

Rockets and Satellites:

World Data Center A: Rockets and
Satellites
Goddard Space Flight Center
Code 601
Greenbelt, Maryland, U.S.A. 20771
[Telephone: (301) 982-6695]

Rotation of the Earth:

World Data Center A: Rotation
of the Earth
U.S. Naval Observatory
Washington, D.C., U.S.A. 20390
[Telephone: (202) 254-4023]

Solar-Terrestrial Physics (Solar and Interplanetary Phenomena, Ionospheric Phenomena, Flare-Associated Events, Geomagnetic Variations, Magnetospheric and Interplanetary Magnetic Phenomena, Aurora, Cosmic Rays, Airglow):

World Data Center A
for Solar-Terrestrial Physics
Environmental Data and Information
Service, NOAA
Boulder, Colorado, U.S.A. 80303
[Telephone: (303) 499-1000, Ext. 6467]

Solid-Earth Geophysics (Seismology, Tsunamis, Gravimetry, Earth Tides, Recent Movements of the Earth's Crust, Magnetic Measurements, Paleomagnetism and Archeomagnetism, Volcanology, Geothermics):

World Data Center A
for Solid-Earth Geophysics
Environmental Data and Information
Service, NOAA
Boulder, Colorado, U.S.A. 80303
[Telephone: (303) 499-1000, Ext. 6521]

NOTES:

1. World Data Centers conduct international exchange of geophysical observations in accordance with the principles set forth by the International Council of Scientific Unions. WDC-A is established in the United States under the auspices of the National Academy of Sciences.
2. Communications regarding data interchange matters in general and World Data Center A as a whole should be addressed to: World Data Center A, Coordination Office (see address above).
3. Inquiries and communications concerning data in specific disciplines should be addressed to the appropriate subcenter listed above.

WORLD DATA CENTER A
for
Solar-Terrestrial Physics

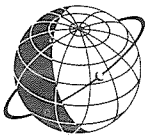

REPORT UAG-72

ENERGY RELEASE IN SOLAR FLARES

Proceedings of the Workshop on Energy Release in Flares 26 February - 1 March 1979 Cambridge, Massachusetts U.S.A.

Edited by

David M. Rust
American Science and Engineering, Inc.
Cambridge, Massachusetts U.S.A.

and

A. Gordon Emslie
Harvard-Smithsonian Center for Astrophysics
Cambridge, Massachusetts U.S.A.

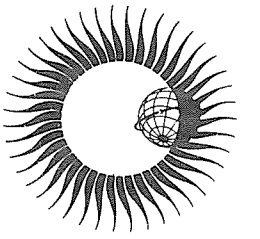

July 1979

Published by World Data Center A for
Solar-Terrestrial Physics, NOAA, Boulder, Colorado
and printed by

U.S. DEPARTMENT OF COMMERCE
NATIONAL OCEANIC AND ATMOSPHERIC ADMINISTRATION
ENVIRONMENTAL DATA AND INFORMATION SERVICE
Boulder, Colorado, USA 80303

SUBSCRIPTION PRICE: $25.20 a year; $17.30 additional for foreign mailing; single copy price varies.*
Checks and money orders should be made payable to the Department of Commerce, NOAA/NGSDC.
Remittance and correspondence regarding subscriptions should be sent to the National Geophysical and Solar–Terrestrial Data Center, NOAA, Boulder, CO 80303.

*PRICE THIS ISSUE $1.50

PREFACE

On February 26, 1979, a workshop was convened in Cambridge, Massachusetts, USA, to devise the scientific program and objectives for the Study of Energy Release in Flares (SERF), a program of the Solar Maximum Year (SMY). The workshop was sponsored by the National Science Foundation, and organized by American Science and Engineering, Inc. Most of the workshop was devoted to parallel meetings of three small teams, where theories of thermalization, particle acceleration, and mass motion in flares were discussed. The teams were led by D. Spicer, R. Lin, and E. Tandberg-Hanssen, respectively. Each team outlined a specific scientific program to test current theories. Because of the nature of the flare problem, most tests require simultaneous observations by ground-based and space observatories, and it is the participants' hope that the present volume will help provide the rationale for world-wide collaboration during the SMY.

Thirty-two scientists, including eighteen from the US, four from the USSR, three from France, two from the UK, two from the Netherlands, two from Japan, and one from West Germany, braved the cruel New England winter to attend the workshop. The names of the participants, the home institutions and the workshop team each served on appear on the the next page. The enthusiam and plain hard work of the participants is evident from the cogent scientific program they created.

An overview of the major scientific issues identified for the Study of Energy Release in Flares is given in Chapter 1. More specific discussions of the three program areas appear in Chapters 2, 3, and 4. Chapter 5 explains the concepts of Joint Observing Sequences and Collaborative Observing Sequences (COSs) developed by NASA's Solar Maximum Mission investigators. Lists of the specific observations needed for each COS of the SERF appear in Chapter 5, also.

At the workshop, A. G. Emslie, J. Heyvaerts, R. MacQueen, S. Mandel'stam, D. Rust, P. Simon, V. Stepanov and E. Tandberg-Hanssen gave keynote talks. Those for which texts are available are reprinted in the appendices. The remainder of the volume was compiled by the editors from discussion notes and from written material provided by the participants. We are grateful to all the participants for their guidance and comments on early versions of these proceedings. Material on the Joint Observing Sequences and characteristics of the experiments on the Solar Maximum Mission (due for launch on 19 October 1979) were provided by G. Withbroe and W. Wagner. F. Orrall provided information on the COSs developed at the SMM Investigators' Working Group meetings.

Mrs. Elaine O'Neill and Mrs. Maureen Gaffney, of American Science and Engineering, Inc., helped greatly to make the workshop a success, from the initial mailings through the daily arrangements to the production of these proceedings. The staff of the Massachusetts Institute of Technology Faculty Club provided warm hospitality and help throughout the meeting.

This work was sponsored by NSF under grant No. ATM78-23322. Publication costs were assumed by the World Data Center A for Solar-Terrestrial Physics in Boulder, Colorado, USA. The WDC-A is sponsored by the National Oceanic and Atmospheric Administration. Any opinions, findings, and conclusions or recommendations expressed in this publication are those of the authors and do not necessarily reflect the views of the National Science Foundation or the National Oceanic and Atmospheric Administration.

David M. Rust
A. Gordon Emslie
Cambridge, Mass.
May 1979

SERF WORKSHOP PARTICIPANTS

(Note: The letters T, A, and M refer to the teams on Thermalization, Particle Acceleration and Mass Motions, respectively; the number refers to the position in the group photograph).

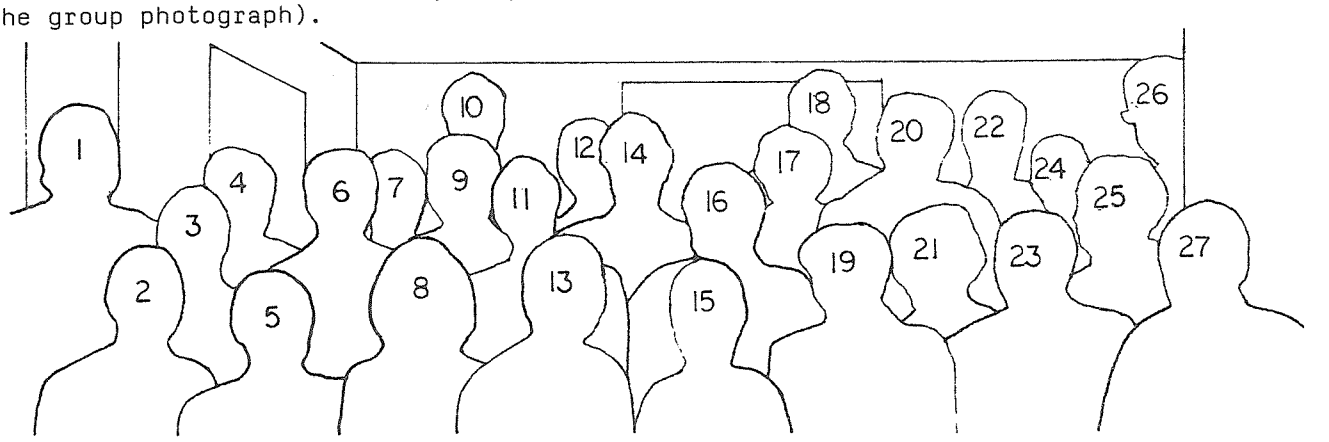

Dr. C. de Jager (A;6)
Space Research Labs.
Beneluxlaan 21
Utrecht
The Netherlands

Dr. Murray Dryer (M;4)
Space Environment Lab
NOAA/ERL
Boulder, CO 80302

Dr. A. Gordon Emslie (T;8)
Center for Astrophysics
60 Garden Street
Cambridge, MA 02138

Mr. Gary Heckman (A;16)
Space Environment Services Center
NOAA-325 Broadway
Boulder, Colorado 80302

Dr. Jean-Claude Henoux (T;12)
Observatoire de Paris
92190 Meudon
France

Dr. Jean Heyvaerts (A;-)
Observatoire de Paris
92190 Meudon
France

Dr. E. Hiei (T; 5)
Tokyo Astronomical Observatory
Mitaka
Tokyo 181
Japan

Dr. S. Hinata (T;21)
Sacramento Peak Observatory
Sunspot, NM 88349

Dr. Gordon Holman (A;-)
Astronomy Program
University of Maryland
College Park, MD 20742

Dr. S. W. Kahler (A;10)
American Science & Engineering, Inc.
955 Massachusetts Avenue
Cambridge, MA 02139

Dr. M. R. Kundu (A;7)
University of Maryland
Astronomy Program
Space Sciences Building
College Park
Maryland 20742

Dr. R. P. Lin (A;-)
Space Science Lab
University of California
Berkeley, CA 94720

Dr. R. M. MacQueen (M;26)
High Altitude Observatory
P. O. Box 3000
Boulder, Colorado 80303

Dr. S. Mandel'stam (M;24)
Institute for Spectroscopy
USSR Academy of Sciences
Troitsk, Moscow obl., 142092, USSR.

Dr. Ron Moore (M;1)
California Institute of Technology
Solar Astronomy
1201 East California Blvd.
Pasadena, CA 91125

Dr. Yoshi Nakagawa (T;13)
ES-51 Space Sciences Laboratory
NASA/Marshall Space Flight Center
Huntsville, AL 35812

Dr. Dennis Peacock (-;18)
Div. of Environmental Sciences
Room 312
National Science Foundation
1800 G. Street, N.W.
Washington, D.C. 20550

Dr. Ken Phillips (T;17)
Astrophysics Research Unit
Culham Laboratory
Abington, Berkshire
United Kingdom

Dr. Reuven Ramaty (A;19)
Goddard Space Flight Center
Building 2, Room 149, Code 611
Greenbelt, Maryland 20771

Dr. David M. Rust (M;22)
American Science & Engineering, Inc.
955 Massachusetts Avenue
Cambridge, MA 02139

Ms. M. A. Shea (A;15)
Air Force Geophysics Laboratory (PHG)
Hanscom AFB
Bedford, MA 01731

Dr. E. J. Smith (A;3)
183-401 Jet Propulsion Lab.
4800 Oak Grove Drive
Pasadena, CA 91104

Dr. P. Simon (M;25)
Observatoire de Paris
Section de Astrophysique
92190 Meudon, France

Dr. Dan Spicer (T;-)
Institute for Physical Sci. & Tech.
Space Sciences Bldg.
University of Maryland
College Park, MD 20742

Dr. V. E. Stepanov (T;27)
P.O. Box 4
Sib IZMIR
Irkutsk 33
U.S.S.R.

Dr. N. V. Steshenko (M;9)
Crimean Astrophysical Observatory
USSR Academy of Sciences
p/o Nauchny
Crimea, 334413
USSR

Dr. Zdenek Svestka (T;20)
Space Research Laboratory
Beneluxaan 21
Utrecht
The Netherlands

Dr. S. I. Syrovatskii (T;23)
P.N. Lebedev Physical Institute
Academy of Science of U.S.S.R.
Leninski Prospekt 53
Moscow, U.S.S.R.

Dr. Katsuo Tanaka (M;14)
Tokyo Astronomical Observatory
Mitaka
Tokyo 181
Japan

Dr. E. Tandberg-Hanssen (M;11)
NASA, MSFC
Code ES-51
MSFC, AL 35812

Dr. G. Wibberenz (A;-)
Institut fur Kernphysik
Universitat Kiel
2300 Kiel, FRG

Dr. Shi Tsan Wu (M;2)
Department of Mechanical Engineering
University of Alabama
P. O. Box 1247
Huntsville, AL 35807

CONTENTS

Page

PREFACE iii

CHAPTER 1: OVERVIEW OF THE STUDY OF ENERGY RELEASE IN FLARES 1

CHAPTER 2: THERMALIZATION OF ENERGY IN FLARES. 3

CHAPTER 3: MECHANISMS OF PARTICLE ACCELERATION 11

CHAPTER 4: MASS MOTIONS. 17

CHAPTER 5: RECOMMENDED OBSERVATIONS. 25

APPENDIX A: SERF ORGANIZATION AND OPERATIONS
David M. Rust. 35

APPENDIX B: SCIENTIFIC PROBLEMS OF THE SMY SERF PROGRAM
A.T. Altyntsev, V.G. Banin, G.V. Kuklin, V.P. Nefedjev,
A.V. Stepanov, V.E. Stepanov, and V.M. Tomozov 37

APPENDIX C: ENERGY TRANSPORT AND THERMALIZATION IN SOLAR FLARES
A. Gordon Emslie 43

APPENDIX D: X-RAY SPECTRA OF SOLAR FLARES
S.L. Mandel'stam 47

APPENDIX E: RESOLUTION
SERF Workshop Participants 59

REFERENCES 61

Chapter 1

OVERVIEW OF THE STUDY OF ENERGY RELEASE IN FLARES

Early in 1980, the Sun promises to pass through one of the highest solar maxima in recent history, thus providing an unprecedented opportunity to observe and study the puzzling phenomena known as solar flares. Realizing the importance of this opportunity, the ICSU Scientific Committee on Solar-Terrestrial Physics (SCOSTEP) accepted a resolution in 1978 to inaugurate the Solar Maximum Year (SMY) program of study, to commence in August 1979 and extend until February 1981. During this period there will be a concerted, world-wide effort to coordinate observations of solar flares and their effects at every possible energy and wavelength, most notably with the Solar Maximum Mission (SMM) satellite, currently planned for launch in October 1979.

The SMY investigations center on three subjects, each an important aspect of the solar flare problem - Flare Buildup Study (FBS), the Study of Traveling Interplanetary Phenomena (STIP), and the Study of Energy Release in Flares (SERF). As part of the organizational effort to ensure that the best and most useful data are obtained during the SMY, it was decided that theoreticians involved in these three aspects of the flare problem should meet to discuss the types of observations that should be made during the SMY to develop and test theoretical models of flares. This was the principal aim of the SERF workshop.

Even after more than a century of observation, with a decade and a half of this spacecraft-based, the solar flare remains basically an object about which very little is known. Even some of the gross characteristics of the flare process elude a definitive explanation. In this brief introductory chapter, we shall briefly discuss a few of the major unresolved problems of energy release in flares, in order to "set the stage" for the more detailed discussions in the chapters to follow.

One of the most basic questions about energy release in flares is of course the following: how does the Sun release some 10^{29} ergs s^{-1} over some 1000 seconds in an area apparently no larger than 10^{19} cm^2? Although it is undoubtedly the case that preflare energy storage is stored in magnetic fields, it is by no means clear how a process of magnetic reconnection can in fact cause such a violent release of energy over such a relatively long period of time. Other, more specific areas of the problem of energy release in flares also have their fair share of unresolved issues, as we now highlight.

(1) Basic questions on the site of the energy release remain unanswered:
- Is the site of the initial flare energy release in the corona, the photosphere, the deep layers of the solar interior, or even a substantial fraction of a solar radius above the photosphere?
- Is the characteristic size of the energy release region of the order of arc seconds (so that resistive magnetic tearing can proceed rapidly enough; cf. also the observed sizes of Hα bright points) or arc minutes (to supply a large enough energy release rate)?

(2) In addition, the nature of the energy release itself is not clear:
- Does the bulk of the flare energy go into macroscopic ejecta or into thermalization of the lower atmospheric layers? The results of Canfield et al. (1979b) and Rust et al. (1979) seem to suggest the former, although no sound theoretical reason for this has yet been given.
- Is the thermalization of the lower layers accomplished by fast non-thermal particles (e.g., electrons) or by thermal conduction and shock fronts? The mechanism actually responsible must be able to explain, among other issues, the synchronism of the flare radiation components at different wavelengths and the relative intensity of these components. There appear to be modeling difficulties with each of the mechanisms mentioned above (see Appendix C), whereas no convincing observational evidence points as yet to either one.

- Are there several different kinds of flares or are there various thresholds at which successively more effective energy release mechanisms take hold? [e.g., is there a clear distinction between "small" and "large" (e.g., proton) events?]

(3) The mechanisms which create the radiation signature of the flare remain ambiguous:

- Are hard X-rays produced by non-thermal bremsstrahlung of a large number of fast-moving, streaming electrons, or are they predominantly thermal in nature?
- In the former case, do the electrons escape out of the bremsstrahlung emitting layers (thin-target model), do they lose all their energy in a high-density target (thick-target model), or are they confined (e.g., magnetically) in a trap?
- In the latter case, what is the density and temperature distribution within the X-ray source?
- Is the white-light flare produced by non-LTE effects at relatively great heights in the atmosphere (cf. Machado and Rust 1974; Lin and Hudson 1976), or does some powerful, as yet undefined, heating mechanism produce it at photospheric depths (Machado, Emslie and Brown 1978; Emslie and Machado 1979)?

(4) The exact sequence of events in the flare is unclear:

- Does the white-light flare precede the hard X-ray burst in some events?
- Are the hard X-ray and EUV time profiles really synchronous enough (Donnelly and Kane 1978) to necessitate a non-thermal excitation mechanism for the latter?
- Does mass ejection occur as a result of the flare energy release, or does it in fact cause the release to occur?

These questions are just some of the many that remain unanswered at this point. However, the spatial, spectral, and temporal resolution of the instruments available to SMY experimenters is conceivably good enough to resolve some of these issues. Thus we hope that the following chapters will clarify the various theoretical points at issue in the study of energy release in flares. These proceedings are being published in the further hope that the best possible sequence of observations will be carried out, and the best possible use of the resulting data made. In the chapters following, the key issues above will be re-raised, along with others. The observing sequences deduced as being possibly capable of resolving the problems identified therein will appear in the final chapter.

Chapter 2

THERMALIZATION OF ENERGY IN FLARES

The problems addressed by the members of this workshop team were the various (sometimes conflicting) theories of energy transport and thermalization in flares (see Appendix C) and the measurements possible during SMY that could conceivably discriminate between, and enhance our knowledge of, these theories.

I. Hard X-Ray Emission

One of the most important and controversial questions addressed by the group was the character of the hard X-ray bursts observed during flares (see, e.g., Hoyng, Brown, and van Beek 1976). Essentially there are two models currently in vogue, which we shall now briefly summarize.

Model N-T (Non-Thermal)

In this model, electrons are accelerated by the action of some non-thermal process, such as a direct electric field or plasma turbulence, and are injected downwards into the solar atmosphere. The beam and its associated return current are considered to be largely stable to the generation of plasma turbulence, and as a result the beam thermalizes by Coulomb collisions deep in the atmosphere, producing the enhanced thermal emission (EUV, $H\alpha$) at these levels (see, for example, Syrovatskii and Shmeleva 1972; Brown 1973; Brown, Canfield, and Robertson 1978; Emslie, Brown, and Donnelly 1978). The X-rays in this model are emitted in a "thick-target" source of high density at the foot of the flare structure (e.g., loop) and have a large amount of polarization and directivity due to the large anisotropy of the electron phase-space distribution function (see, e.g., Brown, 1972).

Model T (Thermal)

In this model, the plasma at, say, the top of an arch-like structure is heated locally to thermal hard X-ray temperatures ($\simeq 3 \times 10^8$ K). Due to the long collisional mean free paths associated with such high temperatures (Spitzer 1962), the electrons form a steady stream down the magnetic field lines in the arch. However, the large return current (required to ensure charge neutrality and zero net current density - see, e.g., Brown and Melrose 1977; Spicer 1977) associated with the stream has a drift velocity which exceeds the local ion sound velocity, thus exciting ion-acoustic turbulence in the plasma. As a result, the X-ray emitting electrons are effectively confined between two conduction "fronts", each moving at the local ion-sound velocity down the arch (Brown, Melrose, and Spicer 1979), with a few "suprathermal" ($v \gtrsim 3 v_e$, where v_e is the mean electron thermal velocity) electrons escaping due to the finite thickness of the conduction front and the long turbulent mean free path of such high energy particles. The velocity distribution function for the confined electrons is a slightly ($\simeq 1\%$) skewed Maxwellian. Thus, in this model, the X-rays are emitted predominantly at the top of the flare structure and are not polarized to such a large degree, although the above anisotropy of the velocity distribution function (caused by the presence of a thermal heat flux) does in fact create finite polarization and directivity (Emslie and Brown 1979).

These two models are illustrated schematically in Figure 2.1., and with these model characteristics in mind, it is a fairly straightforward matter to prepare a number of distinguishing tests, using both satellite (SMM) and ground-based observations.

(1) Using the Utrecht hard X-ray imaging spectrometer (HXIS) on SMM at very high time resolution ($\simeq$ 0.2 seconds), it should be possible to detect the motion of the thermal conduction fronts along the loop. More specifically, such fronts will move at a typical velocity of 2" per second along a structure potentially as long as 1'. Thus some hundred or so consecutive images of the source with the 8" spatial resolution of the instrument could be produced, covering this entire event. If in fact the hard X-ray burst model is non-thermal

(Model N-T), the characteristic propagation velocity of the disturbance is much faster (some 2' per second) and would thus be barely observable with the available time resolution. Further, the location of the hard X-ray source is extremely useful in discriminating between these models: for model N-T, we should expect the brightest X-ray images at the feet of the loop; while for model T, they should be at the top of the structure. This is one of the most vital observations to make. However, a few words of caution regarding observational interpretation are appropriate; namely, the distinction between the motion of a thermal "front" (as described above) or a macroscopic drift of material. These both will occur in flares (although perhaps not the latter in the impulsive flash, due to the long time scales involved - Craig and McClymont 1976) and simultaneous Doppler measurements (using, for example, the SMM X-ray polychromator) are desirable in order to discriminate between these possibilities.

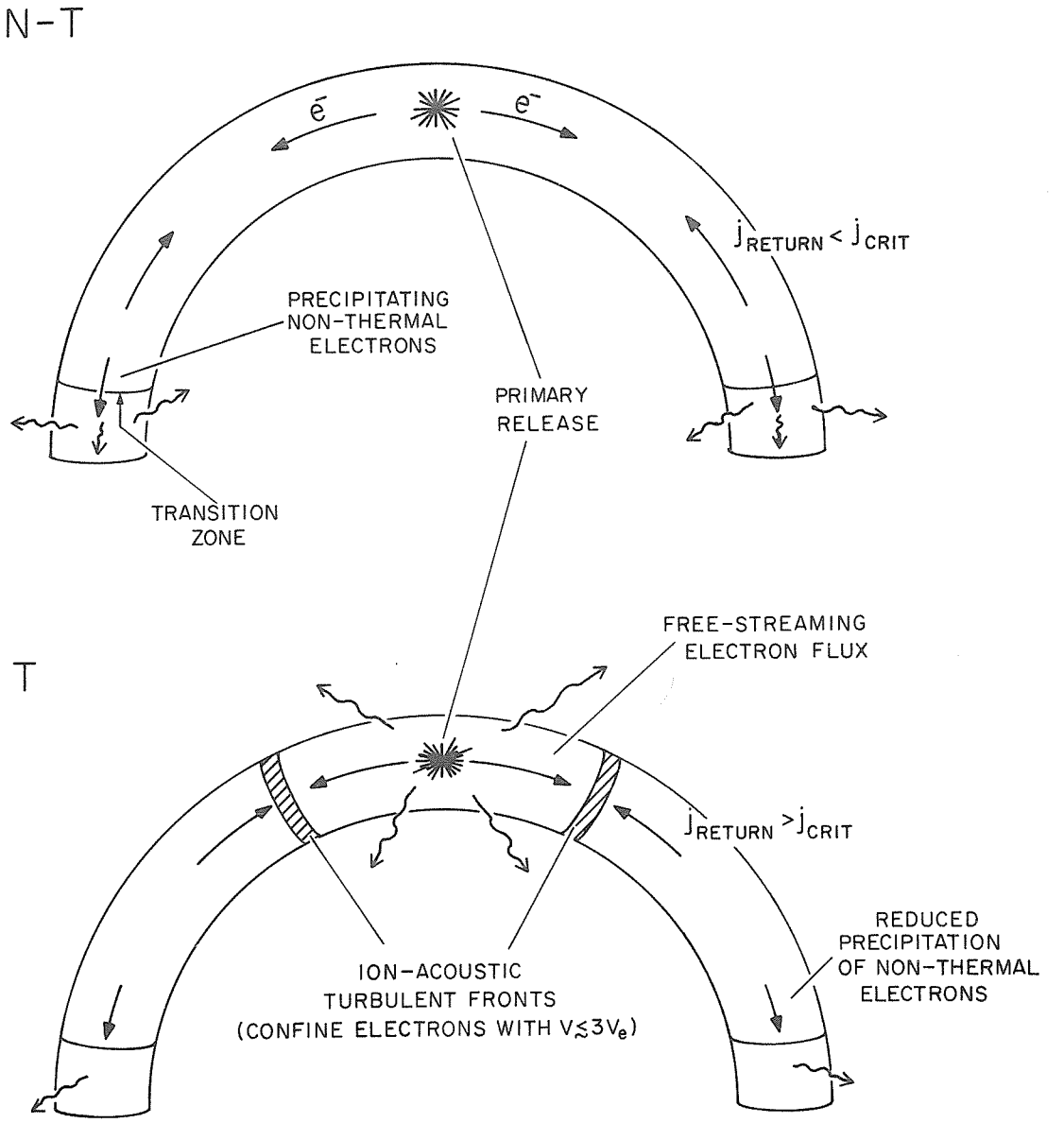

Fig. 2.1: Schematic of the two X-ray burst models N-T and T. In model N-T, the primary release predominately accelerates non-thermal particles, which subsequently thermalize and emit X-ray bremsstrahlung in the dense parts of the loop. In model T, the primary release has predominantly thermal effects; the current due to free streaming electrons is neutralized by a return current j_{RETURN} which has an associated drift velocity higher than the local ion-sound velocity = j_{CRIT}/ne. Thus, turbulent fronts are established which confine the electrons at the top of the arch, where they emit thermal bremsstrahlung; the more energetic electrons ($v \gtrsim 3v_e$; $v_e = (kT/m_e)^{1/2}$) can escape through these fronts and thermalize as in model N-T.

(2) As mentioned above, reliable measurements of the polarization of the hard X-ray bursts provide a clear test between models N-T and T. Since Model T is only capable of producing at most some 5% polarization (Emslie and Brown 1979), while model N-T can produce much more (e.g., Bai and Ramaty 1978), any observation of more than 5% polarization of the emitted X-rays clearly points to Model N-T. However, past polarization observations (Tindo et al. 1972a, b; 1973; 1976) are somewhat uncertain, with polarizations in excess of 10-20 percent claimed in some events, and only a few (2-3) percent in others, but the recent results reported by Mandel'stam (1979) of some 10-20 percent polarization in half of a data sample of 12 events in 1970 clearly require further confirmation. To this end, the Soviet AUOS satellite due to be in operation during SMY, is a potentially very valuable instrument. It will have the ability to deconvolve the effect of an anisotropic X-ray background, and the results it produces should be made an integral part of the SMY observing program.

(3) Radio imaging of the flare in two dimensions, with as high a time resolution as possible will also be a great asset in the discrimination between models N-T and T, especially if polarization measurements are also available. In this way, the location of very high energy (several hundred keV) electrons, and their pitch angle to the magnetic field lines, may be inferred, and compared with the predictions of the two models. These electrons will form part of the suprathermal "tail" in Model T and should therefore manifest themselves outside the X-ray source. They are simply part of the non-thermal (e.g., power-law) distribution in model N-T and should therefore appear cospatially with the X-ray source.

(4) Still, in the radio waveband, it has been observed (Allissandrakis and Kundu 1978) that 6-cm radio bursts, measured with 6" spatial resolution, show an intrinsic polarization during the impulsive phase of the flare which they lose during the post-maximum phase. Kundu and Vlahos (1979) have interpreted this as due to asymmetry in the magnetic field geometry in the flaring loop, and point out that the electrons spiralling down the other (weaker B) leg of the arch should emit most strongly at wavelengths nearer to 20 cm. Thus, simultaneous measurements of the radio emission at 6 cm and 20 cm respectively should provide useful information as to the distribution function for the streaming electrons and so possibly discriminate between models T and N-T.

(5) The measurement, using the SMM Bent Crystal Spectrometer, of the intensities of the Fe XXV resonance line $1s^2\ 1s^2\ {}^1S_0 \rightarrow 1s2p\ {}^1P_1$ (E = 6.701 keV; $\rightarrow$ = 1.850 Å) and its Fe XXIV dielectronic recombination satellites $1s2p^2\ {}^2D_{5/2} \rightarrow 1s^2 2p\ {}^2P_{3/2}$ (n =2; line "j", in the notation of Gabriel 1972) and $1s\ 2p({}^1P)\ 3p\ {}^2D_{5/2} \rightarrow 1s^2\ 3p\ {}^2P_{3/2}$ (n=3; line "d13" in the notation of Bely-Dubau, Gabriel, and Volonte 1979) provide us with samplings of the electron energy distribution function at E = 4.649keV (line j), 5.815 keV (line d13) and E $\gtrsim$ 6.701 keV (resonance line). The satellite lines are excited by electrons having the exact energies quoted above (to within the autoionizing width), due to the absence of a third body to remove excess energy in the dielectronic recombination process. Two temperature values may be obtained from the intensities of these lines: T_1, from the intensity ratio of the satellites; and T_2, from the ratio of either satellite intensity to that of the resonance line (see schematic in Figure 2.2). These two temperatures, and their difference, can be compared with the electron energy distribution function of the two hard X-ray burst models, and the high ($\simeq$ 0.0002 Å) resolution of the BCS instrument, which will observe the 2Å Fe lines continuously, permits measurements of the required quality to be made.

(6) The intercomparison of hard X-ray and EUV fluxes, for which the two hard X-ray models predict a different ratio (Emslie, Brown and Donnelly 1978; Vlahos and Emslie 1979), is also important. It is especially important to know where the EUV radiation originates, and also its spectral distribution, in order to strengthen the previous analysis of Emslie, Brown, and Donnelly (1978) and Donnelly and Kane (1978). This diagnostic clearly requires an interplay between the SMM hard X-ray imager and the ultraviolet spectrometer-polarimeter, although ground-based (e.g., SFD) observations would be also useful.

(7) The study of the general shape of the flux-versus- time profile in a number of different wavelength bands, such as EUV and X-ray, does in fact permit inference of the type of mechanism responsible for the flux enhancement. Using theory due to Nakagawa (1979), the path of a disturbance $\phi(t)$ in the $(\phi,\dot{\phi})$ phase-space (a dot denoting differentiation with respect to time) gives information on the "degree of impulsiveness" (and hence, presumably, of non-thermal/thermal character) of a burst profile. In order to clarify the discussion somewhat, we now briefly reproduce some of the essential theoretical results:

The rate of growth of a quantity ϕ (e.g., X-ray flux) is governed by the action of a driving force $a(t)\phi$ and a restoring force $b(t)\phi$; viz.,

$$\dot{\phi} = [a(t)-b(t)]\phi$$

Further, since $\phi \to 0$ at both $t = 0$ and $t = \infty$, we must have $a(t) \sim t^{-\alpha}$, $\alpha \geq 1$; $b(t) \sim t^{\beta}$, $\beta \geq 0$. If we further relate the magnitudes of $a(t)$ and $b(t)$ by the quantity m, we can formally integrate the linear ordinary differential equation above, using the principle of superposition, to obtain:

$$\phi = \int_{m=0}^{\infty} \int_{\beta=0}^{\infty} \left[\int_{\alpha=1}^{\infty} C_{\alpha,\beta,m} \exp\left(\frac{t^{1-\alpha}}{1-\alpha}\right) d\alpha + C_{1,\beta,m}\, t^{m} \right] \exp\left(\frac{-t^{\beta+1}}{\beta+1}\right) d\beta dm$$

Each "elementary function" $\phi_{\alpha,\beta,m}$ in the above expression has a unique maximum turning point further of Figure 2.3, and therefore gives a unique trajectory in the $(\phi,\dot{\phi})$ plane of Figure 2.4. Thus comparison of the trajectories of different features gives us insight into the closeness of their associated values of α, β and m; i.e., into the possible relation of their physical origin, and it is proposed to treat SMY data in a variety of wavelength intervals in this way.

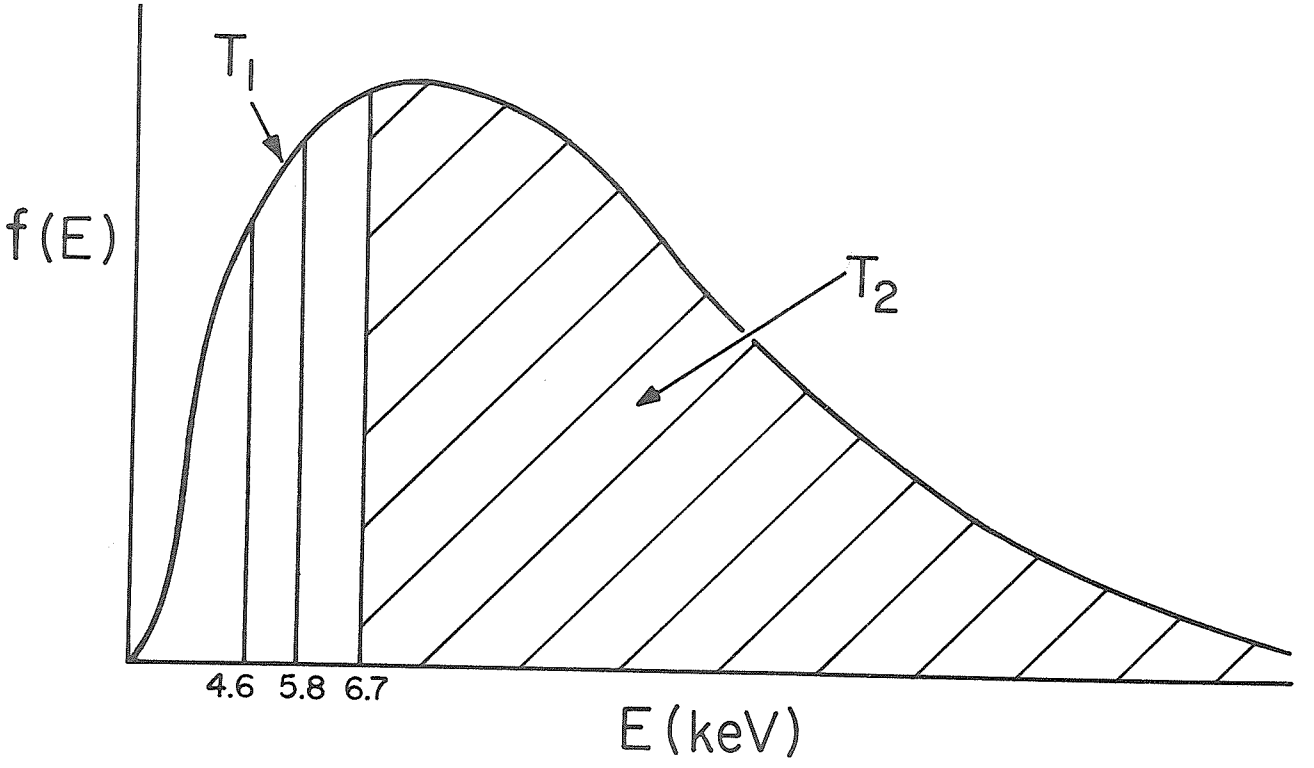

Fig. 2.2: Use of Fe XXV resonance and Fe XXIV satellite lines to determine features of the electron energy distribution. Satellite line strengths give values of the electron distribution function f(E) at 4.649 and 5.815 keV, while combination of these with the resonance line strength gives us $\int_{6.7\ \mathrm{keV}}^{} f(E)dE$, as shown shaded. The temperature T_1, determined by the two satellite line intensities, and the temperature T_2, determined by the ratio of the satellite and resonance line strengths, can be compared with the predictions of flare models.

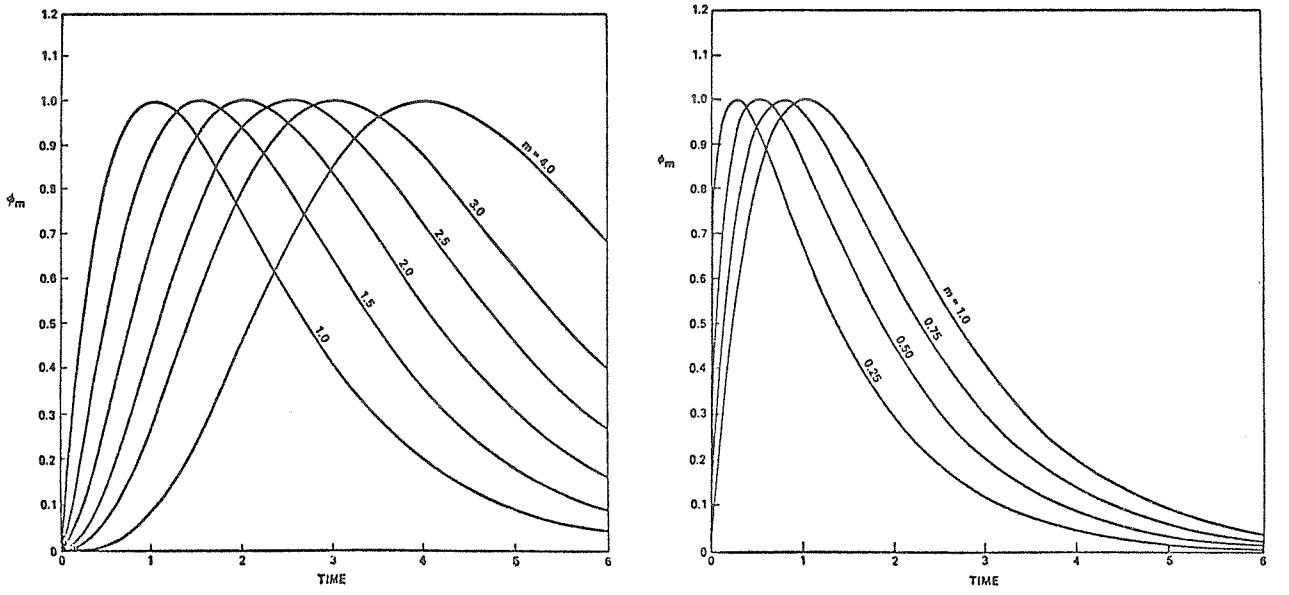

Fig. 2.3: Behavior of an idealized flux-vs-time profile $\phi(t)$, for various values of the "shape parameter" m.

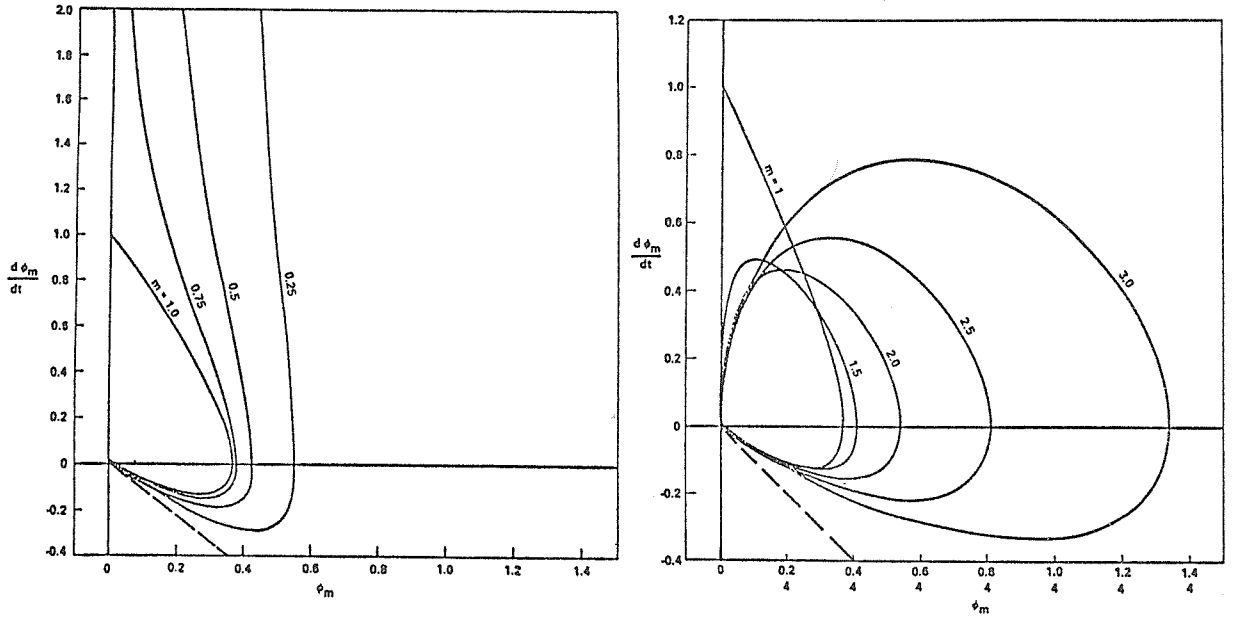

Fig 2.4 : Trajectories in the $(\phi,\dot{\phi})$ plane for each of the functions of Figure 2.3. The general shape of this curve provides an indication of the character of the process responsible for the flux.

(8) The Stark broadening, both linear and quadratic, associated with the presence of an external (beam induced?) electric field permits us to test for such external fields. Such studies naturally subdivide into a number of categories.

(i) Examination of the increase in line half-widths with increasing principal quantum number, or of the continuum merging of the Balmer series or, even better, a series of suitable coronal lines, and use of the Inglis-Teller law to give the local electric field. This has been done for prominences by Hirayama (1963), and flares by Suemoto and Hiei (1959), but primarily as a density diagnostic. In this study we propose to use an Inglis-Teller relationship of the form

$$\ln E = C - 5 \ln n_{max},$$

where E is the electric field strength, n_{max} the principal quantum number of the lowest wavelength line discretely visible, and C is a known constant (Inglis and Teller 1959). A certain part of E will be made up of the local interionic field $E^* = 3.7\, en^{2/3}$, where n is the number density; thus if an independent estimate of n (e.g., by spectroscopic analysis of line intensity ratios) can be made, a value for the external electric field $E_e = E - E^*$ can be found, to be compared with theoretical models.

(ii) Since Model N-T predicts an anisotropy (towards the vertical) of the electron velocity distribution function, the Stark broadening of lines (in itself a useful diagnostic of E fields, if E* can be eliminated) will be directional in strength. Thus, observations of Stark-broadened lines in flares at different central meridian distances provides us with a measure of this anisotropy and so of the likely X-ray emitting mechanism.

(iii) The excitation of forbidden and/or satellite lines by the action of time-independent and time-dependent Stark effects respectively provides another diagnostic of this effect. At this stage suitable candidates for investigation are, however, unclear.

(iv) Finally, it is conceivably possible to measure the quadratic Stark shift in a line, if the instrumentation is accurate enough. Typical values of the quadratic Stark Shift are of order 0.03 Å (observed in the He I lines at 3705 and 4026 Å).

At this point, it is worth remarking on the use of Stark broadening measurements to determine $\underset{\sim}{E}$ fields in the corona. These fields may be capable of creating a $\underset{\sim}{j} \times \underset{\sim}{B}$ drift of material across the magnetic field lines at the top of a coronal loop; this production of material is needed in models which predict a downward convection of coronal material in flares (cf. Craig and McClymont 1976).

(9) Since the SMM hard X-ray imager is capable of unprecedented temporal resolution ($\simeq$ 0.2 seconds), it is capable of perhaps observing real time delays between bursts at different frequencies hitherto considered "synchronous to within the timing accuracy of the data" (cf. Emslie, Brown, and Donnelly 1978, Emslie and Noyes 1978, Donnelly and Kane 1978), even for the non-thermal burst model (a 30 keV electron travels 0.5 arc minutes in 0.2 seconds). Delay times of the form $\Delta\tau = \Delta\bar{\tau} \pm \sigma_{\Delta\tau}$ should be derivable and provide a potentially useful test of theoretical models of energy transport.

(10) In order to assess the importance of thermal effects (such as the thermally driven motion of the conduction fronts in Model T), accurate values of source temperature gradients, inferred from simultaneous density and emission measure determinations, are desirable. At this point, it appears that there are very few density-sensitive spectroscopic diagnostics in the very high temperature regime covered by the available instruments' wavelength range, and theoretical input in this direction from atomic physicists is urged.

Other questions and potential diagnostics addressed by the group will now be presented.

II. Soft X-Ray Irradiation

The study of chromospheric heating by soft X-ray irradiation is a fairly recent aspect of theoretical flare modeling. Analysis for simple source geometries has already been carried out (Somov 1975; Henoux and Nakagawa 1977, 1978; Machado 1978), with very promising results. Recently Henoux and Rust (1979) have carried out a calculation involving the heating of a chromospheric flare by X-ray radiation from an arcade of congruent semi-toroidal loops, with material both uniformly and non-uniformly distributed within them. They find that the degree of illumination of the chromosphere (defined by optical depth unity in "typical" EUV lines) has a geometric structure which bears a strong similarity to the classic two-ribbon Hα structure in flares. Although the analysis is still incomplete (for example, it remains to be shown whether deep chromospheric optically thick radiative transfer leads to a brightening or in fact a darkening in Hα of these brightly illuminated regions), a strong diagnostic of what such a model predicts lies in the comparison of the soft X-ray and Hα radiation geometries. Although care must be exercised due to projection effects when observing loops, this is nevertheless a strong and easily obtained diagnostic, requiring merely the cooperation of SMM X-ray polychromator experimenters and ground-based Hα observatories. Other diagnostics associated with this chromospheric heating model are polarization and non-LTE effects introduced in chromospheric lines by the incidence of photo-electrons (this is theoretically treated very similarly to the case of non-thermal beamed electrons, and shares a number of features in common - Chambe and Henoux 1979). Although a theoretical prediction of the strength of polarization in the Lα wings introduced by this effect gave rather negative results (due largely to the great optical depth of the Lα radiation; Chambe and Henoux 1979) it is hoped that other low-temperature EUV lines, observable with the SMM ultraviolet spectrometer-polarimeter will provide better results, and work is at present in progress along these lines.

As regards NLTE effects, the ionization of Helium is strongly sensitive to an impingent flux of photoelectrons, and careful observations of the He I and II continua, and lines of both species may provide a potential diagnostic of this mechanism. Observations of the spectrum of other atomic species may also be relevant to this study.

III. White-Light Flares

In order to test mechansims responsible for producing white-light flares, simultaneous white-light flare observations and, in particular, Ca II K-line observations, should be made simultaneously with observations in other wavelength bands. In particular, the inference of the accelerated proton flux and the spectrum ($E \gtrsim 10$ MeV) is of great interest in studies of temperature-minimum heating during flares (Machado, Emslie, and Brown 1978). The gamma-ray detector on SMM is sensitive to both of the important 2.2 and 4.4 MeV lines (which permit inference of the proton spectra upwards of 7 MeV) and, when coupled with white-light observations and heating theories of the deep chromosphere, such measurements are potentially capable of increasing our understanding of the deep chromospheric flare. Hard X-ray observations are also of use in this study, since white-light flares may be explainable by electron bombardment alone (Machado and Rust 1974; Lin and Hudson 1976).

IV. Mass Flows

The detection of chromospheric and coronal macroscopic motions and their associated turbulence by measurement of Doppler shifts and broadening of suitable spectral lines is important in assessing the contribution of mass motions as a mechanism of thermalization of energy (Craig and McClymont 1976). Since the initial motion is downward (flare-driven) followed by an upward "evaporation" of overheated chromospheric material some 30 seconds to 1

minute later, quite definite and observable (typical velocities are of order Mach 1 $\simeq 10^6$ cm s^{-1} in the chromosphere) Doppler shifts in both directions (red followed by blue) are predicted by simple theoretical models, and therefore what is required is relatively high time resolution spectral line scans of suitable chromospheric lines.

In summary, therefore, it appears that properly coordinated measurements during SMY are definitely capable of resolving some of the central issues regarding thermalization of energy in flares. It is emphasized, however, that further theoretical input is also needed to a large amount of the above material, in order to make best use of the suggested observations.

Chapter 3

MECHANISMS OF PARTICLE ACCELERATION

Particle acceleration in solar flares can be considered to occur in two distinct classes: the so-called first-stage, common to all flares, in which 10-100 keV electrons are accelerated; and the second-stage acceleration phase, responsible for the production of relativistic electrons and heavy ions, which occurs only in a small number of (usually large) events. In addition to these two main acceleration processes, there is also acceleration of electrons to produce type III radio bursts (which may in fact be due to an entirely different mechanism than that responsible for the first-stage acceleration), and the steady production, for hours or even days, of sub-MeV ions. For a review of these acceleration processes, see Ramaty et al. (1979), while a schematic representation of these processes and their relevance to the flare as a whole is illustrated in Figure 3.1.

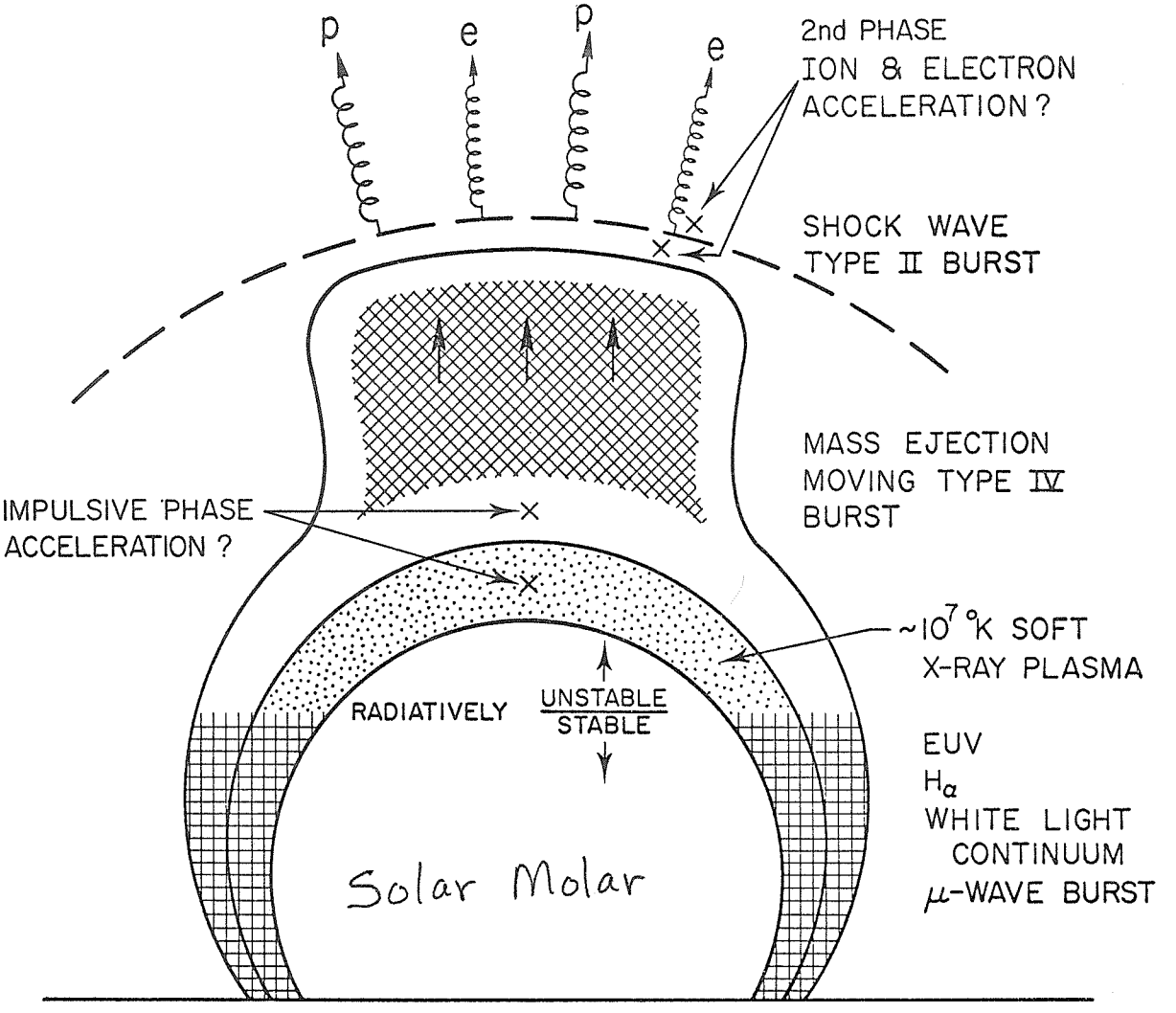

Fig. 3.1: Schematic illustration of the particle acceleration phenomena and their relation to the overall flare process. The existence of a distinct second-stage acceleration process is not clear; nor is the implied cospatiality of the type II shock front and the second-stage acceleration region.

In order to understand the causes and mechanisms of these processes, it is necessary to obtain observations which can satisfactorily define:

(a) the accelerated particle population - its spectrum, temporal evolution, composition, etc.;

(b) the characteristics of the acceleration region - its location, temperature, density, magnetic configuration, etc.;

(c) when and where the particle acceleration takes place;

(d) the responsible accelerating agent - e.g., plasma turbulence, electric fields, shocks, etc.;

(e) the relationship of the particle acceleration process to the flare as a whole - e.g., the fraction of the total flare energy carried by first-stage accelerated particles;

(f) the coronal and interplanetary structure, in order to facilitate the interpretation of terrestrial and spacecraft measurements of particle streams.

In addition, knowledge of the preflare configurations which lead to such acceleration processes is of use; this problem is common to both the SERF and FBS areas of the SMY.

We now discuss each of the broad areas mentioned above in greater detail.

I. The Accelerated Particle Population

This section breaks down naturally into direct detection of particles in the interplanetary medium (including Earth-orbiting satellites), and inference of the particle distribution by means of its associated radiation signatures (X-rays, γ-rays, etc.). We deal with each of these in turn:

Ia. Direct Detection

(1) Spacecraft measurements of the electron spectrum in the MeV range will give information on the likely mechanism for the excess γ-ray emission in the 1 - 2 MeV range which is observed in some flares (e.g., the 4 August 1972 event). At present, this excess emission is interpretable as being due to either the presence of MeV electrons or to the enrichment of heavy nuclei (Mg, Si, Fe) in the particle stream, or ambient solar atmosphere, or both. Deviations in the shape of the electron spectrum from a power-law in the MeV range indicate the former possibility, while no substantial deviation indicates the latter.

(2) Measurements of the energy spectra of protons and heavy nuclei (C, N, O, Ne, Mg, Si, Fe) from a few MeV to at least 100 MeV, are urged. The intercomparison of these spectra will give information on the interaction mode of the particles at the Sun (e.g., thick- or thin-target), and also on the effects of the interplanetary medium on the propagation of these particles (see section V).

(3) Measurements of the charge states of energetic nuclei are potentially capable of determining the electron temperature of the acceleration region (see section II).

(4) Measurements of the abundance ratio of rare nuclides (e.g., D, Li, Be, B) to C and O can place limits on the column density of material encountered by the particles since their production, and hence on the likely interaction mode [cf. (2)]. This information can also be coupled with measurements of the total particle flux (obtained from simultaneous widely-separated multi-spacecraft measurements) and the total γ-ray flux [see (10)] in order to obtain a reasonably complete picture of the confinement and escape mechanisms of accelerated particles.

(5) Since very high energy particles can be detected by terrestrial cosmic-ray neutron monitors, with the low energy cutoff in the instrument response being a function of geomagnetic latitude, use of the world network of neutron monitors can provide information on the energetic particle spectrum in excess of 17 GeV. The SMM γ-ray experiment is conceivably capable of detecting the π^0 decay γ-rays produced by particles with energies of several hundred MeV, and this would provide a comparison flux at lower particle energies.

Ib. Inference From Radiation Signatures

(6) Since particles emitted from flares occurring in the W20 - W90 solar longitude range are most likely to be detected by near-Earth spacecraft, it is strongly urged that SMM and other satellite observations be preferentially made in this region of the solar disk, for comparison with measurements made under program Ia. The location of HELIOS and other interplanetary spacecraft should also be taken into account in deciding the optimum area to be observed.

(7) In principle, the X-ray spectrum observed at the Earth can be inverted to yield the energetic electron spectrum responsible for its production. This process is, however, well known to be mathematically ill-posed, and very accurate X-ray spectral measurements are necessary in order to obtain substantially quantitative results for the electron spectrum. Since the precise form of this electron spectrum has important bearing on the flare problem (e.g., it is substantially different for the two hard X-ray models N-T and T of Chapter 2), we urge that such accurate spectral observations be made, such as with balloon-borne cooled semi-conductor detectors, which have a typical energy resolution of about 1 keV.

(8) The polarization of X-ray bursts has also important implications for the accelerated particle population (cf. discussion in Chapter 2 and Appendices C and D), and cooperation between Russian experimenters and those involved with the solar X-ray polarimeter experiment sheduled for the forthcoming Space Shuttle Orbital Flight Test is encouraged.

(9) It may be possible to determine the relationship between impulsive phase electron acceleration and type III burst electron acceleration by comparing radio and hard X-ray source locations. This involves obtaining two-dimensional high time resolution images of total intensity and circular polarization during impulsive bursts to be compared with information obtained from the SMM hard X-ray imaging spectrometer. Even better would be to directly measure the hard X-ray burst component produced by the type III burst electrons; such measurements are conceivably possible using the cosmic X-ray telescope currently planned for Spacelab 2, suitably modified for a later Spacelab flight.

(10) For diagnostics of the second-stage acceleration, which is characterized by a flux of heavy particles (notably protons) and relativistic electrons, γ-ray measurements are of course of great use. Such observations can be used to infer the energy spectra of the particles (nuclei from line ratios, and electrons from the continuum), the total energy of such particles, the directivity of the accelerated ions (from Doppler shifts and asymmetries in spectral line profiles - cf. Orrall and Zirker 1976; Canfield and Cook 1978), and possibly the enrichment of heavy nuclei in the energetic particle stream [cf. (1) above]. In addition to the γ-ray detector on SMM, cooled semi-conductor detectors, which have a high (a few keV) spectral resolution, are also of use; such detectors are on the Air Force P78-1 spacecraft and scheduled for the HEAO-3 satellite.

II. The Acceleration Region

(1) Spectroscopic measurements made with the SMM X-ray polychromator instrument are capable of determining both the ion (via line widths) and electron (via line intensities and ratios) temperatures in the high temperature regions of the flare. Comparison of these two temperatures permits inference of the likely acceleration agent (cf. section III) and of conditions in the acceleration region, to be compared with models (cf. Chapter 2). In addition to the SMM X-ray polychromator, Russian spacecraft will also be helpful in obtaining this information (cf. Appendix D).

(2) High spatial ($\simeq$1") and temporal ($\simeq$10s) resolution radio mapping of the flare at centimeter wavelengths is necessary to fully study the site of primary energy release and particle acceleration, for it permits inference of the magnetic field structure in such regions; this can again be tested against models of flare energy release.

(3) Determination of the elemental composition of the acceleration region can be carried out using combined measurements of the γ-ray "hump" at 1 - 2 MeV and the electron spectrum in the same energy range [cf. sections I(1) and I(10)].

(4) In order to discriminate between models of ^{3}He rich flares, some of which favor preferential acceleration (Colgate 1978), and some of which favor plasma enrichment in the ambient corona (Fisk 1978), spectroscopic determinations of the abundances of He and heavy nuclei are desirable. In particular, the detection of γ-ray lines from such ^{3}He rich flares would greatly clarify the issue.

(5) In addition, such ^{3}He rich events seem to be correlated with low-speed solar wind regions (Zwickl et al. 1978). Since variation in the solar wind velocity affects interplanetary propagation of particles (Morfill, Richter, and Scholer 1978), observations of these events should be coordinated with measurements of interplanetary structure (section V). In addition, Axford's (1977) model predicts that low solar wind velocities are related to transient open and to closed field regions. Such correlations between field geometry, particle stream speed, and isotopic composition should be investigated.

III. Location and Temporal Behavior of the Primary Energy Release

(1) High resolution hard X-ray images should be capable of determining whether subsequent elementary flare bursts (EFB's - de Jager and de Jonge 1978) are energizations of the same area or of different areas.

(2) High time resolution soft X-ray pictures showing the spread of the energization throughout the flaring volume will also help resolve this question, as well as possibly discriminating between energy release models (cf. models N-T and T of Chapter 2).

(3) Radio observations (Slottje 1978) show that solar microwave fluxes exhibit fluctuations on timescales of the order of milliseconds. The hard X-ray spectrometer on SMM should be able to test for fluctuations in the X-ray flux on similar timescales, and so determine whether the EFB is indeed the fundamental "building block" of the flare energy release.

(4) High spatial resolution vector magnetograms (using the SMM ultraviolet spectrometer and ground-based Stokes polarimeters) could provide important information regarding the magnetic field structure in the preflare configuration, to be compared with the high spatial resolution X-ray pictures mentioned above.

IV. The Accelerating Agent

(1) High time resolution (about 10 ms) measurements of the total flux at centimeter wavelengths are urged, the objective being the detection of source brightness temperatures in excess of 10^{14} K, indicative of a plasma wave acceleration process in centimeter-wave burst sources.

(2) Spectroscopic signatures of strong electric fields are line broadening and shifts due to the linear and quadratic Stark effects respectively (cf. Chapter 2); evidence for a turbulent acceleration mechanism would be the appearance of turbulence-induced forbidden line transitions (Davis 1977).

(3) Simultaneous optical and decametric radio observations of the spatial evolution of the flare disturbance are capable of detecting collisionless bow-shock waves (types II and IV radio bursts). A good estimate of the Alfvenic Mach number of these shocks with time is important for testing theoretical models of particle acceleration by expanding shock waves.

(4) Particle-accelerating shocks should evidence themselves in the Doppler broadening of spectral lines, the typical velocities involved being of the order of 100 km s^{-1}.

(5) Observations of the evolution of coronal mass ejections (cf. Chapter 4) with the SMM coronograph-polarimeter, coordinated with observations of particle fluxes, spectra, and compositions, are required in order to investigate the possible relation between ejections and particle acceleration. HELIOS data are particularly useful for studying the variation of particle flux with size of the coronal mass ejection. Off-band $H\alpha$ measurements should also help to determine the position and velocity of each part of the ejected feature (cf. Chapter 4), to be related to positions of the observed manifestations of the second-stage acceleration process, if any.

V. The Relationship of Particle Acceleration to the Overall Flare

(1) The overall flare energy budget should be derived for a number of events (cf. Canfield et al. 1979b; Rust et al. 1979) and the contribution of energetic particles assessed. This has important implications for mechanisms of primary energy release.

(2) The interaction of accelerated particles with the ambient solar atmosphere needs to be better modeled and understood. We refer the reader to Chapter 2 and Appendix C for a more detailed discussion of this aspect of the flare problem.

VI. Coronal and Interplanetary Structure

Observations of the structure of coronal holes and the solar wind are necessary in order to ease the interpretation of near-Earth observations of particle streams.

(1) Coronal hole maps that define the probable sources of high-speed streams will enable the Sun-Earth propagation of ejected particles to be better modeled. To this end, daily, whole-Sun, soft X-ray spectroheliograms should be made an integral part of the observing program. Also, daily He λ10830 Å images will be of use.

(2) Solar wind plasma and field parameters, obtained from (e.g.) ISEE-3, HELIOS, and Pioneer-Venus, will help define the spatial extent and shape of solar-induced interplanetary disturbances.

(3) We also recommend that three-dimensional probes of the interplanetary medium be carried out using the interplanetary scintillation (IPS) technique, at regular intervals throughout SMY, with specific emphasis on periods of special study as identified by FBS, SERF, and STIP.

With the above observations properly coordinated, we feel that we can make significant progress during SMY toward understanding the causes and effects of particle acceleration in solar flares.

Chapter 4

MASS MOTIONS

Mass motions play an important - perhaps even dominant - role in the flare phenomenon. They can occur on several scales and at various times thoughout the flare, and may be broadly classified into four somewhat overlapping categories:

(1) "Intrinsic" motions; i.e., internal hydrodynamic motions of the heated flare plasma -- these are considered in Chapter 2 [cf. Sections I(1) and I(7) therein], where tests are proposed to distinguish between these motions and thermal conduction fronts.

(2) "Thermally driven" motions; i.e., motions caused by external heating of material. These are also clearly connected with energy thermalization through the process of "evaporation", i.e., upward convection of material (cf. Kostyuk and Pikel'ner, 1975; Antiochos and Sturrock, 1978; Hiei and Widing 1979). Intrinsic motions may result in significant mass and energy transport, but the motions are all constrained by local magnetic flux tubes.

(3) "Infall;" i.e., relaxation of previously evaporated material back into the chromosphere during the decay phase of the flare. Impact of this material may cause further flare brightening (Hyder 1967a, b). These "infall-impact" brightenings will not be considered further in this report, but we note that the pattern of such brightenings can help illuminate the magnetic field configuration of flaring regions.

(4) "Ejections"; i.e., macroscopic motions due to extensive rearrangement of the magnetic field or to large-scale thermodynamic disturbances. These exhibit themselves in the form of (e.g.) spray prominences, eruptive prominences and coronal transients. It is possible also to summarize many optical soft-X-ray, radio and white-light observations of mass ejection events in a common time-height diagram (Figure 4.1).

Mass motions may account for a large fraction of the total flare energy (Canfield et al. 1979b; Rust et al. 1979). In order to fully understand the energy budget in flares, therefore, it is especially necessary to know the nature of large-scale and thermally driven ejections. In what follows, we discuss what seem to us to be the most important questions to be answered about these phenomena. Briefly, an observational program should:

- Determine the total mass and energy losses in mass motions;
- Determine the influence of thermal mechanisms in driving flare ejecta;
- Determine the three-dimensional shape and volume of the various kinds of mass ejecta;
- Determine the spatial relationship of ejecta and particle acceleration regions;
- Differentiate between self-driven expanding magnetic loop and gas-dynamic models of coronal transients;
- Determine whether important motions are present in the corona before flares: e.g., are 'forerunners' initiated prior to flare onset?
- Determine the interplanetary signature of solar mass ejections.

I. Mass and Energy

Ia. Energy of filament eruptions and coronal transients

(1) Filament eruptions accompany the onset of many flares, both in young active regions and in old regions which have lost their sunspots and have weaker magnetic fields. These eruptions are obviously involved in some way in the conversion of magnetic energy to thermal and kinetic energy. To understand this energy release, we need to know the magnetic field configuration. The form and

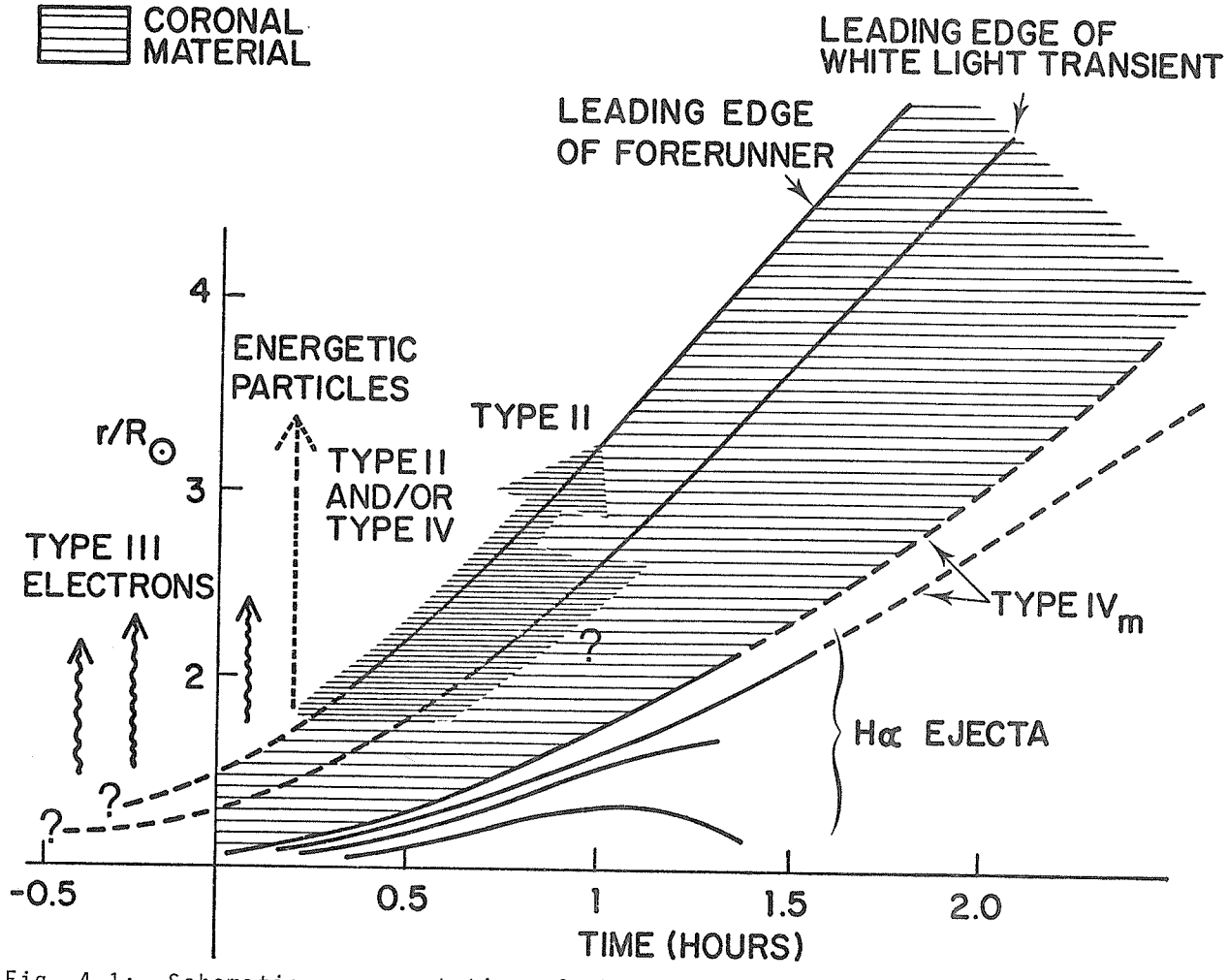

Fig. 4.1: Schematic representation of phenomena associated with large-scale mass ejections. The origin of axes represents flare onset. After flare onset, Hα-emitting ejecta are seen to about 2 $R_\odot$. Coronal transients have been traced from about 1.8 $R_\odot$., but, as the question marks indicate, extrapolation of coronal transients' trajectories back to time zero is uncertain. Metric type III bursts are recorded before time zero, but the starting time and height of coronal transients and their forerunners are uncertain. Energetic particles, revealed by metric type II and type IV emissions, may be accelerated in or near the shocks ahead of fast-moving transients.

structure of a filament prior to and during its eruption gives some indication of the magnetic field structure in the immediate vicinity of the flare. We urge intensive study of high-resolution Hα movies, which are the most effective means of studying this structure.

(2) Observations of coronal transients as well as in situ measurements of travelling interplanetary disturbances give estimates of the total mechanical energy output of a flare. The ratio of the mechanical energy output to the radiative energy output is a fundamental physical characteristic of the energy release process. The best past estimates (Canfield et al. 1979b; Rust et al. 1979) indicate that this ratio may be substantially larger than unity, so that the energy of flare-associated coronal transients and filament eruptions, in addition to the total radiative output, must be documented in order to understand the energy release mechanism of flares.

(3) The total energy of moving material is the sum of the kinetic, potential, magnetic, thermal, and non-thermal energies, and while Hα and white-light images can give good measurements of the kinetic and potential energies, observations of the polarization and intensity of radio emission are necessary in order to infer the magnetic field. Observations of line emission from the outer and inner corona are required to determine the thermal energy of transients. Radio spectroheliograms and interplanetary particle observations (cf. Chapter 3) will give the energy in the non-thermal component.

Ib. Mass of Flare Sprays

(4) Flare sprays are composed of both cool and hot material catapulted into the corona under the action of magnetic (or thermodynamic) forces. The prominence (i.e., flare spray) material, seen in Hα emission, is contained within an expanding or stretching magnetic flux tube and constitutes a substantial mass ejection (Rust et al. 1979). It will be important to obtain optical spectra of this ejected mass to distinguish, by Doppler shift measurements, between genuine mass motions and wave phenomena, where we observe the locus of a density disturbance at successive times. We encourage measurements in some lines formed at higher temperatures than Hα, in addition to Hα measurements, so as to follow the material as it is heated in the corona. Possible lines for these observations are H I 1216 Å, He II 4686 Å, He II 1640 Å, and various lines of Si II, C III, C IV, and Si IV.

(5) Mass ejections reach velocities of several hundred to several thousand kilometers per second, but the material visible in Hα seems to be confined within flux tubes. Broad-band (≃ 10 Å) Hα filtergrams will allow observation of the material moving at an angle with the plane of the sky, so that an accurate estimate of the total mass may be obtained.

Ic. Mass of Coronal Transients

(6) The source of the mass in coronal transients should be investigated with coordinated observations of the low and outer corona. One study (Rust and Hildner 1976) indicated that the mass seen leaving the Sun through the outer corona all came from the inner corona, but some coronal transients may possibly carry off more mass than was present beforehand in the underlying corona. Excess mass may be supplied to the corona during the main flare phase: Hα fibrils connecting the outer borders of flare ribbons to nearby plages have been seen to open up. There follows immediately a surge-like mass ejection from the feet of the opened feature. It is important to determine the mass ejected in the surges and also the surge positions relative to the base of coronal transients, to determine whether the surges could be at the feet of field lines leading into the coronal transient. High-resolution filtergrams, Hα and high Balmer line spectra (to determine the density) as well as coronagraph observations are needed.

II. Thermally Driven Motions

IIa. Flare-initiated Events

(1) The sudden input of heat in the low corona that is a flare should cause an explosive increase in the local gas pressure. Some flare sprays and surges, as well as the sudden coronal loop enhancements found in the Skylab soft X-ray data, may be evidence of mass motions driven by this increased gas pressure. Very little quantitative data are available on such thermally driven motions. A few, rapid, flare-associated coronal loop brightenings were found in the Skylab data (Rust and Webb 1977). (We refer to enhanced loops stretching from the flare kernel to a point $\simeq$ 0.1 $R_\odot$ away as illustrated in Figure 4.2.) The propagation velocity of the excitation is in the range 400 to 1000 km s^{-1}, and a significant fraction of the total flare energy may be carried away in the process (Craig and MacClymont 1976). We recommend that high time resolution, wide-field soft X-ray observations be obtained to quantify the energy in the heated (or shocked) gas.

(2) Hα sprays frequently accompany coronal enhancements, so high time resolution Hα or He λ10830 Å observations should be obtained simultaneously with the above soft X-ray spectroheliograms. Flares with sprays are easiest to study when within 20° (heliographic) of the limb, since the origin of the spray can be compared with the disk position of the flare, while the spray trajectory can be traced easily once it clears the limb. Magnetograms of the active center and its surroundings are useful for understanding how spray trajectories and enhanced coronal loops connect to the flare core.

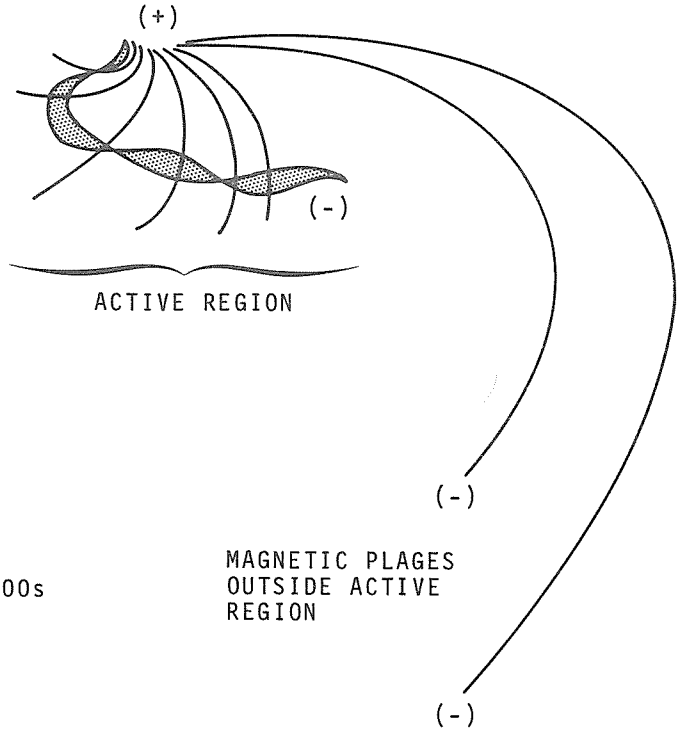

Fig. 4.2, a-c: Schematic model of an active region X-ray enhancement. (a) X-rays (shaded area) are emitted from a filament cavity shortly before the filament explosive phase. The emission seems to come from along the top of or just below a canopy of loops that extend from positive to negative magnetic footpoints in the active region. The emitting region appears 1 - 3 x 10^4 km above the solar surface, and its edges are very sharply defined. (b) Just after filament eruption, X-ray emission is brightest in several low active region loops. Other fieldlines are open and may carry shocks (hatched area) to the outer corona. Slow-mode shocks (see Kopp 1972) also follow extended flux tubes to the chromosphere. (c) About 500 s later, soft X-ray flux is at a maximum with emission from an arcade of loops over the active region. Flux tubes terminating outside the active region brighten, bow out and expand under increasing gas pressure as matter is evaporated from the chromosphere.

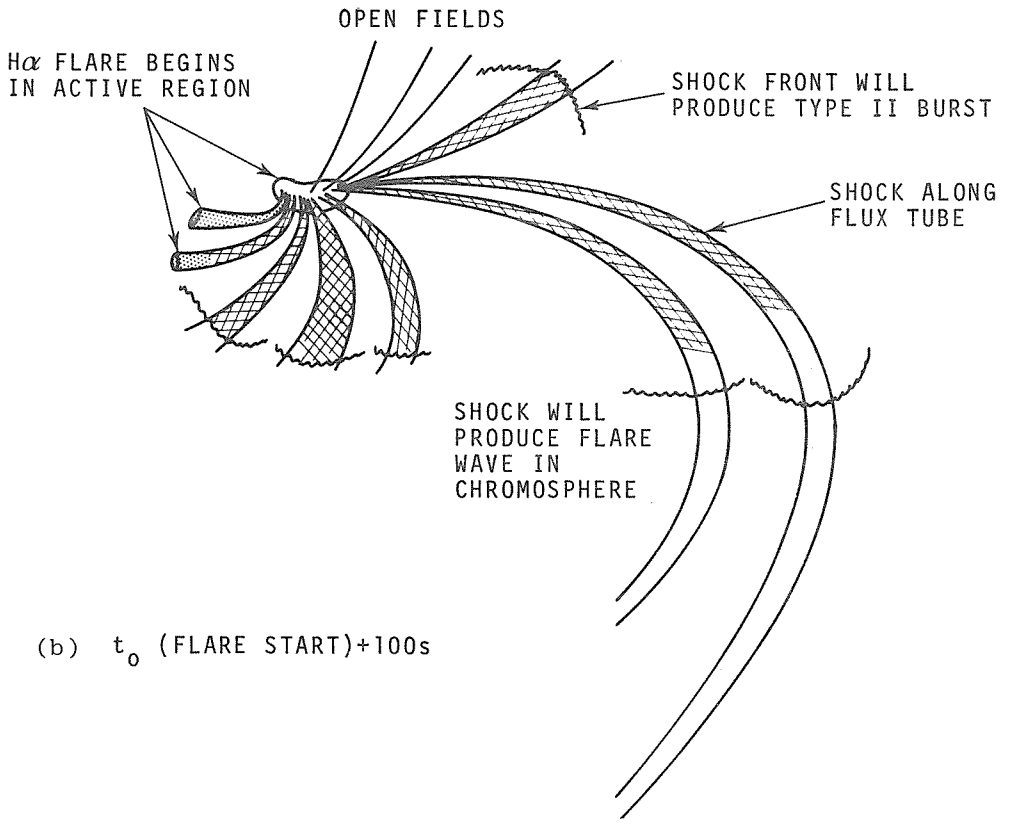

(b) t_o (FLARE START)+100s

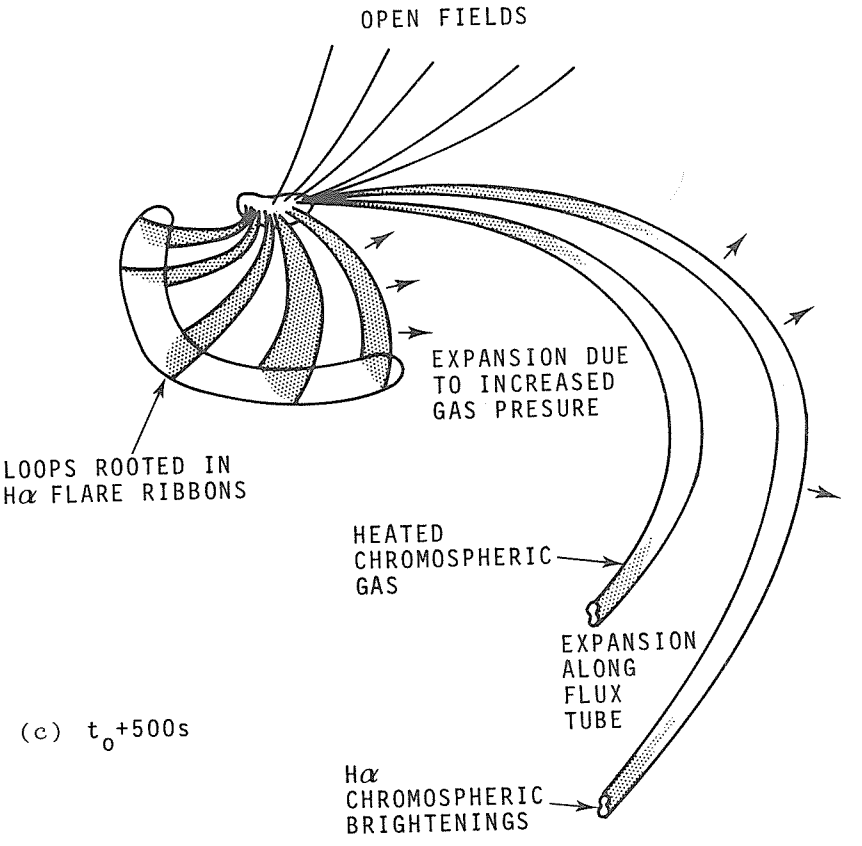

(c) t_o+500s

IIb. Models of Thermally Driven Mass Motion

(3) In order to understand the detailed physics of the observed events, theoretical modeling is needed. A model should be designed to study the dynamical response of a flaring loop of very high β. In this case the shape of the loop is prescribed and will remain unchanged, and the mass motion will be confined by the loop. The thermal pulse takes place at one footpoint of the loop and the effects travel over the top of the loop (in the corona) to the chromosphere at the other footpoint, where reflection and explosive convection must be taken into account. The effects of thermal conduction and radiative losses should also be incorporated. Multiple loop models could be investigated to determine whether the spreading of excitation in the impulsive phase can be simulated.

(4) An alternative to the above model would place the source of loop brightenings outside of the loops themselves. That is, shocks from the flare would strike closed loops broadside and cause brightening at every point almost simultaneously. This model is not excluded by the available data. In order to test these models, we need the magnetic field configuration and strength before and after the event, and the plasma temperature, density and velocity as a function of space and time for each event. By comparing two-dimensional MHD models with observations, we can get some degree of understanding of the physical processes at work during the event; e.g., thermal conduction, shocks, shocks modified by thermal conduction, radiative cooling, etc.

IIc. Filament Activation and Flare Onset

(5) Most, perhaps all, large flares are preceded by a filament eruption. Soft X-ray observations show that some filament material is heated before flare onset, but we do not know whether filament ejection is a result of this heating. Conceivably, heating could signal the destabilization of a magnetic configuration, which then acts directly by Lorentz forces to propel the filament outward. We urge that the source and location of pre-flare filament heating be investigated and that its link to filament motion be clarified. High time resolution observations of soft X-ray emission should be combined with $H\alpha$ observations to determine the degree of filament activation - twisting or untwisting - that is associated with preflare heating. Spectra from the SMM ultraviolet spectrometer-polarimeter, and field measurements in the eruption, will help specify the thermal release process.

III. Loops versus Bubbles

There are two physical models which have been proposed to describe coronal mass ejections. At the risk of oversimplification, we categorize the two approaches as follows:

(a) Discrete ("loop") model - Motivated by the visual appearance of white-light coronal transients, one hypothesizes a loop with plasma confined by a helical magnetic field. One assumes, further, the presence of a low β plasma ($\beta << 1$, where β is the ratio of thermal to magnetic pressure) as well as an uncertain Alfven Mach number motion M_A, where M_A is the ratio of dynamic pressure, $1/2\ nmv^2$, to magnetic pressure. The loop is supposed driven outward by magnetic stresses. Some features of this magnetic loop model can successfully simulate coronal mass ejections of the kind most frequently seen during the Skylab mission. The magnetic loop is considered to be pinched off eventually by reconnection; the inner part returns to the Sun, and the outer plasma bubble moves into the solar wind.

(b) MHD continuum ("bubble") model - Motivated by the successes of collective fluid mechanics in describing explosive phenomena (e.g., bombs), one starts with an atmosphere in stationary equilibrium and introduces an impulsive burst of energy, mass and/or momentum at or near the base of the atmosphere. The fast, slow and intermediate (Alfven) waves propagate anisotropically; the fast waves steepen into an MHD shock. The slow waves

are associated with the compression of the plasma at the "contact surface", i.e., the leading edge of the plasma from the site of the initial burst. The ambient coronal plasma moves ahead of this piston; its leading edge is compressed by the shock wave. The entire ensemble fills a large solid angle, $\simeq \pi/2$ to 2π steradians, which is a function of the energy, momentum, and mass input. If $\beta < 1.0$, the plasma will be constrained: only outward wave motions will occur, and no mass will cross the magnetic field lines.

Answers to the following questions should reveal which model is the more accurate description of mass ejections:

(a) What is the magnetic configuration before, during, and after a mass-ejecting flare?

(b) What are the various energy contents (i.e. kinetic, potential, magnetic, thermal and particles) as a function of time? What are the total outputs in these various forms? How does the radiative flare output vary during periods of large mass motion?

(c) What is the source region of the particles responsible for "prompt" energetic solar protons relative to the flare ejecta?

(d) How does the coronal transient evolve into the travelling interplanetary disturbance? Can we identify one or more interplanetary signatures with different types of coronal transients?

We recommend the following observational studies for answering the above questions:

(1) Use K-coronagraph views at $1 \lesssim R/R_\odot \lesssim 2$ to search for transients.

(2) Radio spectra and spatial views are needed to determine shock velocity (cf. Chapter 3) and type IVm and stationary type IV characteristics in association with the white-light transients.

(3) Determine, using soft X-ray observations, the density and temperature of the plasma at the flare site as a function of time. This information is needed for modeling of input pulse functions. Image the emission-line corona.

(4) Obtain "before" and "after" magnetic field directions in the plane of the sky.

(5) Obtain inner-coronal Faraday rotation of spacecraft telemetry signals to sample magnetic field polarity changes during a transient. Use telemetry phase shifts and dual frequencies to get velocities and densities during and after transients.

(6) Use IPS observations to get the temporal and spatial developments of large-scale mass motion changes in the solar wind.

(7) Use multiple spacecraft observations to detect <u>in situ</u> changes. Obtain unambiguous associations of shocks and pistons with specific solar transient events. Sample energetic particles which come directly from flare sites; distinguish them from locally-accelerated particles.

IV. <u>Precursors and Forerunners</u>

Not all mass motions are consequences of flares. Activated filaments and, perhaps, forerunners precede flare onset. Filament and coronal disturbances may, in fact, <u>cause</u> flares. We urge increased effort to establish the physical reality of the various reported and debated precursors. Specifically, one should search for preflare changes in coronal loops over activated filaments and determine whether such activity is associated with forerunners. The magnetic fields in the photosphere and chromosphere should be monitored for evidence of

emerging flux or shear, which could destabilize the fields supporting filaments. Hα, 5303 Å, and X-ray observations can show precursor activity quite clearly. More patrols in these wavebands are needed. Type III bursts may give a warning that preflare motions are imminent, and microwave interferometer observations will indicate where the preflare heating is occurring. Radioheliograms showing the path of type III and type II bursts can help indicate the rate of propagation of disturbances in the corona near 1.5 $R_\odot$, where coronagraph coverage is poor.

V. Interplanetary Effects

We have barely started to identify, from both observational and theoretical viewpoints, the interplanetary extensions of solar eruptions. During the SMY, we hope to clarify how solar events affect the interplanetary medium and the normal solar wind, to categorize a spectrum of forcing functions, as it were, and to make unambiguous solar-planetary associations with, at least, the most energetic events.

With these observational recommendations carried out to the fullest extent possible, we believe that several key issues regarding the role of mass motions as a mechanism of energy release in flares can be resolved.

Chapter 5

RECOMMENDED OBSERVATIONS

I. Collaborative Observing Sequences

In each of the preceding chapters a group of closely related scientific problems was discussed and appropriate kinds of observations were mentioned somewhat incidentally. In this chapter readers inspired by the scientific discussions will find specific needed observations grouped together as Collaborative Observing Sequences (COSs). During the SMY, whenever it appears that one of the scientific objectives of the SERF subprogram can be pursued profitably, an SMY Coordinator (see Appendix E) will suggest that observers institute a specific COS. (Details of the operations are summarized in Appendix A.)

Following the lead of the Solar Maximum Mission investigators, we recommend that COSs be numbered and identified with Specific Scientific Objectives (SSOs) as follows:

- 001 Chromospheric Evaporation
- 002 Thermalization
- 003 Nature of Electron Acceleration
- 004 Coalignment
- 005 Ejecta
- 006 Flare Energy Budget
- 007 Bright Points
- 008 Impulsive Phase
- 009 Location of Energy Release Sites
- 010 Evolution of Active Regions
- 011 (None)
- 012 Active Region Structure
- 013 Limb and Disk Surveys
- 014 Flare Buildup (FBS objective)
- 015 Flare Precursor (FBS objective)
- 016 Coronal Heating Mechanisms
- 017 Coronal Evolution
- 018 Flare Decay (FBS objective)
- 019 Flare Morphology
- 020 Ion Acceleration
- 021 Hydrodynamics
- 022 Spotless Flares (FBS objective)

Topics without bullets (•) are not SERF objectives, although some like 004 Coalignment are of obvious importance to SERF operations. Very detailed COSs for SSO 014 have been developed by Z. Švestka for the SMY Flare Buildup Study and we will not repeat them.

Table 5.I summarizes the varieties of flare-specific observations that are called for in the SERF COSs. The interval Δt between successive observations is, in most cases, the limit set by available instrumentation. Where instruments are capable of recording data much more rapidly than required by SERF COSs, the shortest required sampling rates are given. In Table 5.I "IP" stands for interplanetary, "SHGs" stands for spectroheliograms, and the Δt intervals given are the approximate times required to complete an SHG of a region of roughly 5 x 5 arc min. The Δt intervals are based on the assumption that the highest possible resolution will be used.

TABLE 5.I

DATA FOR COLLABORATIVE OBSERVING SEQUENCES

Column 1: The kind of flare-specific observation SERF calls for in the Collaborative Observing Sequences. "IP" stands for interplanetary and "SHGs" for spectroheliograms.
Column 2: Time interval in seconds (Δt) between successive observations. In almost all cases Δt represents the limit set by available instrumentation. The table gives the shortest sampling rate for those experiments capable of recording data much more rapidly than required by SERF cooperative observations.

γ-ray	spectra, flux	10,1
X-ray (E>10 keV)	spectra	10^{-3}
	SHGs	1
X-ray (E<10 keV)	spectra	10
	SHGs	10^2
	Doppler shifts	10^2
X-ray	polarization	10
EUV (100 - 3000 Å)	spectra	10
	flux	1
	Dopplergrams	10
UV (1000 - 3000 Å)	spectra	10^2
	SHGs	10^2
	magnetic fields	10^3
	Dopplergrams	10^3
Optical (3000 - 11000 Å)	spectra	10^2
	SHGs	10
	filtergrams (disk, corona)	10
	magnetic fields	10^3
	Dopplergrams	10^3
	photoheliograms (disk, corona)	$10,10^3$
	continuum polarization (disk, corona)	$10,10^2$
cm-λ radio	spectra	10^{-1}
	SHGs, polarization	10
m-λ radio	spectra	10^{-1}
	SHGs, polarization	1
Solar wind	velocity, density, magnetic field	10^2
IP electron	spectra, flux	10^2
IP ion	spectra, flux	10^2
	abundances, charge states	10^3
IP scintillations		10^4

TABLE 5.II

COLLABORATIVE OBSERVING SEQUENCES RELEVANT TO THE STUDY OF ENERGY RELEASE IN FLARES

Column 1: Observations of particular importance to each COS. Magnetograms and other synoptic data (ref. Chapter 5) are highly desirable in each COS. Column 2: Specific objectives, as outlined at the SERF Workshop and in SMM Investigators' Working Group meetings. Spatial resolution: Highest available, generally 1 - 10 arc sec. Field of view: a single active region ~ 5 x 5 arc min, or one quadrant of the solar limb, unless otherwise noted. Time resolution: See Table 5.I.

COS-001 Chromospheric Evaporation (ref. Chapters 4 and 2)

Scheduling criteria: Initiate following flare onset.

Hard X-ray spectra	identify heating agent
SHGs	locate heating agent
Soft X-ray spectra	define heated region (e.g. emission measure)
SHGs	locate ejecta
Doppler shifts	energy in ejecta
EUV spectra, flux	define heated region (e.g. emission measure)
EUV Dopplergrams	locate ejecta
UV Dopplergrams	locate ejecta
Chromospheric spectra	study ejecta sources
D_3, Hα filtergrams	locate ejecta
Dopplergrams	locate ejecta
Coronal photoheliograms	follow material through corona
cm-λ radio spectra, SHGs	define heated region (e.g. emission measure)
m-λ radio spectra	follow material through corona
SHGs, polarization	follow material through corona

COS-002 Thermalization (ref. Chapter 2)

Scheduling criteria: Initiate before or as soon as possible after flare onset.

γ-ray spectra, flux	define particle beam and target properties
Hard X-ray spectra, flux	define electron energy distribution
SHGs	locate energy release region
Soft X-ray spectra, flux	sample electron temperature, get emission measures
SHGs	locate energy release region
X-ray polarization	seek confirmation of electron beam
EUV spectra, flux	compare fluctuations with NT emissions
UV spectra	compare fluctuations with NT emissions
Optical spectra	seek evidence of electric fields
D_3, Hα filtergrams	compare fluctuations with NT emissions
photoheliograms	white-light flare search
continuum polarization	synchrotron emission test
cm-λ radio SHGs, polarization	locate electron beams
m-λ radio SHGs, polarization	locate electron beams

TABLE 5.II (continued)

COS-003 Nature of Electron Acceleration (ref. Chapter 3)

Scheduling criteria: Initiate upon reasonable probability of flare occurrence.

γ-ray spectra, flux	infer beam and target properties
Hard X-ray spectra, flux	infer beam and target properties
SHGs	find acceleration region size and location
Soft X-ray spectra	sample electron temperature
SHGs	follow spread of energization
X-ray polarization	search for electron beam effects
UV polarization	search for electron beam effects
Hα filtergrams	locate flare kernels, other phenomena associated with electron beam evidence, e.g., Type III bursts
Magnetograms	show field structure and changes
Coronal photoheliograms	define Type III burst trajectories
cm-λ radio spectra, flux	measure NT source brightness temperature
SHGs polarization	locate acceleration region
m-λ radio spectra	follow accelerated beam
SHGs, polarization	seek second-stage acceleration region
IP electron spectra, flux	define particle population

COS-005 Ejecta (ref. Chapter 4)

Scheduling criteria: Initiate with active prominence at $R/R_{\odot} > 0.7$

Hard X-ray SHGs	burst location re. ejecta position
Soft X-ray SHGs	locate heated ejecta
Doppler shifts	infer kinetic energy of hot ejecta
UV SHGs	define mass as a function of temperature
Dopplergrams	infer kinetic energy and trajectories
Optical spectra	infer sources and sinks of kinetic energy
5303 Å, Hα, D_3 filtergrams (limb)	infer kinetic energy and trace material through low corona
Off-band Hα filtergrams (full disk)	search for Moreton waves
Dopplergrams (Hα)	infer sources and sinks of kinetic energy
Coronal photoheliograms	follow mass ejection through corona
Continuum polarization (corona)	determine shape of coronal transients
Magnetograms	infer magnetic field in prominence
m-λ radio spectra	follow shock through corona
SHGs, polarization	infer magnetic field and location of shock
Solar wind velocity, density, magnetic field	infer mass and energy of ejecta
IP ion abundances, charge states	infer conditions in source region
IP scintillations	infer size, field and velocity of IP disturbance

TABLE 5.II (continued)

COS-006 Flare Energy Budget

Scheduling criteria: A large flare-prone active region is required. Weather must be clear at an adequate number of ground-based observatories. Interplanetary probes must be on alert.

Very complete observations are required to specify the total energy output, especially in the optical spectrum and in interplanetary space. Special coordination will be required at least on some occasions when this COS is carried out, since an energy measurement in every waveband and for each form of ejection is required. In addition, magnetograms before and after the event are required for estimates of the available energy. While SMM is admirably suited to obtain the total energy of the hotter and energetic plasma, it does not have the diagnostic capability to derive either the total mass or energy flux of the lower temperature component. An intensive effort at ground-based observatories is required to specify the total energy.

COS-008 Implusive Phase (ref. Chapters 3 and 2)

For the study of impulsive phase questions the SMM investigators have defined a series of JOS's for which the collaborative observations are essentially the same as those for COS-003, Nature of Electron Acceleration.

COS-009 Location of Energy Release Sites (ref. Chapter 2)

Distinctions between this COS and COS-002, Thermalization, have not yet emerged. Basic observation sequences are the same as for COS-002.

COS-015 Flare Precursor (ref. Chapter 4)

Scheduling criteria: Initiate on reasonable probability of flare occurrence, esp. when many ground-based observatories are clear (ref. Flare Build-Up Study).

Soft X-ray SHGs	search for preflare heating
UV SHGs	search for preflare heating
Dopplergrams	search for preflare heating
Optical SHGs (D_3, 10830 Å)	preflare motions, absorption
Hα filtergrams	preflare motions, absorption
Coronal emission-line filtergrams	preflare coronal motions
Magnetograms	emerging flux; other field changes
Dopplergrams	photospheric shear; filament activation
Photoheliograms (disk)	sunspot changes
Photoheliograms (corona)	look for forerunners
cm-λ radio SHGs	search for preflare heating
m-λ radio spectra	record preflare bursts
SHGs	locate preflare bursts

TABLE 5.II (concluded)

COS-018 Flare Decay (FBS objective)

Scheduling criteria: Initiate following flare maximum. Continue intermittently for several days following large flares.

Soft X-ray spectra	define emission-measure changes
SHGs	define morphology of cooling regions
Doppler shifts	seek hot component of cooling loops
EUV spectra	define emission-measure changes
Dopplergrams	identify precipitating material
UV spectra	examine line wings for evidence of asymmetries induced by non-thermal particles
UV SHGs	structure of cooling region
Optical spectra	search for electric field and energetic particle effects
Hα, 5303 Å filtergrams	morphology vs time
Magnetograms	magnetic field relaxation
Disk photoheliograms	sunspot changes
Coronal photoheliograms	streamer reformation; coronal transients
cm-λ radio spectra	define emission-measure changes
Solar wind velocity, density, magnetic field	decay of flare effects on IP medium
IP electron spectra, flux	particle acceleration or trapping with leakage in decay phase
IP ion spectra, flux	(same as above)
IP scintillations	persistence of flare effects

COS-019 Flare Morphology

Scheduling criteria: Initiate on regions producing frequent flares.

This COS is a sequence of pre-flare, flare onset and flare decay COSs. See COS-015, Flare Precursor; COS-002, Thermalization; and COS-018, Flare Decay.

COS-020 Ion Acceleration (ref. Chapter 3)

Scheduling criteria: Initiate on reasonable probability of flare occurrence.

γ-ray spectra, flux	seek evidence of heavy nuclei enrichment
Hard X-ray spectra, flux	provide electron temperature and energy data
Soft X-ray spectra	yield ion and electron temperatures
Soft X-ray SHGs	provide flare morphology
X-ray polarization	seek evidence for particle beams
UV spectra (Lyα)	proton beam effects in line profile
UV SHGs	provide flare morphology
Optical spectra	search for deuterium lines
magnetograms	magnetic gradients
Photoheliograms (disk)	white-light flare search
m-λ radio spectra	presence of shocks in corona
SHGs, polarization	shape of coronal shocks; magnetic fields
IP ion spectra, flux	infer interaction with ambient medium, total energy
abundances	infer interaction mode with ambient medium
charge states	infer electron temperature in acceleration region
Solar wind data	separate propagation effects from acceleration mechanism
Neutron-monitor data	define deka-GeV particle population

II. SMM Joint Observing Sequences

Observations with the SMM instruments will be made in Joint Observing Sequences (JOSs) that are numbered in the same way as the SSOs and COSs. Each JOS has many variations. A complete list of instrument modes for all JOSs would double the size of this report and so it is not reproduced; however, the JOSs relevant to SERF are compatible with the observing sequences in Table 5.II and, in fact, this table is based in part on the JOSs available in May 1979.

In order to indicate the general nature of the observations of which SMM is capable, we reproduce below summaries of the SMM instrument characteristics that G. Withbroe, JOS coordinator for SMM, kindly provided.

(1) Gamma Ray Experiment (GRE)
Spectrograms 0.3 - 17 MeV every 16s (7% resolution at 0.6 MeV).
Photometry in 100 - 300 keV band every 64 ms and 300 - 500 keV band every 1s.
Also 10 - 160 MeV gamma rays in 4 channels every 2s, 10 - 160 MeV neutrons every 2s, and 10 - 160 keV X-rays in 4 channels every 1s.
Whole-Sun resolution.
Single-point sampling time = 0.064s.

(2) Hard X-Ray Burst Spectrometer (HXRBS)
Spectrograms in 16 energy channels every 100 ms.
Photometry (flux integrated over all energies) to 1 ms resolution.
Triggerable memory freezes previous 120-s and succeeding 180-s data (at 10 ms resolution). Constant count or time bins.
Whole-Sun resolution; FOV = ±45°.
20 - 300 keV; 30% resolution at 100 keV.
Single-point sampling time = 0.001s.

(3) Hard X-ray Imaging Spectrometer (HXIS)
6 spectroheliograms of an area of the Sun in 6 energy channels; various channels may be added together.
Provides S/C flare alarm (position and intensity) after 2s.
At 8 arc sec resolution FOV = 2.8 x 2.8 arc min and at 32 arc sec resolution FOV = 6.4 x 6.4 arc min.
3.5 - 30 keV; 18% resolution at 6 keV (mini-proportional counters).
Single-point sampling time = 0.125s.

(4) X-Ray Polychromator (XRP) - Flat Crystal Spectrometer (FCS)
7 spectroheliograms in fixed wavelengths of a rastered area, e.g., "Home Position" (O VIII He-like ions) for T_{ion}.
7 spectroheliograms in flux from "Integral Scans" across short wavelength bands.
7 short spectrograms/Dopplergrams of a point, e.g., "O VII Components" for N_e.
Can locate bright points.
10 x 10 arc sec resolution; FOV ≤ 7 x 7 arc min.
1.4 - 22.4 Å; 10^3 to 10^4 resolving power.
Single-point sampling time = 0.25s.

(5) X-Ray Polychromator (XRP) - Bent Crystal Spectrometer (BCS)
Spectrograms of HXIS region, especially in Fe XXV, Fe XXVI, Ca XIX, and Fe Kα lines with 8 detectors.
Recirculating queue memory triggerable to store previous 45s of data.
6 x 6 arc min resolution and FOV.
1.769 - 3.231 Å; 5 x 10^3 resolving power.
Single-point sampling time = 0.064s.

(6) Ultraviolet Spectrometer/Polarimeter (UVSP)
4 spectroheliograms of a rastered area in any of several sets of lines.
2 Dopplergram rasters produced by slit pairs on 2 different lines.
4 spectrograms (line profiles) across short spectral bands.
2 magnetograms (or polargrams) of a rastered area using waveplates on a pair of lines.
Coronal spectroheliograms in Lyα to $R/R_\odot$ = 10.
Can locate bright points.
S/C pointing = ±2 arc min
1 x 1 arc sec resolution; FOV ≤ 4 x 4 arc min.
1100 - 3000 Å; 0.01 Å resolution.
Magnetic field noise level ∿ 50 G.
Velocity noise level ∿ 60 km/s.
Single-point sampling time = 0.016s (one detector operating).

(7) Coronograph/Polarimeter (C/P)
Filtergrams of the corona; in white light, coronal emission line FeXIV and Hα polarization techniques for plane of the sky, magnetic field direction, and resonance scattering information.
Dopplergrams from tuneable Fe XIV filter.
6.4 arc sec; FOV ≤ 6 x 6 $R_\odot$ (at 8 limb positions).
4448 - 6585 Å (7 passbands).
Single-point sampling time = 60s.

(8) Active Cavity Radiometer Irradiance Monitor (ACRIM)
Total solar irradiance measurements from three dual conical cavity radiometers.
FOV = 5°.
UV to IR spectral coverage.
Absolute accuracy ±0.1% (S.I.); precision ±0.02%.
Single-point sampling time = 2s.

III. Synoptic Observations

Most of the observations to be made during the SMY will provide high time and spatial resolution measurements that will comprise the primary set of data for attacking the problems of energy release in flares. As a complement to these intensive data sets, selected synoptic observations, made daily over the period of the SMY and covering the entire Sun, are essential to providing a comprehensive survey of solar flare activity. The following specific problems require synoptic data:

(1) Establishment of trends of solar activity. Initiation of COSs depends on a knowledge of the recent trend of development of active regions and the rates of flare occurrence. Synoptic data, such as full-disk and large-scale Hα and white-light images, if made available on a rapid time scale will provide a sound basis for selection of SMY target regions. Magnetograms are also especially important for this purpose.

(2) Provision of a continuous record of the development of each active region studied. By the time of solar maximum, active regions may persist for several months, as magnetic field structures decay and are replaced by new fields in the same general location. Synoptic observations will provide the record necessary to follow the evolution and topology of the magnetic field and emission sources in target regions.

(3) Isolation of sources of particles observed by interplanetary satellites. Major flares often occur within hours in widely separated active regions. A knowledge of all possible sources of energetic particles at any given time is necessary before initiating studies that relate interplanetary particle fluxes and spectra to specific flare sources.

(4) Study of important events in regions not selected as SMY targets. In particular, great particle events may occur in active regions other than those being observed by the high spatial resolution instruments participating in the SMY. Analysis of the gamma ray and hard x-ray observations will then depend on the availability of lower resolution but temporally complete synoptic observations.

Primary sources of synoptic data include the following:

(1) The U.S. Air Force Solar Observing Optical Network (SOON). The SOON telescopes produce regional and whole-Sun Hα and continuum images, providing a consistent and nearly continuous record of almost all flares and sunspot activity. The digital SOON flare histograms are the most precise way of differentiating between flares that occur almost simultaneously in different active regions. Whole-Sun radiation measurements of soft x-rays, hard x-rays, gamma rays, and radio emission can be differentiated and attributed to the correct flare sources by using these regional histograms. Recognizing the unique capabilities of the Solar Observing Optical Network, we strongly recommend the timely dissemination of the SOON data to the scientific community and the permanent archival of these data by a World Data Center.

(2) The U.S. Air Force Radio Solar Telescope Network (RSTN). The RSTN provides the only source of continuous whole-Sun radio flux measurements in microwave and meter wavelengths. Thus, these measurements are capable of showing probable times of high energy particle acceleration in all solar flares. We recommend that (a) routine 1-s data be rapidly disseminated to the scientific community in digital form and archived by a World Data Center and that (b) for designated periods of detailed interdisciplinary solar flare and particle event studies, solar radio data acquisition rates be increased to give significantly higher time resolution.

(3) The NOAA GOES Satellite Whole-Sun X-Ray Monitor. The GOES X-ray measurements provide the only source of continuous soft X-ray fluxes, and since it is a whole-Sun instrument, it is the only comprehensive record of X-ray emission for all solar flares. GOES data should continue to be archived through established procedures.

IV. Coronal Hole Observations

Reconstruction of energetic particle spectra at the Sun, based on observations made at distances greater than several solar radii, can be improved by a knowledge of the structure of the solar wind. Sun-to-Earth propagation and interplanetary acceleration can both be better described with knowledge of the location of high-speed solar wind streams. Coronal hole maps that define the probable sources of high-speed streams and *in situ* measurements of solar wind plasma characteristics are essential for this reconstruction. Access to the following observations, through established data centers, should be facilitated during the SMY:

(1) daily whole-Sun, moderate-resolution soft X-ray heliograms, e.g., those from the U.S. Air Force satellite P78-1;

(2) daily He 10830 full-disk solar images, e.g., those made at Kitt Peak National Observatory and

(3) solar wind plasma parameters of which the primary sources are ISEE-3, HELIOS, and Pioneer-Venus.

V. In-Situ Plasma and Interplanetary Magnetic Field Observations

Recognizing the value of solar plasma and interplanetary magnetic field measurements, particularly in the Earth-Sun region, in defining the spatial extent and shape of solar-induced interplanetary disturbances, we recommend rapid dissemination of "quick look" plasma and field measurements from satellites such as ISEE-3 and the Venus orbiter, and the timely reduction and deposit of these data into the World Data Centers.

Moreover, recognizing that the interplanetary scintillation (IPS) technique offers a three-dimensional probe of the interplanetary medium, we recommend that solar wind and interplanetary disturbance measurements by the IPS technique be routinely performed during the SMY and that they include specific emphasis on periods of special studies as identified by FBS, SERF, and STIP. We further encourage the rapid dissemination of these data, particularly when these routine measurements indicate a current disturbance in the interplanetary medium.

VI. A Final Comment

The advanced solar instrumentation that will be used during the SMY is at a point where resolution is not a strong function of wavelength. Almost all Sun-viewing instruments except meter-wave radio telescopes and gamma ray detectors can resolve 1 - 10 arc sec. This is an important point to remember, since it facilitates intercomparison of observations, but if the fundamental physical processes in flares take place on a scale of less than 1 arc sec, progress in the SERF subprogram will be limited and we must await the arrival of the next generation of instruments. Nevertheless, we certainly do not wish to end on a pessimistic note. The instruments available now are an order of magnitude better than those available during the last solar maximum. These instruments will answer most of the questions raised in Chapters 2 - 4, and therefore our understanding of flares and flare-associated phenomena will be much greater.

APPENDIX A

SERF ORGANIZATION AND OPERATIONS

David M. Rust
American Science and Engineering, Inc.
Cambridge, Massachusetts U.S.A.

I. Introduction

The SERF is one of three subprograms of the SMY. The other two subprograms are the Flare Buildup Study (FBS) and the Study of Traveling Interplanetary Phenomena (STIP). Each of these subprograms is guided by an organizing committee headed by the individuals listed below.

FBS -- Z. Sveštka, Space Research Laboratory, Beneluxlaan 21, 3527 HS Utrecht, The Netherlands.

SERF -- D. Rust, American Science and Engineering, Inc., 955 Massachusetts Ave., Cambridge, MA 02139, U.S.A.

STIP -- M. Dryer, Space Environment Laboratory, NOAA/ERL, Boulder, CO 80303, U.S.A.

The actions of the three subprograms are coordinated and integrated by a Steering Committee appointed by SCOSTEP, COSPAR, IAU, IUPAP and IUGG with C. de Jager (Chairman), Z. Sveštka (deputy-Chairman), P. Simon (Secretary): DASOP, Observatoire, 92190 Meudon, France, and members M. Dryer, M. Kundu, D. Rust, E.J. Smith, V.E. Stepanov, G. Wibberenz, and R. MacQueen.

II. Operations During the SMY

Based on the COSs defined in Chapter 5, SERF "ACTION" intervals will be declared as special opportunities for observations arise throughout the SMY. The first SERF ACTIONS will be scheduled during a special ALERT period shortly after the launch of the SMM satellite. This period is likely to be 1 - 22 November 1979. All subprograms of the SMY will be involved. The goal of this first ALERT is to obtain some simultaneous ground and satellite data as early as possible in the SMM flight. Thus, should any satellite experiment fail in the first month of operation at least the best advantage will have been taken of the period of successful operation. To this end, the SERF program will follow SMM operations rather closely during this initial interval.

During the rest of the SMY, it appears that the following two modes of collaboration will be most effective:

(1) "Á la carte" - observing efforts built around Specific Scientific Objectives (SSOs) and particular observing opportunities. This is basically to say that the whole of the SMY is an ALERT interval for SERF, except for May and June 1980, when the Flare Buildup Study will be the main subject of the SMY. STIP will assign ALERT intervals to coincide with SERF and FBS ALERTS when appropriate.

Observing efforts called "ACTIONS", of 1 to 3 days, will be triggered by good prospects for collaborative observations. Although notice of the ACTION (including coordinates of the activity center) will be distributed by Telex and telephone to all interested participants, it is understood that not everyone will be able to react to every call for observations. We hope, in the course of a year's work, however, to obtain simultaneous and relatively complete coverage of several dozen flares for most, if not all, of the specific scientific objectives of the SERF program. ACTIONS may be called at the average rate of 2 or 3 per month. Advance notice for ACTIONS will vary from 1 to 7 days.

(2) "Menu conseillé" - one or more pre-established intervals for especially intense efforts. This is the same as an ALERT-ACTION interval in the FBS program, and we hope that all participants will schedule their telescopes, maintenance programs, vacations, etc., in order to ensure that a set of observations as complete as possible will be obtained during this period. The candidate time for a special SERF ALERT is 15 September - 15 October 1980. During this month, or during another period to be chosen at the IAU meeting in Montreal, the ACTION intervals should yield especially complete coverage.

III. Newletter and Communications

The SMY Newsletter will be the principal means of informaing SERF participants of Collaborative Observing Sequences and Joint Observing Sequences, of planned observations and special intervals, and of meetings and recent observational results. The newsletter will be mailed monthly to all interested parties. In May 1979 there were about 800 subscribers to the newsletter. News of past and future observations relevant to the scientific objectives of the SMY and requests for newsletters should be sent to

Mr. J.H. Allen
Central Information Exchange Office
World Data Center A for Solar-Terrestrial Physics
NOAA, D64
Boulder, Colorado 80303 U.S.A.

The newsletter is composed with a computerized text editor, and all material is stored on computer files. By using a system of key words and dates, all references to observations of a given flare or to a given scientific objective can be recalled and summarized. A suitable code for the scientific programs, kinds of observations, and observatory names will be developed from codes already in use at World Data Center A for Solar-Terrestrial Physics and at the SMM Investigator Working Group meetings.

The purpose of the newsletter is only to supplement such volatile communications as telephone and Telex, which will be used heavily before, during and after ACTION intervals. Before an ACTION, participants should Telex or call the SERF coordination center about observing conditions, predictions of activity, activity in progress, and recommended ACTION intervals. Before an ACTION is called, the coordinator will consult with participating observatories, according to the scientific objective of the contemplated ACTION, and especially with the following centers:

(1) SibIZMIR (via the Sun-Earth Council)
(2) NOAA and the Solar Observing Optical Network
(3) Solar Maximum Mission Operations
(4) Meudon Observatory

We emphasize, however, that SERF ACTION intervals in the "á la carte" mode can be built around requests for assistance from any source, including experimenters on satellites such as ISEE-3 or Interkosmos and theoreticians who desire observational tests of hypotheses about flare energy release. For practical reasons, SERF will not normally be able to help with collaborations on problems not concerned with solar flares.

After ACTIONS, participating observatories will be asked to communicate a summary of observations obtained. This can be done in condensed formats, to be developed, that will describe the instrument, the observing mode, and the intervals successfully covered during the ACTION. Codes for this purpose will be included in the catalog of participants' equipment, interests, and research programs to be issued by the Meudon Observatory for the Flare Buildup Study and for SERF. Most prospective participants have already responded to questionnaires circulated by Sveštka, Zirin, or Rust. Additional data will be requested in future mailings to make it easy for us to communicate with you and to understand what you want from the Study of Energy Release in Flares.

IV. Data Exchange and Collaborative Data Analysis

In contrast to the FBS plan and because of the anticipated volume of data, SERF presently does not plan to be directly involved in data analysis except to indicate to the participants those data sets that seem applicable to the study of energy release in flares. Periodically, throughout the SMY, the SERF Organizing Committee and the SMY Steering Committee will review progress made toward each Specific Scientific Objective. Periods of successful observations will be identified. Through personal contacts and via the newsletter information on the flares most successfully observed during ACTIONS will be publicized. We also hope to facilitate data exchanges through meetings sponsored by international bodies such as COSPAR and SCOSTEP. We recommend that summaries of data obtained for outstandingly successful ACTIONS be published by World Data Center A for Solar-Terrestrial Physics under their series of UAG Reports. Then, workshops will be organized around the scientific objectives. The participants in the workshops will establish the level of collaborative data analysis. It is presumed, however, that all participants in the SMY will be willing to share data obtained during ACTIONS with others via collaborative analyses and scientist-to-scientist or institution-to-institution exchanges.

APPENDIX B

SCIENTIFIC PROBLEMS OF THE SMY SERF PROGRAM

A.T. Altyntsev, V.G. Banin, G.V. Kuklin, V.P. Nefedjev
A.V. Stepanov, V.E. Stepanov, and V.M. Tomozov

USSR Academy of Sciences
Siberian Branch
Siberian Institute of Terrestrial Magnetism, Ionosphere and Radio Wave Propagation
Irkutsk, USSR

We propose to concentrate our attention on the two problems which have bearing not only on the SERF problem but also on the FBS problem.

Problem I. Investigation of particle-heating and acceleration processes in the flare region.

Problem II. Determination of the flare triggers.

1. Let us consider problem I in more detail.

According to current knowledge, the solar flare is associated with the formation, interruption and turbulization of the current sheet. Plasma heating and particle acceleration are accompanied by the excitation of ion-acoustic(s) and Langmuir (ℓ) turbulence at a comparatively high intensity: $W_\ell \lesssim W_s \sim 0.1\ nk T_e$, where W is the wave energy density. Such a high level of ion-acoustic turbulence results also from laboratory experiments on current sheets.

Fast particles are assumed to contain about 10 percent of the flare energy and to be accelerated by plasma turbulence. Therefore it is essential to acquire observational data which permit the determination not only of the plasma heating rate and of the efficiency of particle acceleration but also of the plasma turbulence level in the acceleration region. These data can be inferred from radio, X-ray and optical observations of flares.

1.1 Radio emission. Plasma heating in the flare region and the existence of plasma turbulence both will cause radio emission. Theoretically the electron density in the current sheet $n \sim 10^{12} - 10^{14}$ cm^{-3}, i.e., the radio emission frequency in the transmittance region ($\omega \geq \omega_{pe}$) corresponds to the millimeter and centimeter range. Knowing from observations the characteristics of the current-sheet radio emission and having available an appropriate theory one can create the flare (current sheet?) diagnostics from radio emission.

The current-sheet radio emission theory is only in its first stages. Kuznetsov and Syrovatskii (1977) made an estimate of the level of the current sheet bremsstrahlung emission. Zheleznyakov and Zlotnik (1979) calculated the thermal cyclotron emission of the Harris sheet (1962) - a classical model of the current sheet. It resembles a series of relatively narrow spectral lines with a simple ratio of their frequencies. The formation of individual lines is explained by cyclotron emission only on the periphery of the current sheet, where the magnetic field has quasi-homogeneous features. Therefore, the frequencies of the lines correspond to electron cyclotron harmonics in this magnetic field. Detection of cyclotron harmonics at the background of a slowly varying component is possible for sufficiently hot current sheets with a temperature of $10^7 - 10^8$ K. Using these lines, diagnostics of the magnetic fields and kinetic temperature in the current sheet is possible.

But the chief problem of the current sheet radio emission theory is the problem of radio emission of the ion-acoustic(s) turbulence of a comparatively high level: $W_s \sim 0.1\ nk T_e$. The point is that if together with s-waves also ℓ-waves of approximately the same level exist, the problem then reduces to calculation of the plasma electromagnetic wave conversion coefficients under conditions of strong turbulence. However, the statement that in the flare $W_\ell \sim (10^{-2} - 1) W_s$ cannot be regarded as substantiated. The linear mechanism of Langmuir wave generation by the current is not realized. With the current speed $u > v_{te}$, Buneman instability with a real part of the frequency $R_e\omega \sim (m_e/m_i)^{1/3} \omega_{pe}$ arises. If u exceeds the sound velocity ($u > c_s$), ion-acoustic waves are then generated. The non-isothermicity of plasma ($T_e > T_i$) is provided either from the preliminary electron heating in the Buneman stage of current instability or by Joule heating. Generation of Langmuir waves of a sufficiently high energy density level

NOTE: Some minor, stylistic changes have been made from the text supplied by the authors.

by "runaway" electrons (Kaplan et al., 1974) is problematic since it is difficult to estimate the density of fast particles. Consequently, only ion-acoustic turbulence is fairly substantiated in the current sheet.

Ion-acoustic waves have a frequency much less than the electron plasma frequency ω_{pe}. Therefore for the conversion of s-waves to high-frequency ($\omega \geq \omega_{pe}$) Langmuir and electromagnetic waves, for example, by scattering on particles (inverse Compton-effect), a sufficient number of superthermal particles is needed.

The processes of particle acceleration, plasma heating and generation of plasma turbulence in the flare seem to be interconnected. Consequently, using the radio emission characteristics one may in principle determine not only the levels of the s- and ℓ-turbulence but also get information regarding the spectrum of particles directly in the acceleration region. For this purpose, in our opinion, observations of flare radio emission at millimeter, centimeter and decimeter wavelengths are needed. In addition, for the current sheet diagnostics during the flash-phase of the flare measurements of polarization are important. In this connection, let us mention the work of Nefedjev (1979), in which the growth of the linear polarization at $\lambda = 3.2$ cm prior to the flash phase of the flare is linked with the presence in the corona of a sheet about 10^2 cm thick and with an electron density of $n \sim 10^{12}$ cm^{-3}.

Linear polarization of radio emission, as is well known (Zheleznyakov, 1970), arises by radio wave propagation through a region of the quasi-transversal magnetic field. If the waves then get into a region where the geometrical optics approach is violated, polarization can remain also during further propagation. Thus linear polarization of a microwave burst can be accounted for by the presence of a large density gradient in or just above the burst source. According to simple estimates performed on the basis of the bremsstrahlung mechanism, linearly polarized emission originating from a dense sheet should be observed in a narrow wavelength range ($\Delta\lambda \sim 0.5$ cm) at wavelengths between 2 cm and 6 cm.

Note that a very promising diagnostic of current sheets is the method of the sheet "transillumination" by radio emission from a local source. The current sheet formation process must be accompanied by a decrease in emission of the local source (absorption burst) located below the current sheet.

1.2 X-Ray Emission. Measurements of X-ray emission from the flare should be performed simultaneously with optical and radio observations. These data are essential for the determination of fast particle spectra. Particularly useful are observations of the hard X-ray emission polarization of the flare. These allow one to select among different theoretical models which explain the nature of hard X-ray bursts: deceleration of electron beams in dense layers of the solar atmosphere (thick and thin targets), Thompson scattering of X-ray quanta in the solar atmosphere (Beigman, 1974), or the multitemperature model (Colgate, 1978).

Somov (FIAN) suggested a program "Hard X-rays and brightening of the lower layers of the Sun's atmosphere from flares" (and for a flare on the limb - investigation of coronal condensations) with the aim to compare the X-ray image with the supposed illumination of the lower atmospheric layers by flare X-rays and to verify the reality of the low chromosphere and high photosphere heating by flare short-wave radiation at $\lambda < 912$ Å. Three mechanisms of energy transfer from the source above the chromosphere (magnetic reconnection region) into the low-temperature (optical) part of a chromospheric flare are widely discussed and investigated. These are heat conduction, energetic particles, and generally speaking, gasdynamic flows. However, as was shown by Somov (1975), the radiation from low-lying X-ray structures can make an important contribution to the heating of the under-lying Hα (and other line) flare structures. X-ray flare radiation may also cause diffuse optical haloes around the flare, as a whole, or around flare kernels. The X-ray heating efficiency depends essentially on the X-ray source geometry.

The HXIS experiment will be the first and only one to allow a possible illumination of the low solar atmosphere by flare X-rays to be tested. The whole necessary calculation has been published by Somov (1975, 1976) (see also Somov and Syrovatskii, 1977). The HXIS data will offer the possibility of checking the X-ray heating theory both in principle and quantitatively. Data to be used:

1. The X-ray images to be obtained with the HXIS instrument at different spectral channels from 3.5 to 30 keV with spatial resolution 8" x 8". (It would be very useful for comparison to have EUV-images of the same flare with $\lambda > 912$ Å because this non-ionizing radiation can also make a contribution to heating the solar atmosphere at large depths near the temperature minimum (Somov and Syrovatskii, 1977).

2. Optical images of flares in lines and continuum formed at low heights ($Z \lesssim 500$ km in the model of Vernazza et al. (1973) for X-ray energies $E_x \geq 3.5$ keV) above the photosphere. To compare optical and X-ray images there is no need for high spatial resolution. It will be enough to compare the X-ray images with optical images having the same (8" x 8") resolution. Another reason that high spatial resolution is not required is that radiative heating (unlike heat and particle fluxes traveling along magnetic tubes) produces diffuse flare images. The program can be implemented jointly with the Space Research Laboratory of the Astronomical Institute, Utrecht, The Netherlands.

1.3 Optical. To solve the problem of the role of plasma turbulence in the flare mechanism it is advisable to obtain spectrograms of hydrogen lines of the Balmer series (Hα, Hβ, Hγ ... to H_7, and probably of the HeI 3705 and 4026 Å lines) with good time resolution (as much as 5 s) with coverage of all phases of the flare. Analysis of line profiles with due regard for the Stark-effect will permit determination of the electron density and the level of plasma turbulence.

Traditional mechanisms determining the behavior of flare hydrogen lines are the Doppler effect due to unresolved mass motions and the Stark-effect associated with the electric fields of thermal electrons and ions. However, if plasma turbulence is excited in the solar flare and the amplitude of electric field oscillations exceeds the value $E_0 = 2.6\, e\, n^{2/5}$ (Holtsmark field), then a dominating role will be played by the Stark effect in turbulent electric fields. This possibility was first indicated by Tomozov (1973), Tsytovich (1973), Dolginov and Yakovlev (1973).

The Stark effect theory in turbulent electric fields stems from a separate consideration of the effect on the emitting atom by the low-frequency and high-frequency components of the turbulent electric field (HF-oscillations of the field are produced by Langmuir turbulence, and the LF-fields by the ion-acoustic one). According to Ox's estimates (1978), HF-noise in the flare plasma has a stochastic character and appearance of nonadiabatic effects should be expected. These arise when $\omega_F = 3\, nea_0 F/2\hbar \approx \omega_{pe}$ (a_0 is the Bohr radius, R is the amplitude of the quasi-static field) and are characterized by the appearance of gaps on the spectral line profile at frequencies:

$$\omega_\alpha = [\,(n_1 - n_2)_\alpha - (n_\beta/n_\alpha)\,(n_1 - n_2)_\beta\,]\,\omega_{pe},$$

$$\omega_\beta = [\,(n_\alpha/n_\beta)\,(n_1 - n_2)_\alpha - (n_1 - n_2)_\beta\,]\,\omega_{pe},$$

which correspond to the distances λ_α and λ_β from the line center λ_0

$$\lambda_\alpha = (\omega_\alpha/\omega_{pe})\lambda_p, \quad \lambda_\beta = (\omega_\beta/\omega_{pe})\lambda_p, \quad \lambda_p = \omega_{pe}\lambda_0^2\, 2\pi c\,.$$

Here α and β are the initial and final states of the atom, n_1 and n_2 are the parabolic quantum numbers. Using the gap half-width determined from the line profile, one can calculate the amplitude of Langmuir noise (Zhuzhunashvili and Ox, 1977):

$$E\ (\mathrm{kV/cm}) = \frac{7.6 \times 10^9\ \Delta\lambda_{1/2}}{[\,n^2 - (n_1 - n_2)^2 - m^2 - 1\,]_\gamma^{1/2}\left|n_\alpha (n_1 - n_2)_\alpha - n_\beta (n_1 - n_\beta)_\beta\right|\lambda_0^2}$$

Here $\gamma = \alpha$, β and λ_0 and $\Delta\lambda_{1/2}$ are expressed in angstroms, m is the parabolic quantum number.

Banin et al. (1978) have investigated the profiles of the central and middle parts of the Hα and Hβ lines in the spectrum of the 26 September 1963 large flare. Using the locations of typical gaps, they determined the electron density in the Hα, Hβ emitting region to be 3×10^{13} cm^{-3}, whereas the corresponding level of Langmuir turbulence was $W_\ell / nk\,T_e$ is too large. Its real value seems to be much less than that obtained since the electron temperature in the flare region generally exceeds the ion temperature.

Unlike Langmuir turbulence, ion-acoustic turbulence determines the character of the line profile as a whole by changing the intensity decrease law in the line wings. Ox's estimates (1978) also yield a large value for the ion-acoustic turbulence level:

$$W_s \sim 0.1\, nk\, T_e.$$

The processing of spectrograms is generally complicated by various photometric errors. Furthermore, when flares on the Sun's disk are observed the determination of the flare emission is complicated by the effect of spectral lines in the photosphere. To eliminate the effect of the Fraunhofer spectrum of the "substrate" it is necessary to obtain spectra of flares at the limb of the Sun. The quantity W_ℓ determined independently using the Stark effect can be compared with the value W_ℓ obtained from radio data.

1.4 Laboratory experiment. Laboratory experiments serve as a check of the correctness of the theory of particle heating and acceleration in current sheets. A part of the results concerning annihilation of opposite magnetic fields has already been achieved at SibIZMIR and FIAN. The neutral current sheet that forms in the theta-pinch device has been selected as an objective of investigations. The description of the device is given by Altyntsev et al. (1973). To study the tearing-instability, a sheet with a width one order more than its thickness is formed. The main parameters are: Magnetic field $B \lesssim 10^3$ G, density $n \simeq 10^{12} - 10^{14}$ cm^{-3}.

With the aim to use the results of the experiment for the interpretation of solar flares, the parameters of the process as a function of B and n are investigated, which provides a possibility in many cases of describing these parameters in dimensionless quantities. Assuming that the sheet under study is a fraction of the solar current sheet, when modeling one can assume the scaling parameter to be equal to unity for such results as the maximum rate of the magnetic field energy conversion into plasma energy, the current dissipation mechanism, fast electron density and rate of electron acceleration.

The first problem of the experiment which has been mainly solved so far is to study the magnetic field topology in the sheet (Altyntsev and Krasov, 1974). From the experiments it follows that the sheet thickness is $\Delta \approx 100/\omega_{pe}$.

By direct measurements of the magnetic field vector it has been shown for the first time that the evolution of the magnetic field structure in the sheet is consistent with the development of the collisionless tearing-instability. The ratio of perturbation wavelength to sheet thickness is constant and equals six. The instability stabilizes and does not lead to a catastrophic sheet interruption. The stabilization level, $B_\perp/B_{th} = 0.2 - 0.3$, where $B_\perp$ is the maximum value of the resulting transversal field component in the sheet and B_{th} is the value of magnetic field at the sheet boundary. This phenomenon was explained theoretically by Galeev and Zelenyi (1975).

The second problem is to study plasma heating and acceleration in the sheet. The experiment (Altyntsev and Krasov, 1977, 1978) has shown that the electron temperature reaches the values of 0.5 - 1 keV and is due to the attainment in the sheet of the quasi-linear stage of the ion-acoustic instability. Electron energy distributions are measured in a turbulent current sheet. Spectra characterized by γ from 0.5 to 8 have been obtained if the distribution is approximated by a power law $n(E) \propto E^{-\gamma}$ and is a function of initial conditions and recording site with respect to the sheet. The acceleration rate can be accounted for by the existence in the sheet of a superthermal Langmuir turbulence.

Applications of these results to the problem of solar flares are given in the work of Altyntsev et al. (1978). The efficiency of the process investigated is sufficient for the observed energy release rate in flares with an exclusively small total volume of current sheet fractions.

The technique developed at SibIZMIR permitted the first detection of accelerated electrons in the experiment of Frank's group (FIAN) at the interruption of the current sheet produced from the zero line of the multipole magnetic field (Altyntsev et al., 1978).

The chief trend of further experiments is to study the efficiency of annihilation with due regard for the effects of plasma compression into a sheet, conductivity, etc. Study of the generation mechanism of Langmuir oscillations and of their effect on the spectrum of accelerated electrons is being planned. The lifetime of the current sheet in the experiment was 5×10^{-7} s. This time it is intended to increase it up to 4×10^{-5} s.

1.5 Summary. Above we have mainly dealt with the processes occurring directly in the acceleration region (current sheet). To get a more comprehensive picture about the dynamics of particles and emissions in the flare it is necessary to investigate other possible mechanisms of particle acceleration and the behavior of energetic particles in solar magnetic traps.

(a) Dynamics of energetic particles and emissions in coronal magnetic traps. After a large flare, there arises a broad-band (cm-dm) radio emission from energetic particles trapped in magnetic bottles in the corona (type IV, flare continuum, etc.). The trapping of particles by magnetic bottles may be the cause of the extended duration (up to 10 - 15 hours) of the particle flux from flares. It is not excluded that energetic particles may additionally be accelerated by MHD-oscillations of the traps (betatron acceleration, Fermi mechanism, magnetic pumping).

Using X-ray and radio emissions one can determine the energetics of post-flare particles, the processes of their accumulation and escaping from traps as well get information regarding the power of fast particle sources. In this respect, of special importance and interest are observations of X-ray and radio emission pulsations (periods $0.1 - 10^2$ s) probably associated with the modulation of high-frequency radiations by a vibrating magnetic bottle (Brown and Hoyng, 1975; McLean et al., 1971). Such oscillations can arise when energetic protons with $\beta_p \gtrsim 0.1$, where $\beta_p = 4\pi n_p m_p V^2/B^2$, are injected into the magnetic trap (Meerson et al., 1978). Note that type IV radio pulsations correlate with solar proton satellite-borne observations (McLean et al., 1971).

(b) Proton acceleration in a flare. From observations it follows that energetic protons are accelerated in the solar corona. Gubchenko and Zaitsev (1977) proposed a mechanism of injectionless regular proton acceleration. This implies a repeated reflection of proton from the front of the perpendicular collisionless shock wave playing a role of a moving "mirror." It is clear that in order to study the particle acceleration due to shock waves it is necessary to know the shock wave front structure. Only shock waves propagating in the solar atmosphere across the magnetic field have been studied in sufficient detail up to now with due regard for the effect of the plasma turbulence on the front structure (Zaitsev et al., 1979). It is not excluded however that effective mechanisms of proton acceleration also exist in longitudinal and oblique shock waves. In this connection, observations of type II radio bursts made together with the recording of protons on satellites and observations at optical and X-ray wavelengths are useful. In addition, we recommend that observations of type IV bursts linked with type II radio emission be performed. The point is that shock waves can supply energetic particles into magnetic traps which are sources of type IV bursts. Using the intensity of type IV bursts or the manner of pulsations of type IV emission, one can estimate the energy of particles supplied to the trap.

Sometimes, type III bursts display an intensity modulation with a characteristic period of about 1 s (Santin, 1971). Zaitsev (1974) suggested that such bursts are generated by energetic protons rather than electrons. Generation of plasma waves by a proton beam due to induced wave scattering on the coronal plasma occurs periodically with $T \sim 1$ s. The electron beam does not lead to any modulation of plasma wave energy density. Therefore, when performing investigations of type III bursts together with optical and X-ray observations and with the recording of particles at the Earth's orbit, one will be able to get information on which types of magnetic structure in the Sun's atmosphere are associated with proton acceleration during the flare and which accelerate electrons only. Also, the bandwidth of the receiver at a frequency of 100 MHz should be not greater than 1 MHz.

1.6 To sum up, the following list of observational data needed to solve the first problem can be given:

a. Data on intensity and linear polarization of radio emission at the centimeter wavelength for diagnostics of current sheets. In particular, at 2, 3 and 5 cm wavelengths.

b. Radio emission (intensity, polarization) at decimeter and meter wavelengths to get additional information regarding spectra of particles and the plasma turbulence level in a current sheet to establish the mechanisms of proton acceleration during flares. Of special interest are observations of type II bursts and pulsations of type IV bursts (radioheliograph, spectrograph).

c. Data on X-ray emission of flares to investigate spectra of energetic particles and the possibility of solar atmosphere heating due to X-ray emission of the flare.

d. Spectrograms of H and He lines for an independent determination of the plasma wave level using the Stark effect.

2. The Problem of the Determination of the Flare Triggers.

It is not yet clear where the disturbance which initiates a flare comes from: from the lower layers of the solar atmosphere or from above. Is any external disturbance necessary for the onset of a flare at all or is it a self-exciting system? Finally, one should know the triggering mechanism, the threshold of instability leading up to a flare. Formulation of the following observational programs is advisable.

2.1 Assessment of the degree of deviation of the character of the magnetic field of the active region in the upper layers of the solar atmosphere from a potential field and interpretation of these deviations. It should be determined whether these deviations of the magnetic field from the potential field are associated with the existence of an internal current system in the magnetic structure or due to an external current system from neighboring structures (Molodenskii and Syrovatskii, 1977). The recording of magnetic fields prior to a flare, of the full vector H at the photospheric level and $H_{\parallel}$ in the chromosphere in the H-line and acquisition of solar images in UV and X-rays are indispensable here to construct a three-dimensional magnetic configuration of the active region. In addition, data on soft X-rays will permit determination of the location of the feet of loop structures of the magnetic field.

2.2 In bipolar arch-like structures, the links between the triggering mechanism and the manner of the movement of arch feet should be established (Spicer, 1977) and the reason of loops twisting found out. For this purpose, it is advisable to acquire data in UV and X-rays. By using them, one can reveal the plasma temperature distribution in the loop configuration, determine the type of plasma MHD-instability in the arch-like structure and the typical size of this instability at different stages of development of this structure.

2.3 Recording of the metastable current sheet being in the pre-flare state. This is necessary to determine the phases of the active region where the current sheet can exist and to determine the parameters of the sheet. With this purpose, in addition to the radio observations mentioned in 2.1, spectral lines at 300 - 1500 Å should be investigated. In particular, the HeI, HeII, CII, CIII, NeII, SII lines (Syrovatskii, 1977) and possibly lines at optical wavelengths whose emission may be invoked by secondary effects of the current sheet. Syrovatskii (1976) showed that prior to the thermal instability switch-on in the sheet and consequently prior to the flare process development, the current sheet can represent a thin and comparatively cold plasma formation with dimensions of 10^{10} cm x $2\ 10^{9}$ cm x 20 cm with a particle density $n = 2 \times 10^{14}$ cm^{-3} and a temperature $T \lesssim 10^{5}$ K, located in the solar corona. Such a sheet can persist for a relatively long time in a stationary state until the temperature in it exceeds a critical value (Tur and Priest, 1978).

2.4 To clear up the nature of the agents which cause sympathetic flares, radio pictures of the Sun obtained with the radiospectrograph and heliograph (Wild, 1969) at cm, dm and m wavelengths and acquisition of photoheliograms of the full disk of the Sun in the Hα-line, are needed.

2.5 During the flare process development, the program of observations with the panoramic magnetograph with indispensable control of the magnetosensitive line profile variation is required. This will allow one to establish a link between magnetic field variations and flare location.

ACKNOWLEDGMENTS

In conclusion, we express our gratitude to the members of the "Solar Plasma Physics" Workshop of SibIZMIR who took part in the discussion of the problems stated above as well as to Dr. B.V. Somov, Professor V.V. Zheleznyakov and Dr. E.Ya. Zlotnik for useful information.

APPENDIX C

ENERGY TRANSPORT AND THERMALIZATION IN SOLAR FLARES

A. Gordon Emslie
Harvard-Smithsonian Center for Astrophysics
60 Garden Street
Cambridge, Massachusetts 02138

The means by which energy, liberated by magnetic field annihilation in the primary release site, is transported and subsequently thermalized throughout the flare atmosphere provides us with a potentially important set of signatures of the physical processes responsible for, and operating within, a solar flare.

A solar flare is characterized by its thermal emission in optical and EUV wavelengths and by its non-thermal emission in microwave and X-rays [although the X-ray burst may in fact be significantly thermal (see below)]. Any model which contends to explain the solar flare phenomenon must be capable of reproducing the characteristics (intensity, spectral distribution, and polarization) of this composite radiation field.

One of the most obvious mechanisms for thermalizing energy in the lower atmosphere is thermal conduction (Sveštka 1973). In fact, it is apparent (Machado and Emslie 1979) that this is the dominant energy redistribution mechanism during the post-flash and decay phases of the flare, although the significantly long timescales associated with conductive transport (Bessey and Kuperus 1970; Craig and McClymont 1976) seem to effectively rule this out as a viable heating mechanism during the impulsive phase of the event. However, these timescales may be somewhat overestimated (Shapiro and Moore 1977; Spicer 1979), and I shall return to this point later.

Similar timescale arguments rule out convection as flash-phase transport and thermalization mechanism (Craig and McClymont 1976), although study of the full set of hydrodynamic equations (instead of the frequency assumed static energy equation) is doubtless necessary for later stages in the flare and is a very worthwhile pursuit. The original work in this area by Kostyuk and Pikel'ner (1975) is somewhat lacking in detail (in particular, no density values are presented; see Canfield et al. 1979a for more details), and further hydrodynamic modeling, including the very difficult treatment of the behavior of a pressure shock wave upon encountering the sudden density discontinuity at the transition zone, is at present is progress (McClymont and Canfield 1979). Such studies will hopefully enable us to construct reasonably accurate theoretical atmospheric structures which can then be tested against empirical structures (Machado and Linsky 1975; Machado, Emslie and Brown 1978; Lites and Cook 1979; Canfield et al. 1979a), based on observation of spectral features.

Another mechanism which undoubtedly plays an important role in the heating of the lower atmosphere, particularly in the post-impulsive phase, is irradiation by both soft X-ray and EUV flux. Modeling of soft X-ray heating was first carried out by Somov (1975) and subsequently developed (a) in steady-state and (b) including hydrodynamic terms by Henoux and Nakagawa (1977, 1978 respectively). These authors demonstrated that significant chromospheric heating could be indeed produced by this process. Also Machado (1978) has demostrated that observed Skylab SO55 L_α intensities over the flare area correspond very well to those expected on the basis of a point source of X-ray emission with a temperature of some 10^7K. However, Machado, Emslie, and Brown (1978) have demonstrated that plausible soft X-ray sources cannot in fact produce enough heating at photospheric levels to be compatible with observation (see below). These authors suggested that, instead, EUV radiation might be responsible for the heating and cited the very strong C IV λ1549 Å line as a possible source; however, Emslie and Machado (1979) have now shown that insufficient heating is in fact produced by this process. Nevertheless, it is clear that a fully consistent treatment of chromospheric modeling must take both radiation sources into account in the local energy balance.

Of course, one of the mechanisms of thermalization which has received a great deal of attention in the literature is the collisional degradation of a non-thermal beamed electron flux. First proposed by Dubov (1963) and subsequently developed in some detail by Brown (1972, 1973), Lin and Hudson (1976), Emslie (1978), and others, this mechanism remains one of the most viable mechanisms of transport and thermalization of energy in a solar flare. Transport

of energy by non-thermal electrons enables the close synchronism of emission at widely separated wavelength ranges (Zirin and Tanaka 1973; Emslie, Brown, and Donnelly 1978; Emslie and Noyes 1978; Donnelly and Kane 1978) and so, presumably, depth in the atmosphere, to be realized. Whether this synchronism of emission over the bulk of the electromagnetic spectrum can be effected by other transport mechanisms, such as conduction, depends on the temperature gradients in the atmosphere, coupled with a knowledge of the characteristic velocity associated with the transport mechanism (cf. Craig and McClymont 1976). Further development of this line of reasoning requires the inclusion of some a priori concept of the atmospheric structure in the flare (e.g. plane-parallel geometry - Machado and Linsky 1975; Brown, Canfield and Robertson 1978) and a determination (Emslie and Noyes 1978; Machado and Emslie 1979) of the differential emission measure function $\xi(T)$ (Craig and Brown 1976), and is still in fact an open question (cf. Emslie and Noyes 1978). Energy transport by non-thermal electrons beams also affords a straightforward interpretation of the hard X-ray bursts, i.e. via non-thermal bremsstrahlung of the beam electrons [although an inverse Compton mechanism, requiring fewer electrons but of higher individual energy, has also been proposed (Korchak 1971)], and a great deal of analysis concerning the intensity, spectrum, and polarization of this bremsstrahlung carried out (e.g. Brown 1971, 1972; Hoyng, Brown, and van Beek 1976; Lin and Hudson 1976; Bai and Ramaty 1978).

There are, however, a number of problems with the above electron beam model scenario. Firstly, it is long recognized that the number of electrons required to produce typical hard X-ray fluxes by thick-target bremsstrahlung (Hoyng, Brown, and van Beek 1976) places great constraints on particle acceleration mechanisms (cf. Heyvaerts 1979) and so on the primary energy release mechanism [these problems are made even worse if a thin-target (Datlowe and Lin 1973) source is postulated, or if the importance of return current ohmic losses is recognized (Emslie 1979b; see below)]. Secondly, recent studies of the inter-relationship of hard X-ray fluxes with fluxes in other (thermal) wavebands, such as EUV (Emslie, Brown, and Donnelly 1978); Donnelly and Kane 1978) and H (Brown, Canfield, and Robertson 1978), have strongly suggested that approximately one to two orders of magnitude less electrons thermalize in the lower atmosphere than are required to produce the hard X-ray burst by a non-thermal thick-target bremsstrahlung process. Further, overall estimates of the energy released over all wavelengths (Canfield et al. 1979b) fall short of the total electron energy by a similar amount, thus suggesting that in fact the degree of electron beam thermalization in the chromosphere is less than previously estimated.

Attempts have been made to resolve some of these discrepancies, such as invoking detailed source geometries (in the EUV case; Donnelly and Kane 1978), attempting refinements to existing theoretical models (McClymont and Canfield 1979), or assuming that thermal emission such as $H\alpha$ in fact originates not in the chromosphere, but in low-temperature coronal loops (Zirin 1978). However, there is growing evidence to suggest that the simple collisional degradation model is not a completely accurate picture. Firstly, it has been frequently noted (Hoyng, Brown, and van Beek 1976; Knight and Sturrock 1977; Brown and Melrose 1977; Hoyng and Melrose 1977; Colgate 1978; Hoyng, Knight, and Spicer 1978) that there is a strong need for a charge-neutralizing return current in beamed flux models, in order to avoid the establishment of unacceptably large electrostatic fields and magnetic energy densities associated with an un-neutralized beam[1]. However, little work has been done in incorporating the associated return current joule heating into such beam models, and in fact this joule heating can dominate over standard collisional losses for sufficiently large events at sufficiently great heights in the atmosphere (Knight and Sturrock 1977; Emslie 1979b). More specifically (Emslie 1979b), the effect of this joule heating is to overheat the corona (thus possibly creating a substantial thermal X-ray component; this problem is still under development) and underheat the chromosphere (for a given

[1] This return current is not so important if the electrons have a low degree of anisotropy (such as in trap models - e.g. Takakura and Kai 1966; Brown and Hoyng 1975; Melrose and Brown 1976; Bai and Ramaty 1979; Emslie, McCaig, and Brown 1979), and its presence or absence, as evidenced by the microwave signature caused by runaway electrons accelerated by the induced E_c field, could well be an important flare diagnostic.

injected flux, as compared to the purely collisional model), and to cause a reduced non-thermal X-ray flux (since the electrons are stopped quicker in the target by the additional deceleration of the $\underset{\sim}{E}$ field). While not satifactorily resolving the X-ray/(EUV, $H\alpha$) inter-relationship difficulties of Emslie, Brown, and Donnelly (1978) and Brown, Canfield, and Robertson (1978) respectively, the inclusion of ohmic heating terms does, however, on a purely non-thermal interpretation of the X-ray event, worsen the electron number problem to a degree which might well be considered totally unacceptable.

It thus appears that the present view of the thermalization of electron beams is very much in need of repair and review. This has led to a renewed interest in thermal models of the hard X-ray burst (Chubb 1971; Brown 1974; Smith and Lilliequist 1979; Brown, Melrose and Spicer 1979; Vlahos and Papadopoulos 1979), in which the X-rays are emitted from a very hot ($\simeq 3 \times 10^8$K) source, the bulk of whose electrons are prevented from free-streaming out of the source (e.g. Kahler 1971) by the ion-acoustic turbulence created by instabilities in the aforementioned beam return current. A small, high energy, fraction of the electrons are not effectively confined by the thin turbulent fronts bounding the source and can escape to, and thermalize in, the chromosphere. In this way, a number of the problems mentioned above are possibly resolved: the greater efficiency of thermal (as opposed to non-thermal) bremsstrahlung results in a reduced number of electrons requiring to be accelerated, and the precipitation rate into the chromosphere is reduced, easing the X-ray (EUV, $H\alpha$) inter-relationship difficulties mentioned above (for more details, see Vlahos and Papadopoulos 1979; Vlahos and Emslie 1979). Further, the anisotropy in the source effected by the heat flux along the arch results in finite polarization and directivity of the X-rays (Emslie and Brown 1979) which is quite compatible with current observational requirements (Tindo, Shuryghin, and Steffen 1976; Datlowe et al. 1977), and the computed X-ray spectrum from such a source (Emslie and Brown 1979, Smith and Lilliequist 1979) compares very favorably with those observed (e.g., Hoyng, Brown, and van Beek 1976).

Finally turning to the deeper layers of the atmosphere, it is apparent that significant temperature enhancements are produced at photospheric depths during flares (Machado, Emslie and Brown 1978; Cook and Brueckner 1979). Various attempts at reproducing these enhancements on the basis of standard mechanisms (electron impact, X-ray and EUV irradiation, joule heating) have met with little or no success (Machado, Emslie, and Brown 1978; Emslie and Machado 1979) and it appears that we must either invoke a very high flux of deka-MeV protons or a separate primary energy release at photospheric levels. Proton fluxes as high as those necessary should evidence themselves in strong γ-ray bursts and therefore SMM is ideally suited to testing the first of these hypotheses. Further, as Machado, Emslie, and Brown (1978) point out, more ground-based (Ca II H and K and Mg II h and k line) data are necessary to strengthen their observational claims; this is also appropriate to the proposed high level of co-operation of satellite and terrestrial observations during SMY.

In conclusion, the task facing modelers of energy tranport and thermalization is to construct, to as high a level of self-consistency and exactness as possible, theoretical emission measure profiles and other such signatures of their theories, to such a level that the SMY network of satellite and ground-based observations is capable of discriminating observationally between such models.

APPENDIX D

X-RAY SPECTRA OF SOLAR FLARES

S. L. Mandel'stam
USSR Academy of Sciences
Institute of Spectroscopy
Troitsk, Moscow

Spectra of solar flares provide vast information on the physical parameters of the plasma of the flare region. In the present communication the results of recent evaluation of the spectra of large X-ray flares at the Sun on 24 October, 5 November and 16 November 1970 are presented.

Observations were performed from the satellite "Intercosmos-4" launched on 14 October 1970 (Mandel'stam 1978). The principal layout of this satellite-borne instrument is shown in Fig. D1. The instrument contained two spectrometers with quartz crystals with spacings d = 1.800 Å and d = 4.2546 Å, an X-ray heliograph and an optical sensor. The instrument was mounted on the front panel of the satellite; the longitudinal axis of it was pointed at the Sun and the solar disk was scanned automatically three times at each orbit. By scanning the angle of incidence for the radiation from the flare region onto the crystal θ varies and, therefore - according to Wulf-Bregg law - the radiation wavelength recorded at the moment is $\lambda = 2d \sin \theta$. By fitting two of the lines in the solar spectra with two reference lines in laboratory spectra and knowing the scanning velocity $d\theta/dt$, wavelengths of other lines in the spectrum were determined. Scanning velocities were determined by passing the flare region through three collimator slits of the heliograph and from the optical sensor data. The error in the λ determination with regard to the possible error of alignment of spectrometer and heliograph axes ($\simeq$ 1') and the dimensions of the flare radiation region ($\simeq$ 1') did not exceed +0.0004 Å; spectral resolution (depending on scanning velocity) was 3×10^{-4} - 1×10^{-3} Å (Zhitnik 1974).

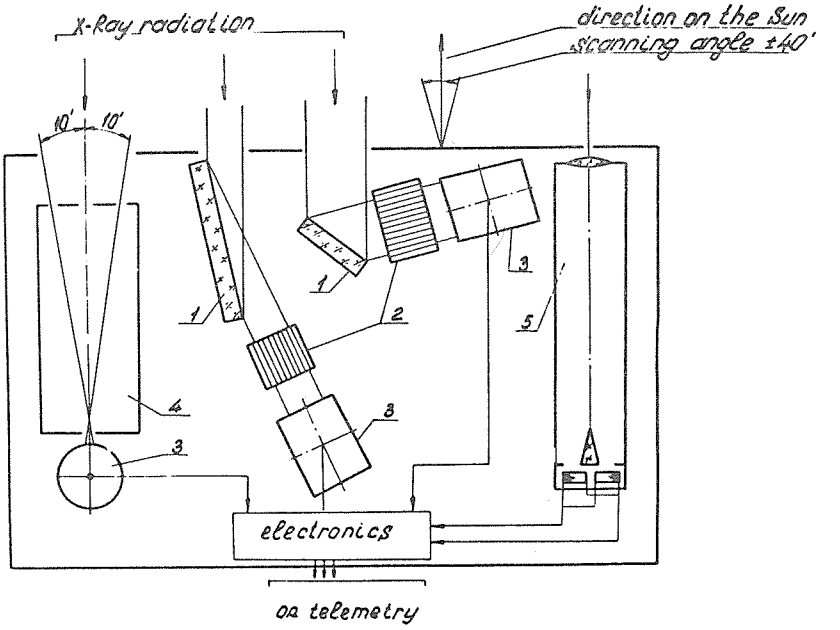

Fig. D1: Layout of X-Ray spectrometer-heliograph: 1 - quartz crystals; 2 - collimators; 3 - photon counter; 4 - heliograph collimator; 5 - optical sensor.

NOTE: Some minor, stylistic, changes have been made to the text supplied by the author (editors).

Fig. D2 shows records of 6 high resolution spectra in the region of lines of the helium-like ion Fe XXV, λ = 1.85-1.87 Å. In Fig. D3 one of these spectra is fitted with the laboratory one (Zhitnik et al. 1979 a). One can see the resonance line 1s 2p $^1P_1 \rightarrow 1s^2\ ^1S_0$, λ = 1.8506 Å (w), the intercombination line 1s 2p $^3P_1 \rightarrow 1s^2\ ^1S_0$, λ = 1.8596 Å (y), the forbidden magneto-dipole line 1s 2s $^3P_1 \rightarrow 1s^2\ ^1S_0$, λ = 1.8685 Å (z), and the forbidden magneto-quadrupole line 1s 2p $^3P_1 \rightarrow 1s^2\ ^1S_0$, λ = 1.8557 Å (x) (these two lines cannot be seen in the laboratory spectrum due to large electron density). Moreover, a large number of satellite lines are observed. These lines are due to transitions 1s 2l 2l' $\rightarrow$ $1s^2$ 2l" in the lithium-like ion Fe XXIV; the upper levels of these lines correspond to the excitation of two electrons and lie above the ionization limit of Fe XXIV ions. Fig. D4 shows a section of the solar and the laboratory spectra in the region 1.70-1.80 Å. One sees the unresolved resonance line L_α of the hydrogen-like ion Fe XXVI 2p $^2P_{1/2,3/2} \rightarrow$ 1s $^2S_{1/2}$, λ = 1.78 Å and the adjoining group of unresolved satellite lines which correspond to transitions 2l 2l' $\rightarrow$ 1s 2l" in helium-like ions. The upper levels of these lines also lie above the ionization limit of the ion Fe XXV. Table D1 contains experimental and theoretically calculated wavelengths for the observed lines of Fe XXV and for the satellite lines.

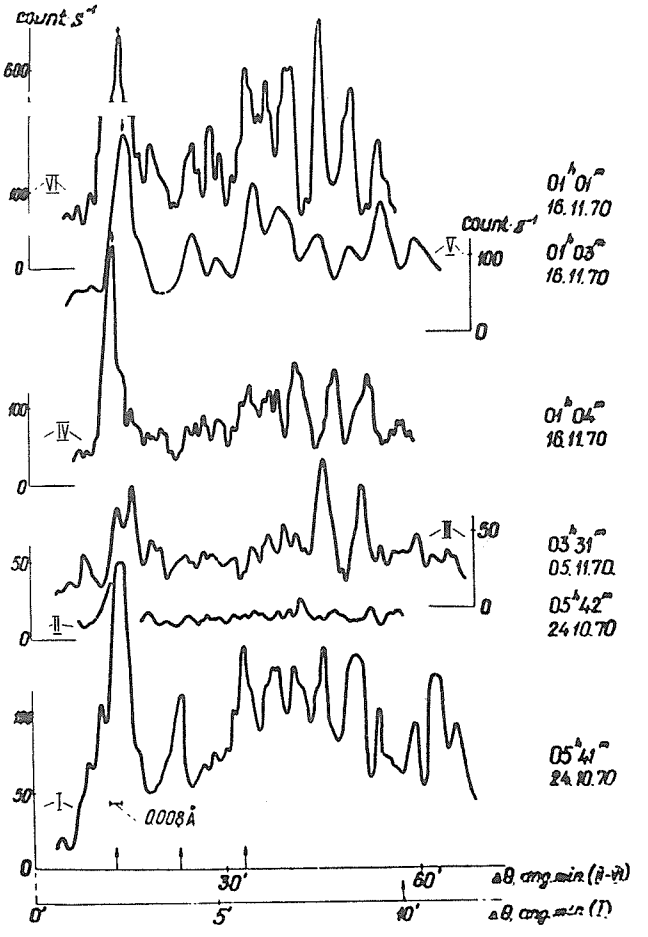

Fig. D2: Spectra in the Region 1.85-1.87 Å of 6 solar flares

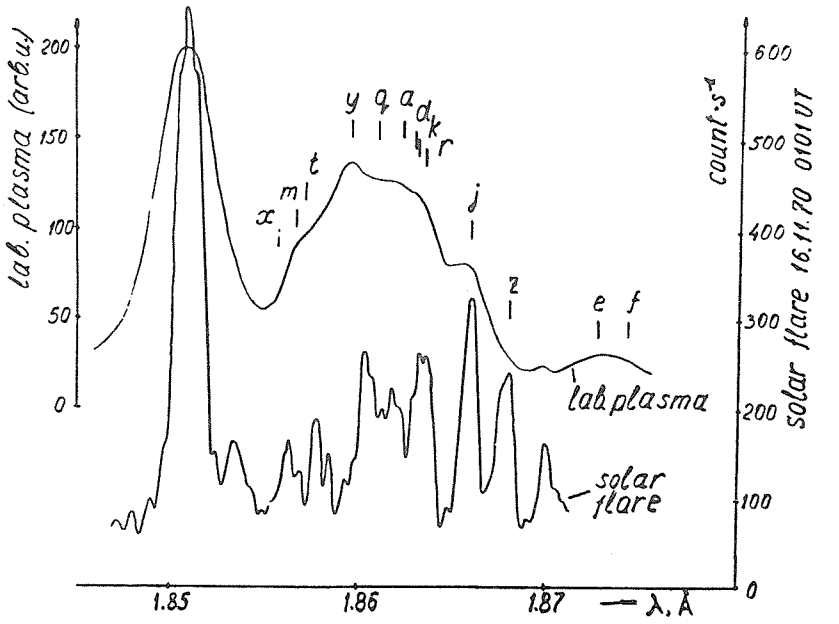

Fig. D3: Comparison of Flare and Laboratory Spectra within the Region of Fe XXV Lines

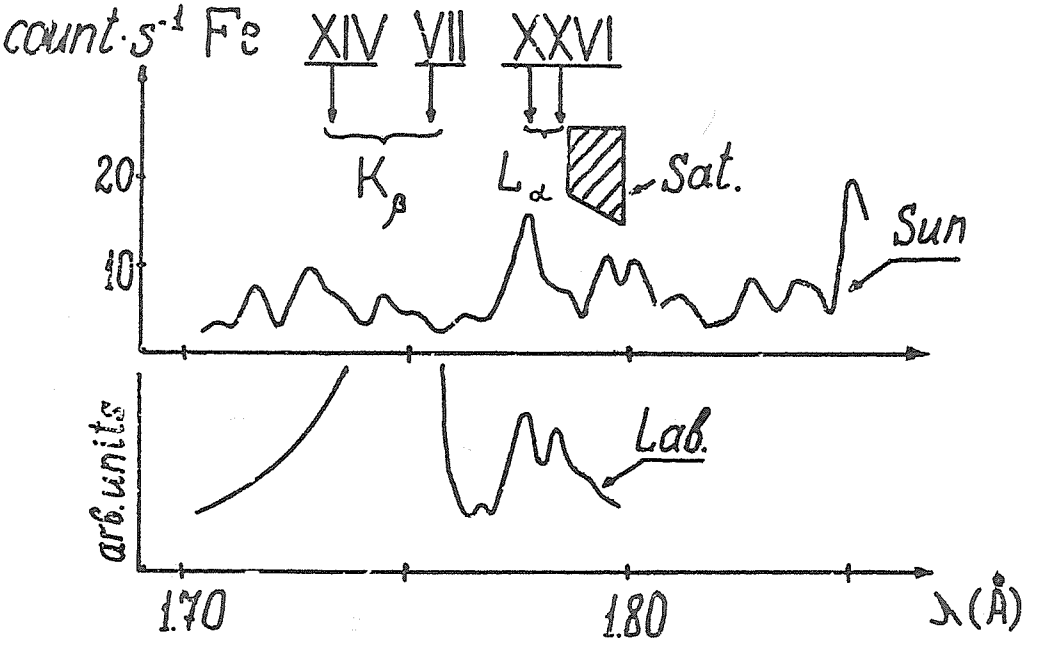

Fig. D4: Comparison of Flare and Laboratory Spectra within the region of Fe XXVI Lines

Table D I. Wavelengths of most prominent Fe XXIV-XXV lines in the region 1.85 - 1.87 Å

Date	10/24/70		11/05/70		11/16/70					
UT	I 05 41	II 05 42	III 03 31	IV 01 04	V 01 03	VI 01 01	Averaged Values	Theory (Vainstein & Safronova)	Key	Transition
Lines										
1	[1.8506]	[1.8506]	[1.8506]	[1.8506]	[1.8506]	[1.8506]	[1.8506]	[1.8506]	w	$1s2p\,^1P_1 \rightarrow 1s^2\,^1S_o$
2	-	1.8526	1.8528	1.8538	(1.8524)	1.8534	1.8530	1.8534	-	$1s2p3p\,^2P_{3/2}\,;\,^2D_{5/2,3/2} \rightarrow 1s^2 3p\,^2P_{3/2}$
3	1.8552	1.8555	1.8552	1.8560	1.8559	1.8561	1.8557	1.8556	x	$1s2p\,^3P_2 \rightarrow 1s^2\,^1S_o$
4	1.8580	(1.8576)	1.8568	1.8576	1.8580	1.8578	1.8576	1.8573	t	$1s2s2p_2^2\,^2P_{1/2} \rightarrow 1s^2 2s\,^2S_{1/2}$
5	1.8600	1.8606	1.8591	1.8597	1.8610	1.8603	1.8601	1.8596	y	$1s2p\,^3P_1 \rightarrow 1s^2\,^1S_o$
6	(1.8616)	1.8615	1.8605	1.8611	1.8609	1.8619	1.8611	1.8612	q	$1s2s2p_1^2\,^2P_{3/2} \rightarrow 1s^2\,2s\,^2S_{3/2}$
7	(1.8626)	1.8620	1.8617	1.8625	1.8629	(1.8629)	1.8624	1.8624	a	$1s2p^2\,^2P_{3/2} \rightarrow 1s^2 2p\,^2P_{3/2}$
8	1.8640	1.8636	1.8629	1.8629	1.8636	1.8635	1.8634	1.8631	k	$1s2p^2\,^2D_{3/2} \rightarrow 1s^2 2p^2 P_{1/2}$
9	(1.8644)	(1.8640)	1.8638	1.8636	1.8643	1.8642	1.8641	1.8638	r	$1s2s2p\,^2P_{1/2} \rightarrow 1s^2 2s\,^2P_{1/2}$
10	[1.8661]	[1.8661]	[1.8661]	[1.8661]	[1.8661]	[1.8661]	[1.8661]	1.8662	j	$1s2p^2\,^2D_{5/2} \rightarrow 1s^2 2p\,^2P_{3/2}$
11	(1.8680)	(1.8686)	1.8684	1.8671	(1.8678)	(1.8681)	1.8680	1.8678	l	$1s2p^2\,^2D_{3/2} \rightarrow 1s^2 2p\,^2P_{3/2}$
12	1.8687	1.8689	1.8690	1.8678	1.8685	1.8684	1.8685	1.8684	z	$1s2s\,^3S_1 \rightarrow 1s^2\,^1S_o$

x) The values of all wavelengths are shifted on 0.0007 Å due to Lamb-correction. Brackets ( ) show the suggested position of unresolved lines; [ ] point to the reference lines measured in laboratory with the help of vacuum spark.

The upper levels of satellite lines in the hydrogen line spectra and some of satellite lines (e.g. j,k,a) in the helium- like spectra are populated by dielectronic recombination:

$$Fe^{+25} + e^- \rightarrow Fe^{+24**}\ (2l\ 2l') \rightarrow Fe^{+24*}\ (1s\ 2l') + h\nu$$
$$Fe^{+24} + e^- \rightarrow Fe^{+23**}\ (1s\ 2l\ 2l') \rightarrow Fe^{+24*}\ (1s^2\ 2l') + h\nu$$

and the ratio of their intensity to the intensity of the resonance line is given by:

$$I_s/I_r = \frac{\delta E}{kT_e} \exp\left(\frac{\delta E}{kT_e}\right),$$

where $\delta E = Z^2 Ry/h^2$, the binding energy of the electron, is sufficiently large.

This makes the ratio I_s/I_r a rather sensitive "thermometer" to measure the electron temperature T_e of the flare plasma (cf. Chapter 2; Section I.5, Figure 2.2). It is important to note here that this ratio is independent of the ion number density and can therefore be used for plasma which is nonstationary and spatially inhomgeneous - in temperature and in density. Table DII gives values of T_e thus determined by the use of the Fe XXV spectra and emission measures obtained from absolute values of radiation fluxes in the resonance line for four flares.

These data refer to the time which corresponds approximately to the flare maxima. Recently evaluated spectra (Zhitnik et al. 1979b) which refer to initial and final stages of flares are of obvious interest.

Fig. D5 shows several spectra which refer to the inital stage of the flare 16 November 1970 (which began at 0045 UT) and to the vicinity of its maximum. The intensity of resonance and satellite lines Fe XXV in spectra of the initial phase are 30-50 times less than in spectra close to the flare maximum. However, in spectra of the initial phase one can clearly see resonance lines of hydrogen-like ions Fe XXVI and lines K_α and K_β, which correspond to inner-shell transitions $L \rightarrow K$ and $M \rightarrow K$ in "colder" iron ions. These lines are not seen and, perhaps, are absent altogether in the spectra near the maximum stages of flares.

The K_α lines were observed previously, but with lower dispersion (Doschek et al. 1971, Neupert 1971). The K_β lines apparently are observed for the first time. Our preliminary identification suggests for K_α and K_β lines, according to laboratory data and calculations, ions with ionization stage beginning within the interval from Fe^{+16} to Fe^{+3}.[1]

In Fig. D6 several spectra of the initial phase and spectra close in time to the flare maximum for the flare 5 November 1970 are presented. The same picture is observed: 30-40 times lower intensity of resonance and satellite lines Fe XXV and relatively high intensity of the line K_α, K_β of lower ions, and Fe XXVI $L\alpha$.

The same picture is also observed for the flare 24 October 1970 (Figs. D7, D8): low intensity of resonance and satellite lines Fe XXV at the initial and final stages as compared to the maximum, and relatively high intensity of lines K_α, K_β of lower ions and the Fe XXVI $L\alpha$ line in relation to the Fe XXV lines.

Fe^{+15} ions and those of lower ionization degrees where the 1s electron is removed have their their maximum concentration within the temperature range 2×10^6 - 5×10^4 K, i.e., in the lower layers of the corona and the transition region.

---

1 Lines K_α correspond to the transitions:
Fe XVII: $1s2s^22p^63s \rightarrow 1s^22s^22p^53s$; $\lambda = 1.927$Å
Fe IV: $1s2s^22p^63s^23p^63d^6 \rightarrow 1s^22s^22p^63p^53d^6$; $\lambda = 1.936$Å

Lines K_β correspond to the transitions:
Fe XIV: $1s2s^22p^63s^23p^2 \rightarrow 1s^22s^22p^63s^23p$; $\lambda = 1.739$Å
Fe VII: $1s2s^22p^63s^23p^63d^3 \rightarrow 1s^22s^22p^63s^23p^53d^3$; $\lambda = 1.756$Å

TABLE DII. Solar Flare Data

Date	Start UT	Maximum UT	End UT	Importance	Mc Math Region	Temperature T_e (10^6 K)	Emission Measure Y (cm^{-3})
10/24/70	0447	0552	0631	2N	11002	18	3.0×10^{49}
11/05/70	0310	0335	0437	3B	11019	15	7.5×10^{48}
11/16/70	2215	2221	2233	1N	11029	20	1.5×10^{48}
11/16/70	0045	0052	0139	2B	11029	23	2.5×10^{49}

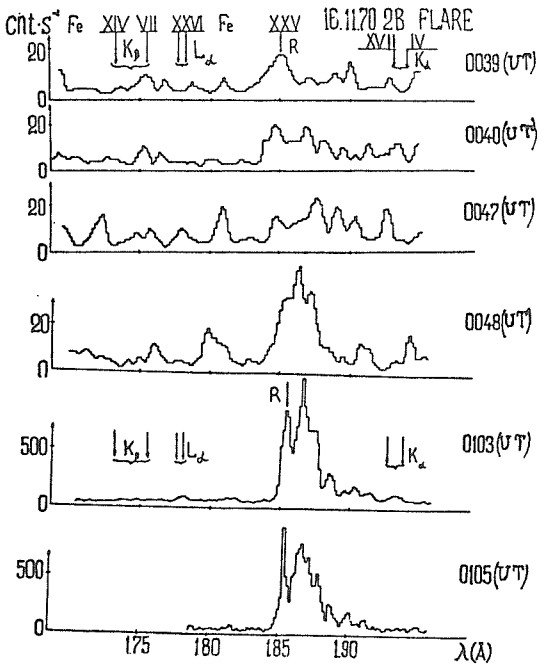

Fig. D5: Spectra of the Initial Stage and Maximum for the Flare 16 November 1970 (Spectra 0039-0048 have somewhat lower spectral resolution.)

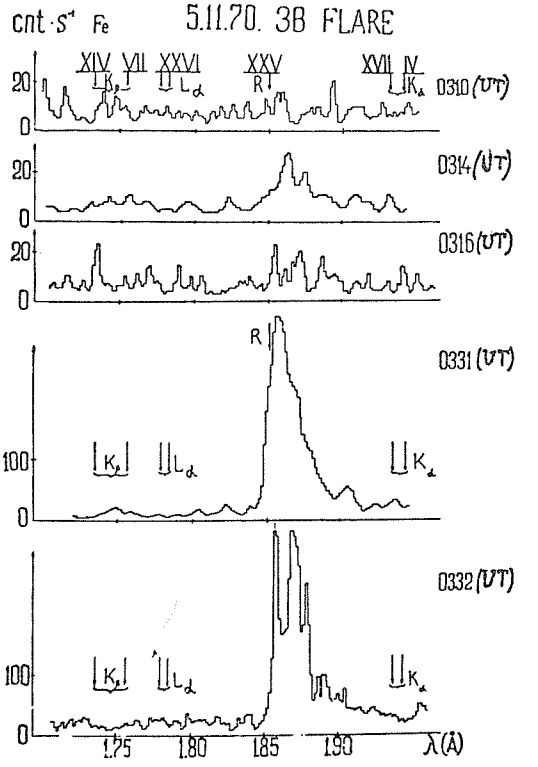

Fig. D6: Spectra of the initial State and Maximum for the Flare 5 November 1970 (The spectra at 0314 and 0331 UT have somewhat lower resolution.)

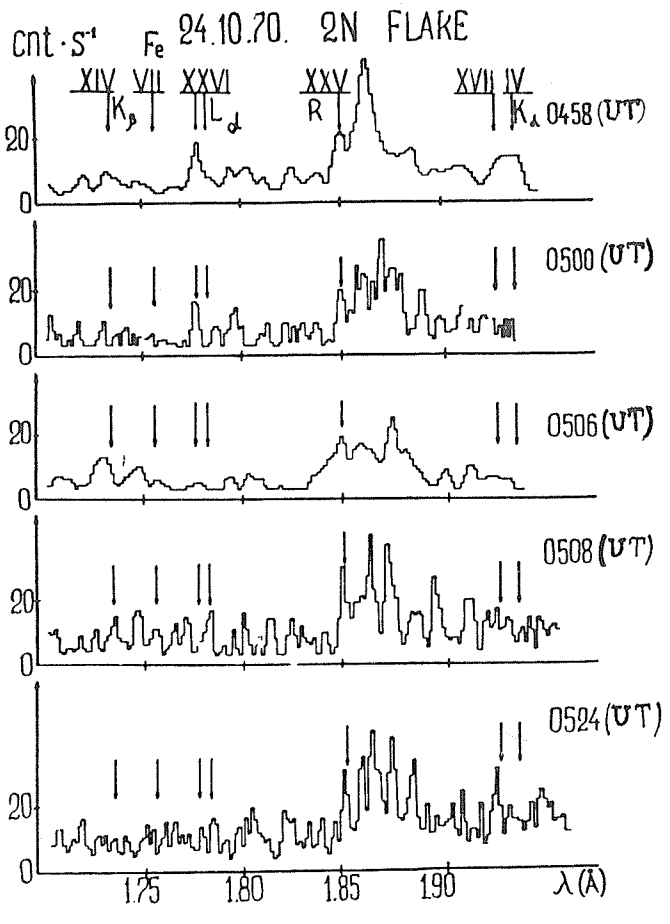

Fig. D7: Spectra of the initial stage for the flare 24 October 1970 (The spectra at 0458 and 0506 UT have somewhat lower spectral resolution.)

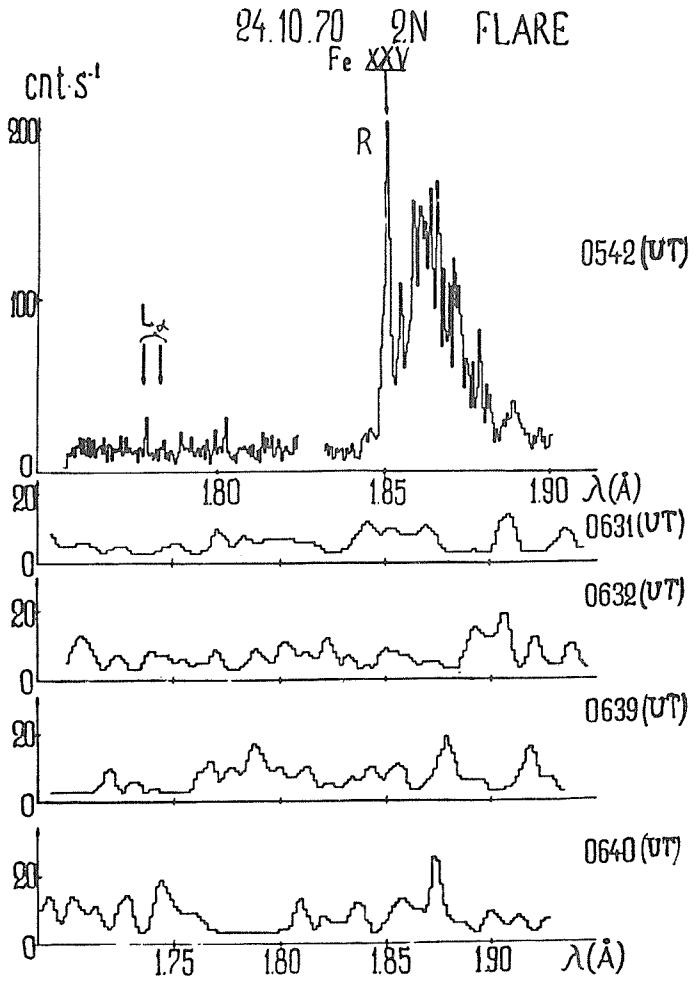

Fig. D8: Spectra of the maximum and the final stage of the flare 24 October 1970 (The spectra 0631-0640 UT have somewhat lower spectral resolution.)

The binding energy of the electron is about 7 keV. Thus, this ionization process is realized by means of electrons accelerated up to energies $\simeq$ 10 keV coming from outside, i.e., with a directional velocity distribution.[2]

From this point of view it is interesting to compare spectra with polarization of the X-ray radiation of the flare (Tindo et al. 1972b). This comparison is presented in Figs. D9 and D10. It can be seen that at the initial and final stages of flares where the relative intensity of lines K_α and K_β of lower ions is comparatively high, the polarization value is also high, indicating directly the presence of directed electron beams. Note that appreciable polarization was observed in 9 flares out of 14 studied (Tindo and Somov 1978).

Thus, the results of spectral interpretation and polarization measurements indicate that at the initial stage of the flare some directed accelerated electrons evidently appear, which penetrate rather deep into the solar atmosphere and give raise to hard bremsstrahlung hard X-ray emission and K_α and K_β lines of ions in rather low ionization stages as was suggested earlier. Then near the maximum stage of the flare the flux of high energy electrons increases so that a certain volume of plasma is heated and the electrons are thermalized both in velocity value and direction. We cannot say whether the fluxes of directed electrons are still preserved at this stage since the lines K_α , K_β are lost in the strong continuous background of thermal radiation. At the final stage of flares, the accelerated electrons again play an important role, although in large flares the accelerated mechanism is likely to be different from that at the initial stage of the flare (de Jager 1976).

Table DIII gives experimental values of radiation fluxes for different lines in flare spectra taken on 5 November 1970 and evaluations of physical parameters of the flare region obtained on the basis of these data. As is seen from the Table, the whole picture is described well within the supposition of a comparatively small flux of accelerated nonthermal electrons. Our attention is attracted by the fact that temperature values in the flare region determined by the ratio of intensities of the resonance and satellite lines of Fe XXV, and also by the distribution of satellite line intensities, are in good agreement. The value of the temperature determined by the intensity ratio of resonance lines of Fe XXVI and Fe XXV turns out to be much higher. This fact also points to the important additional ionization and excitation of the $L\alpha$ line of Fe XXVI by non-thermal electrons.[3]

The role of accelerated electrons as a dominant agent which is responsible for most of a flare's manifestations is confirmed by a number of experimental facts (Sveštka 1976): the power law character of bremsstrahlung spectra $\gtrsim$ 10 keV, the fine structure of this radiation in the form of "elementary bursts" with the duration of seconds or less (van Beek, de Feiter, and de Jager 1974), the presence of accelerated electrons in the interplanetry space, and other phenomena. On the other hand, this hypothesis has lately met serious theoretical difficulties (Hoyng, Brown, and van Beek 1976; Emslie 1979b). This problem should be studied further both experimentally and theoretically.

We think that important information can be obtained if generation heights in the solar atmosphere of X-ray flare radiation of different energy can be observed with sufficiently high spatial and temporal resolution. Our measurements of the height of the soft X-ray radiation region $E \lesssim 1$ keV and also Skylab photos, show that this radiation appears at the height 20^{0} - 25000 km in the tops of "arches" or "loops" (Zhitnik 1974; Pallavicini, Serio, and Vaiana 1977; Vorpahl et al. 1975). It is possible that just in this very region of the corona accelerated electrons appear, either as a result of the rupture of current sheets (Somov and Syrovatskii 1976), or due to another mechanism. These particles are indicated by polarization values, although up to now we have these data only for three flares (Tindo et al. 1972b).

[2] Possibly a contribution to this ionization is made by hard X-ray emission from the outside flare regions (Basko 1977).

[3] An attempt to interpret this by a two-component plasma model failed because the intensity ratio of Fe XXVI satellite and $L\alpha$ lines also gives a temperature of about 20 x 10^6 K (Grineva et al. 1975).

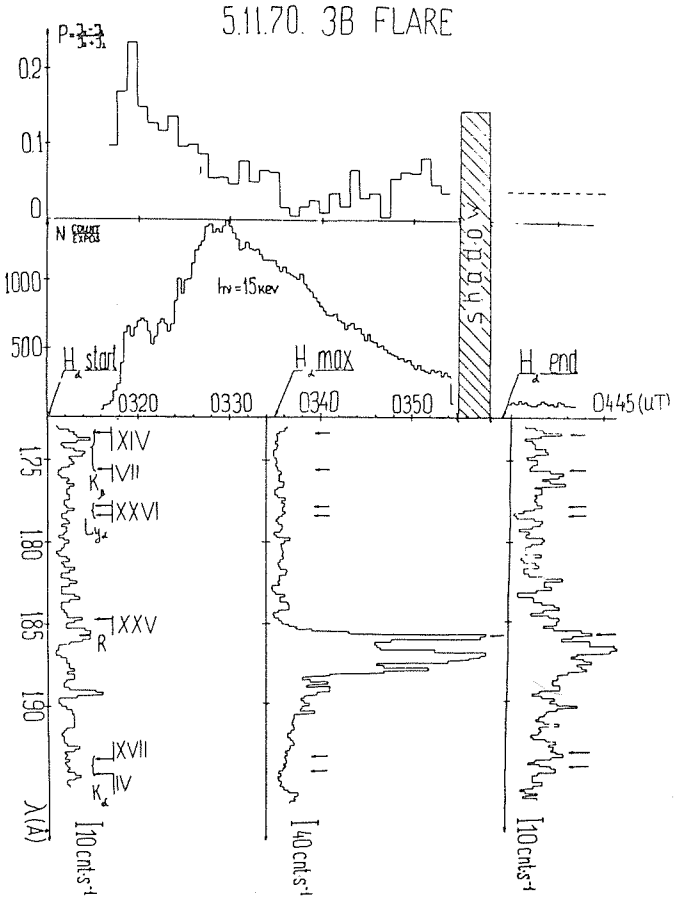

Fig. D9: Comparison of radiation polarization and spectra of the flare 5 November 1970

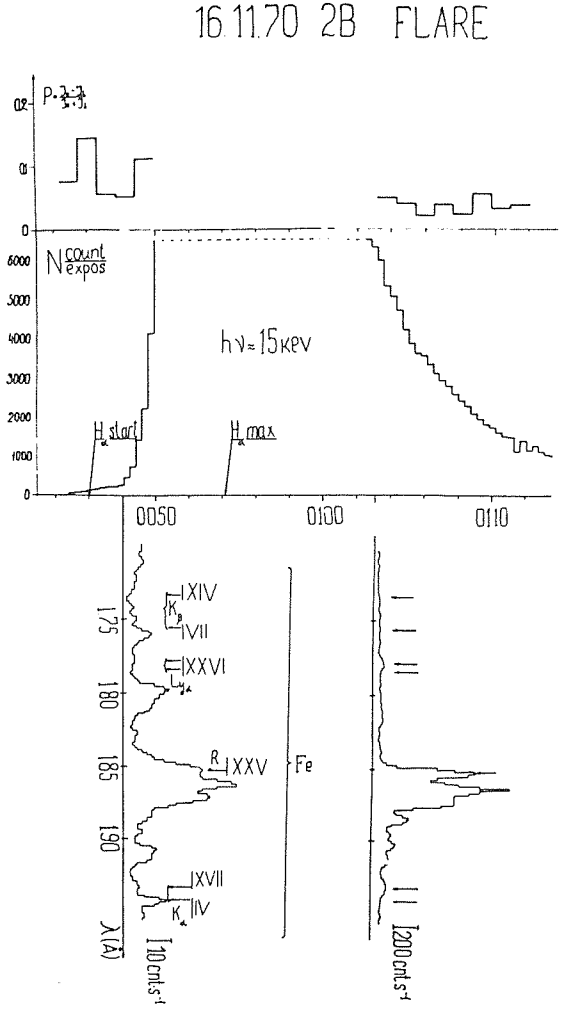

Fig. D10: Comparison of radiation polarization and spectra of the flare 16 November 1970

TABLE DIII. Energy Fluxes and Physical Parameters for the Flare on 11/05/70

Optical Flare	Time [UT]	Flux [erg - cm^{-2}-s^{-1}]					T_e [10^6 K]			Parameters		
		Res Fe XXV	L_α Fe XXVI	Σ Sat Fe XXIV	K_α Fe XVII-IV	K_β Fe XIV-VII	$\frac{\Sigma I_S(XXIV)}{I_R(XXV)}$	$\frac{\Sigma I_S(XXIII-XVIII)}{I_R(XXV)}$	$\frac{L_\alpha(XXVI)}{I_R(XXV)}$	Y [cm^{-3}] therm	Y [cm^{-3}] beam	$\frac{n_e}{n_e^t}$ (E $\geq$ 7 keV)
Start 03 10	03 10	5.0×10^{-6}	4.0×10^{-6}	1.3×10^{-5}	7×10^{-6}	3×10^{-5}	18	12	100	10^{47}	3×10^{46}	$\approx$ 90
	03 14	6.0×10^{-6}	$<1.5\times10^{-6}$	3.6×10^{-5}	-	3×10^{-5}	14	18	60	1.5×10^{47}	3×10^{46}	$\approx$ 80
	03 16	8.7×10^{-6}	-	1.8×10^{-5}	2×10^{-6}	2×10^{-5}	20	15	-	2×10^{47}	2×10^{45}	$\approx$ 40
	03 31	1.7×10^{-4}	1.3×10^{-5}	3.0×10^{-4}	3×10^{-6}	4×10^{-5}	21	20	[40]	10^{49}	4×10^{46}	$\approx$ 18
maximum	03 32	1.7×10^{-4}	7.0×10^{-5}	5.0×10^{-4}	$<3\times10^{-6}$	$<3\times10^{-6}$	20	20	40	10^{49}	$<3\times10^{45}$	$\approx$ 2
03 45	04 35	1.7×10^{-5}	4.0×10^{-6}	5.7×10^{-5}	1×10^{-5}	1×10^{-5}	17	19	55	5×10^{48}	1×10^{46}	$\approx$ 10
end 04 37	04 40	1.0×10^{-5}	5.0×10^{-6}	6.2×10^{-5}	8×10^{-6}	5×10^{-6}	13.5	17.5	73	5×10^{48}	5×10^{45}	$\approx$ 5
	04 49	4.5×10^{-6}	6.0×10^{-6}	3.0×10^{-5}	6×10^{-6}	2×10^{-5}	13.0	16	110	10^{47}	2×10^{46}	$\approx$ 60
	05 03	1.1×10^{-5}	7.5×10^{-6}	3.0×10^{-5}	6×10^{-6}	1×10^{-5}	17.5	17	82	10^{47}	1×10^{46}	$\approx$ 50

As to the generation regions of more hard radiation (greater than 10 keV), direct experimental data are lacking. From the viewpoint of the picture developed here, the excitation of the K_α and K_β lines and further heating of plasma take place within a volume of about 10^{27}-10^{29} cm^3 at a height of several thousand km or less with the density in the range 10^9-10^{11} cm^{-3} (Kane and Lin 1972), though we cannot exclude a somewhat higher density. Thus, determination of the regions of generation of X-ray radiation of various energies can be very useful for clarification of flare development mechanism.

We are planning to investigate, during the year of maximum solar activity, spectra, polarization and localization of generation regions of X-ray radiation for different energies. These studies will be performed by means of AUOS stations - a new generation of satellites for solar research.

APPENDIX E

The following resolution was adopted unaminously at the Workshop on Energy Release in Flares on 1 March 1979.

The SERF (Study of Energy Release in Flares) Workshop collectively recommends the establishment of the position of an SMY (Solar Maximum Year) coordinator, whose role is to

(a) provide a central focus for the communication of detailed observational plans and priorities between observatories (ground and space-borne), and

(b) assist in the development of the plans to carry out coordinated observing sequences, and

(c) assist in the coordination of the scientific goals of the individual ground and space-borne observatories toward the ultimate goal of maximizing the collective science.

REFERENCES

Allissandrakis, C.E. and Kundu, M.R. 1978, Ap. J., 222, 342.

Altyntsev, A.T., Kosholev, N.A., Krasov, V.I., Masolov, V.I., Parfenov, O.G., and Shishko, A.A. 1973, Soviet Phys. JETP, 18, 397.

Altyntsev, A.T. and Krasov, V.I. 1974, ZhTF, 44, 2629.

Altyntsev, A.T. and Krasov, V.I. 1977, ZhTF, 47, 44.

Altyntsev, A.T. and Krasov, V.I. 1978, SibIZMIR Preprint # 22-78.

Altyntsev, A.T., Krasov, V.I., and Tomasov, V.M. 1977, Solar Phys., 55, 69.

Altyntsev, A.T., Krasov, V.I., Markov, V.S., Petrov, M.F., Frank, A.G., and Khodsaev, A.Z. 1978, Fizika Plasmii, 4, 18.

Antiochos, S.K. and Sturrock, P.A. 1978, Ap. J., 220, 1137.

Anzer, U. 1978, Solar Phys., 57, 111.

Axford, W.I. 1977, in (M.A. Shea et al., eds.) "Study of Travelling Interplanetary Phenomena", Ap. and Space Sci. Library, 71, 45. [Dordrecht: Reidel]

Bai, T. and Ramaty, R. 1978, Ap. J., 219, 705.

Bai, T. and Ramaty, R. 1979, Ap. J., 227, 1072.

Banin, V.G., Maksimov, V.P., and Tomozov, V.M. 1978, in "Issledovanija po Geomagnetizmu, Aeronomii, i Fisika Soltsna", No. 45, Moscow, "Nauka", 54.

Basko, M.M. 1977, Institute of Space Research preprint #379.

Beigman, I.L. 1974, Astron. Zhurn., 51, 1017.

Bely-Dubau, F., Gabriel, A.H., and Volonte, S. 1979, MNRAS, 186, 405.

Bessey, R.J. and Kuperus, M. 1970, Solar Phys., 12, 216.

Bohme, A., Furstenberg, F., Hildebrandt, J., Saal, O., Kruger, A., Hoyng, P., and Stevens, G.A. 1977, Solar Phys., 53, 139.

Brown, J.C. 1971, Solar Phys., 18, 489.

Brown, J.C. 1972, Solar Phys., 26, 441.

Brown, J.C. 1973, Solar Phys., 31, 143.

Brown, J.C. 1974, in (G.A. Newkirk, Jr., ed.) "Coronal Disturbances", I.A.U. Symp., 57, 395.

Brown, J.C. and Hoyng, P. 1975, Ap. J., 200, 734.

Brown, J.C. and Melrose, D.B. 1977, Solar Phys., 52, 117.

Brown, J.C., Canfield, R.C., and Robertson, M.N. 1978, Solar Phys., 57, 399.

Brown, J.C., Melrose, D.B., and Spicer, D.S. 1979, Ap.J., 228, 592.

Canfield, R.C. and Cook, J.W. 1978, Ap.J., 225, 650.

Canfield, R.C., Brown, J.C., Brueckner, G.E., Cook, J.W., Craig, I.J.D., Doschek, G.A., Emslie, A.G., Henoux, J.-C., Lites, B.W., Machado, M.E., and Underwood, J.H. 1979a, in (P.A. Sturrock, ed.) "Solar Flares", proceedings of the Skylab Solar Flare Workshop.

Canfield, R.C., Cheng, C.-C., Dere, K.P., Dulk, G.A., McLean, D.J., Robinson, R.D., Schmahl, E.J., and Schoolman, S.A. 1979b, in (P.A. Sturrock, ed.) "Solar Flares", proceedings of the Skylab Solar Flare Workshop.

Chambe, G. and Henoux, J.-C. 1979, Astr. Ap., submitted.

Chubb, T.A. 1971, in (E.R. Dyer, ed.) "Solar Terrestrial Physics", Part I [Dordrecht:Reidel].
Colgate, S.A. 1978, Ap. J., 221, 1068.
Cook, J.W. and Brueckner, G.E. 1979, Ap. J., 227, 645.
Craig, I.J.D. and Brown, J.C. 1976, Astr. Ap., 49, 239.
Craig, I.J.D. and McClymont, A.N. 1976, Solar Phys., 50, 133.
Datlowe, D.W. and Lin, R.P. 1973, Solar Phys., 32, 459.
Datlowe, D.W., O'Dell, S.L., Petersen, L.E., and Elcan, M.J. 1977, Ap. J., 212, 561.
Davis, W.D., 1977, Solar Phys., 54, 139.
de Jager, C. 1976, in "Solar Flares and Space Research", North Holland Publishing Company.
de Jager, C. and de Jonge, G. 1978, Solar Phys., 58, 127.
Dolginov, A.Z. and Yakovlev, D.G. 1973, Astron. Zhurn., 50, 1001.
Donnelly, R.F. and Kane, S.R. 1978, Ap. J., 222, 1043.
Doschek, G.A., Meekins, I.E., Kreplin, R.W., Chubb, T.A., and Friedman, H. 1971, Ap. J., 170, 573.
Dryer, M., Wu, S.T., Steinolfson, R.S., and Wilson, R.M. 1979, Ap. J., in press.
Dubov, E.E. 1963, Soviet Phys. Doklady, 8, 543.
Dulk, G.A., Smerd, S.F., MacQueen, R.M., Gosling, J.T., Magun, A., Stewart, R.T., Sheridan, K.V., Robinson, R.D., and Jacques, S. 1976, Solar Phys., 49, 369.
Emslie, A.G. 1978, Ap. J., 224, 241.
Emslie, A.G. 1979a, Ap. J., submitted.
Emslie, A.G. 1979b, these proceedings (Appendix C).
Emslie, A.G. and Brown, J.C. 1979, Ap. J., submitted.
Emslie, A.G. and Machado, M.E. 1979, Solar Phys., in press.
Emslie, A.G. and Noyes, R.W. 1978, Solar Phys., 57, 373.
Emslie, A.G., Brown, J.C., and Donnelly, R.F. 1978, Solar Phys., 57, 175.
Emslie, A.G., McCaig, M.G., and Brown, J.C. 1979, Solar Phys., in press.
Fisk, L.A. 1978, Ap. J., 224, 1048.
Gabriel, A.H. 1972, MNRAS, 160, 99.
Gabriel, A.H. and Phillips, K.J.H. 1979, preprint.
Galeev, A.A. and Zelenyi, L.M. 1975, Soviet Phys. JETP, 69, 882.
Grineva, Yu. I., Karev, V.I., Korneev, V.V., Krutov, V.V., Mandel'stam, S.L., Safronova, U.I., Urnov, A.M., Vainstein, L.A., and Zhitnik, I.A. 1975, Space Research, 15, Berlin, 637.
Gubchenko, V.M. and Zaitsev, V.V. 1977, Abstracts of the X Conference on Radio Astronomy, Irkutsk, 43.
Harris, E.C. 1962, Il Nuovo Cimento, 23, 115.
Henoux, J.-C. and Nakagawa, Y. 1977, Astr. Ap., 57, 105.
Henoux, J.-C. and Nakagawa, Y. 1978, Astr. Ap., 66, 385.
Henoux, J.-C. and Rust, D.M. 1979, in preparation.
Heyvaerts, J. 1979, these proceedings (cf. Chapter 3).

Hiei, E. and Widing, K.G. 1979, Solar Phys., in press.
Hildner, E. 1977, in (M.A. Shea et al., eds.) "Study of Travelling Interplanetary Phenomena", Ap. and Space Sci. Library, 71 [Dordrecht:Reidel].
Hirayama, T. 1963, Publ. Astr. Soc. Japan, 15, 122.
Hoyng, P. and Melrose, D.B. 1977, Ap. J., 218, 866.
Hoyng, P., Brown, J.C., and van Beek, H.F. 1976, Solar Phys., 48, 197.
Hoyng, P., Knight, J.W., and Spicer, D.S. 1978, Solar Phys., 58, 139.
Hyder, C.L. 1967a, Solar Phys., 2, 49.
Hyder, C.L. 1967b, Solar Phys., 2, 267.
Hudson, H.S. 1978, Solar Phys., 57, 237.
Inglis, D.R. and Teller, E. 1959, Ap. J., 90, 439.
Jackson, B.V. and Hildner, E. 1978, Solar Phys., 60, 155.
Kahler, S.W. 1971, Ap. J., 168, 319.
Kahler, S.W., Hildner, E., and van Hollebeeke, M.A.I. 1978, Solar Phys., 57, 429.
Kane, S.R. and Lin, R.P. 1972, Solar Phys., 23, 457.
Kaplan, S.A., Pikel'ner, S.B., and Tsytovich, V.N. 1974, Phys. Reports, 150, #1.
Knight, J.W. and Sturrock, P.A. 1977, Ap. J., 218, 306.
Kopp, R.A. 1972, Solar Physics, 27, 373.
Korchak, A.A. 1971, Solar Phys., 18, 284.
Korchak, A.A. 1978, Solar Phys., 56, 223.
Kostyuk, N.D. and Pikel'ner, S.B. 1975, Soviet Astron. - AJ, 18, 590.
Kundu, M.R. and Vlahos, L. 1979, Ap. J. in press.
Kuznetsov, V.D. and Syrovatskii, S.I. 1977, Pisma v. AZh, 3.
Lin, R.P. and Hudson, H.S. 1976, Solar Phys., 50, 153.
Lites, B.W. and Cook, J.W. 1979, Ap. J., 228, 598.
Machado, M.E. 1978, Solar Phys., 60, 341.
Machado, M.E. and Emslie, A.G. 1979, Ap. J., in press.
Machado, M.E. and Linsky, J.L. 1975, Solar Phys., 42, 295.
Machado, M.E. and Rust, D.M. 1974, Solar Phys., 38, 499.
Machado, M.E., Emslie, A.G., and Brown, J.C. 1978, Solar Phys., 58, 363.
McClymont, A.N. and Canfield, R.C. 1979, in preparation.
McLean, D.B., Sheridan, K.V., Stewart, R.T., and Wild, J.P. 1971, Nature, 234, 140.
Mandel'stam, S.L. 1978, in "Advances of the Soviet Union in Space Research", Moscow, Nauka, 209. (in Russian)
Mandel'stam, S.L. 1979, these proceedings (Appendix D)
Meerson, B.I., Sasorov, P.V., and Stepanov, A.V. 1978, Solar Phys., 58, 165.
Melrose, D.B. and Brown, J.C. 1976, MNRAS, 176, 15.
Molodenskii, M.M. and Syrovatskii, S.I. 1977, Astron. Zhurn., 54, 1293.
Morfill, G., Richter, A.K., and Scholer, M. 1978, J. Geophys. Res., in press.
Mouschovias, T. Ch. and Poland, A.I. 1978, Ap. J., 220, 675.
Munro, R.H., Gosling, J.T., Hildner, E., MacQueen, R.M., Poland, A.I., and Ross, C.L. 1979, Solar Phys., in press.
Nakagawa, Y. 1979, preprint.

Nefedjev, V.P. 1979, Pisma v. AZh, 5, #2.
Neupert, W.M. 1971, Solar Phys., 18, 474.
Orrall, F.Q. and Zirker, J.B. 1976, Ap. J., 208, 618.
Ox, E.A. 1978, Pisma v. AZh, 4, 415.
Pallavicini, R., Serio, S., and Vaiana, G.S. 1977, Ap. J., 216, 108.
Pneuman, G.W. 1979, Solar Phys., in press.
Ramaty, R., Colgate, S.A., Dulk, G.A., Hoyng, P., Knight, J.W., Lin, R.P., Melrose, D.B., Palzis C., Orrall, F.Q., Shapiro, P.R., Smith, D.F., and Van Hollebeeke, M.A.I. 1979, in (P.A. Sturrock, ed.) "Solar Flares", Proceedings of the Skylab Solar Flare Workshop.
Robinson, R.D. 1978, Solar Phys., 60, 383.
Roy, J.R. and Tang, F. 1975, Solar Phys., 42, 425.
Rust, D.M. and Hildner, E. 1976, Solar Phys., 48, 381.
Rust, D.M. and Webb, D.F. 1977, Solar Phys., 54, 403.
Rust, D.M., Hildner, E., Dryer, M., Hansen, R.T., McClymont, A.N., McKenna Lawlor, S.M.P., McLean, D.J., Schmahl, E.J., Steinolfson, R.S., Tandberg-Hanssen, E., Tousey, R., Webb, D.F., and Wu, S.T. 1979, in (P.A. Sturrock, ed.) "Solar Flares", proceedings of the Skylab Solar Flare Workshop.
Sakurai, T. 1976, Publ. Astr. Soc. Japan, 28, 177.
Santin, P. 1971, Solar Phys., 18, 87.
Shapiro, P.R. and Moore, R.J. 1977, Ap. J., 217, 621.
Shea, M.A., Smart, E.F., and Wu, S.T. (eds.) 1977, "Study of Travelling Interplanetary Phenomena", Ap. and Space Sci. Library, 71 [Dordrecht:Reidel]
Slottje, C. 1978, Nature, 275, 520.
Smith, D.F. and Lilliequist, C.G. 1979, Ap. J., in press.
Somov, B.V. 1975, Solar Phys., 42, 235.
Somov, B.V. 1976, P.N. Lebedev Institute Report 88, 127.
Somov, B.V. and Syrovatskii, S.I. 1976, Soviet Phys. Usp., 19, 813.
Somov, B.V. and Syrovatskii, S.I. 1977, Solar Phys., 55, 393.
Spicer, D.S. 1977, Solar Phys., 53, 305.
Spicer, D.S. 1979, unpublished.
Spitzer, L.J. 1962, "Physics of Fully Ionized Gases" [2d. ed., New York: Interscience].
Suemoto, Z. and Hiei, E. 1959, Publ. Astr. Soc. Japan, 11, 185.
Sveštka, Z. 1973, Solar Phys., 31, 389.
Sveštka, A. 1976, "Solar Flares" [Dordrecht:Reidel]
Syrovatskii, S.I. 1976, Pisma v. AZh, 2, 35.
Syrovatskii, S.I. 1977, Pisma v. AZh, 3, 133.
Syrovatskii, S.I. and Shmeleva, O.P. 1972, Soviet Astron. - AJ, 16, 273.
Takakura, T. and Kai, K. 1966, Publ. Astr. Soc. Japan, 18, 57.
Tindo, I.P. and Somov, B.V. 1978, in "New Instrumentation for Space Astronomy", [Oxford: Pergamon] 131.

Tindo, I.P., Ivanov, V.D., Mandel'stam, S.L., and Shuryghin, A.I. 1972a, Solar Phys., 24, 429.
Tindo, I.P., Ivanov, V.D., Valnicek, B., and Livshits, M.A. 1972b, Solar Phys., 27, 426.
Tindo, I.P., Mandel'stam, S.L., and Shuryghin, A.I. 1973, Solar Phys., 32, 469.
Tindo, I.P., Shuryghin, A.I., and Steffen, W. 1976, Solar Phys., 46, 219.
Tomozov, V.M. 1973, Astron. Circular #749, 1.
Tsytovich, V.N. 1973, Ann. Rev. Astr. Ap., 11, 363.
Tur, I.J. and Priest, E.R. 1978, Solar Phys., 58, 181.
van Beek, H.F., de Feiter, L.D., and de Jager, C. 1974, Space Research, 14, 447 Berlin.
Vernazza, J.E., Avrett, E.H., and Loeser, R.K. 1973, Ap. J., 184, 605.
Vlahos, L. and Emslie, A.G. 1979, in preparation.
Vlahos, L. and Papadopolous, K. 1979, Ap. J., in press.
Vorpahl, J., Gibson, E., Landecker, P., MacKenzie, D., and Underwood, J.H. 1975, Solar Phys., 45, 199.
Wild, J.P. 1969, Proc. ASA, 1, 181.
Zaitsev, V.V. 1974, Radiofizika, 17, 1438.
Zaitsev, V.V., Parfenov, O.G., and Stepanov, A.V. 1979, Solar Phys., in press.
Zheleznyakov, V.V. 1970, "Radio Emission of the Sun and Planets" [Oxford: Pergamon].
Zheleznyakov, V.V. and Zlotnik, E. Ya. 1979, Solar Phys., in press.
Zhitnik, I.A. 1974, in "Advances in Science and Technology", Ser. Astron., Vol. 9, Moscow, VINITI (in Russian).
Zhitnik, I.A., Kononov, E. Ya., Korneev, V.V., Krutov, V.V., Silvester, V., Silvester, I., Mandel'stam, S.L., and Urnov, A.M. 1979a, Solar Phys., in press.
Zhitnik, I.A., Korneev, V.V., Krutov, V.V., Mandel'stam, S.L., Tindo, I.P., and Urnov, A.M. 1979b, Solar Phys., to be submitted.
Zhuzhunashvili, A.I. and Ox, E.A. 1977, Soviet Phys. JETP, 73, 2142.
Zirin, H. 1978, Solar Phys., 58, 95.
Zirin, H. and Tanaka, T. 1973, Solar Phys., 32, 173.
Zwickl, R.D. and Webber, W.R. 1977, Solar Phys., 54, 457.
Zwickl, R.D., Roelof, E.C., Gold, R.E., Krimigis, S.H., and Armstrong, T.P. 1978, Ap. J., 225, 281.

UAG Series of Reports

UAG Reports are issued on an irregular basis, with 6 to 12 reports being issued each year. Subscriptions may be ordered through the National Geophysical and Solar-Terrestrial Data Center, Environmental Data and Information Service, NOAA, Boulder, CO 80303, USA. The annual subscription price is $25.20 ($17.30 additional for foreign mailing). In years when the single price copies are less than $25.20, arrangements will be made to extend the subscription duration. Single issues are also available at the prices shown below. Some of the issues are now out of print and are available only on microfiche. Orders must include check or money order payable in U.S. currency to the Department of Commerce, NOAA/NGSDC. $2.00 handling charge per order.

UAG-1 "IQSY Night Airglow Data", price $1.75.
UAG-2 "A Reevaluation of Solar Flares, 1964-1966", price 30 cents.
UAG-3 "Observations of Jupiter's Sporadic Radio Emission in the Range 7.6-41 MHz, 6 July 1966 through 8 September 1968", microfiche only, price 45 cents.
UAG-4 "Abbreviated Calendar Record 1966-1967", price $1.25.
UAG-5 "Data on Solar Event of May 23, 1967 and its Geophysical Effects", price 65 cents.

UAG-6 "International Geophysical Calendars 1957-1969", price 30 cents.
UAG-7 "Observations of the Solar Electron Corona: February 1964-January 1968", price 15 cents.
UAG-8 "Data on Solar-Geophysical Activity October 24-November 6, 1968", price (includes Parts 1 & 2) $1.75.
UAG-9 "Data on Cosmic Ray Event of November 18, 1968 and Associated Phenomena", price 55 cents.
UAG-10 "Atlas of Ionograms", price $1.50.

UAG-11 "Catalogue of Data on Solar-Terrestrial Physics" (now obsolete).
UAG-12 "Solar-Geophysical Activity Associated with the Major Geomagnetic Storm of March 8, 1970", price (includes Parts 1-3) $3.00.
UAG-13 "Data on the Solar Proton Event of November 2, 1969 through the Geomagnetic Storm of November 8-10, 1969, price 50 cents.
UAG-14 "An Experimental, Comprehensive Flare Index and Its Derivation for 'Major' Flares, 1955-1969", price 30 cents.
UAG-15 "Catalogue of Data on Solar-Terrestrial Physics" (now obsolete).

UAG-16 "Temporal Development of the Geographical Distribution of Auroral Absorption for 30 Substorm Events in each of IQSY (1964-65) and IASY (1969)", price 70 cents.
UAG-17 "Ionospheric Drift Velocity Measurements at Jicamarca, Peru (July 1967-March 1970)", microfiche only, price 45 cents.
UAG-18 "A Study of Polar Cap and Auroral Zone Magnetic Variations", price 20 cents.
UAG-19 "Reevaluation of Solar Flares 1967", price 15 cents.
UAG-20 "Catalogue of Data on Solar-Terrestrial Physics" (now obsolete).

UAG-21 "Preliminary Compilation of Data for Retrospective World Interval July 26 - August 14, 1972", price 70 cents.
UAG-22 "Auroral Electrojet Magnetic Activity Indices (AE) for 1970", price 75 cents.
UAG-23 "U.R.S.I. Handbook of Ionogram Interpretation and Reduction, Second Edition, November 1972", edited by W. R. Piggott and K. Rawer, NGSDC/EDS/NOAA, November 1972, 324 pages, price $1.75.

UAG-23A "U.R.S.I. Handbook of Ionogram Interpretation and Reduction, Second Edition, November 1972", Revision of Chapters 1-4, edited by W. R. Piggott and K. Rawer, NGSDC/EDS/NOAA, July 1978, 135 pages, price $2.14.

UAG-24 "Data on Solar-Geophysical Activity Associated with the Major Ground Level Cosmic Ray Events of 24 January and 1 September 1971", price (includes Parts 1 and 2) $2.00.
UAG-25 "Observations of Jupiter's Sporadic Radio Emission in the Range 7.6-41 MHz, 9 September 1968 through 9 December 1971", price 35 cents.

UAG-26 "Data Compilation for the Magnetospherically Quiet Periods February 19-23 and November 29 - December 3, 1970", price 70 cents.
UAG-27 "High Speed Streams in the Solar Wind", price 15 cents.
UAG-28 "Collected Data Reports on August 1972 Solar-Terrestrial Events", price (includes Parts 1-3) $4.50.
UAG-29 "Auroral Electrojet Magnetic Activity Indices AE (11) for 1968", price 75 cents.
UAG-30 "Catalogue of Data on Solar-Terrestrial Physics", price $1.75.

UAG-31 "Auroral Electrojet Magnetic Activity Indices AE (11) for 1969", price 75 cents.
UAG-32 "Synoptic Radio Maps of the Sun at 3.3 mm for the Years 1967-1969", price 35 cents.
UAG-33 "Auroral Electrojet Magnetic Activity Indices AE (10) for 1967", price 75 cents.
UAG-34 "Absorption Data for the IGY/IGC and IQSY", price $2.00.
UAG-35 "Catalogue of Digital Geomagnetic Variation Data at World Data Center A for Solar-Terrestrial Physics", price 20 cents.

UAG-36 "An Atlas of Extreme Ultraviolet Flashes of Solar Flares Observed Via Sudden Frequency Deviations During the ATM-SKYLAB Missions", price 55 cents.
UAG-37 "Auroral Electrojet Magnetic Activity Indices AE (10) for 1966", price 75 cents.
UAG-38 "Master Station List for Solar-Terrestrial Physics Data at WDC-A for Solar-Terrestrial Physics", price $1.60.
UAG-39 "Auroral Electrojet Magnetic Activity Indices AE (11) for 1971", by Joe Haskell Allen, Carl C. Abston and Leslie D. Morris, National Geophysical and Solar-Terrestrial Data Center, Environmental Data Service, February 1975, 144 pages, price $2.05.

UAG-40 "H-Alpha Synoptic Charts of Solar Activity For the Period of Skylab Observations, May, 1973-March, 1974", by Patrick S. McIntosh, NOAA Environmental Research Laboratories, February 1975, 32 pages, price 56 cents.

UAG-41 "H-Alpha Synoptic Charts of Solar Activity During the First Year of Solar Cycle 20, October, 1964 - August, 1965", by Patrick S. McIntosh, NOAA Environmental Research Laboratories, and Jerome T. Nolte, American Science and Engineering, Cambridge, Massachusetts, March 1975, 25 pages, price 48 cents.

UAG-42 "Observations of Jupiter's Sporadic Radio Emission in the Range 7.6-80 MHz 10 December 1971 through 21 March 1975", by James W. Warwick, George A. Dulk, and Anthony C. Riddle, Department of Astro-Geophysics, University of Colorado, Boulder, Colorado 80302, April 1975, 49 pages, price $1.15.

UAG-43 "Catalog of Observation Times of Ground-Based Skylab-Coordinated Solar Observing Programs", compiled by Helen E. Coffey, World Data Center A for Solar-Terrestrial Physics, May 1975, 159 pages, price $3.00.

UAG-44 "Synoptic Maps of Solar 9.1 cm Microwave Emission from June 1962 to August 1973", by Werner Graf and Ronald N. Bracewell, Radio Astronomy Institute, Stanford University, Stanford, California 94305, May 1975, 183 pages, price $2.55.

UAG-45 "Auroral Electrojet Magnetic Activity Indices AE (11) for 1972", by Joe Haskell Allen, Carl C. Abston and Leslie D. Morris, National Geophysical and Solar-Terrestrial Data Center, Environmental Data Service, May 1975, 144 pages, price $2.10.

UAG-46 "Interplanetary Magnetic Field Data 1963-1974", by Joseph H. King, National Space Science Data Center, NASA Goddard Space Flight Center, Greenbelt, Maryland 20771, June 1975, 382 pages, price $2.95.

UAG-47 "Auroral Electrojet Magnetic Activity Indices AE (11) for 1973", by Joe Haskell Allen, Carl C. Abston and Leslie D. Morris, National Geophysical and Solar-Terrestrial Data Center, Environmental Data Service, June 1975, 144 pages, price $2.10.

UAG-48A "Synoptic Observations of the Solar Corona during Carrington Rotations 1580-1596 (11 October 1971 - 15 January 1973)", [Reissue with quality images] by R. A. Howard, M. J. Koomen, D. J. Michels, R. Tousey, C. R. Detwiler, D. E. Roberts, R. T. Seal and J. D. Whitney, E. O. Hulbert Center for Space Research, NRL, Washington, D. C. 20375 and R. T. and S. F. Hansen, C. J. Garcia and E. Yasukawa, High Altitude Observatory, NCAR, Boulder, Colorado 80303, February 1976, 200 pages, price $4.27.

UAG-49 "Catalog of Standard Geomagnetic Variation Data", prepared by Environmental Data Service, NOAA, Boulder, Colorado, August 1975, 125 pages, price $1.85.

UAG-50 "High-Latitude Supplement to the URSI Handbook on Ionogram Interpretation and Reduction", by W. R. Piggott, British Antarctic Survey, c/o SRC, Appleton Laboratory, Ditton Park, Slough, England, October 1975, 292 pages, price $4.00.

UAG-51 "Synoptic Maps of Solar Coronal Hole Boundaries Derived from He II 304Å Spectroheliograms from the Manned Skylab Missions", by J. D. Bohlin and D. M. Rubenstein, E. O. Hulbert Center for Space Research, Naval Research Laboratory, Washington, D. C. 20375 U.S.A., November 1975, 30 pages, price 54 cents.

UAG-52 "Experimental Comprehensive Solar Flare Indices for Certain Flares, 1970-1974", compiled by Helen W. Dodson and E. Ruth Hedeman, McMath-Hulbert Observatory, The University of Michigan, 895 Lake Angelus Road North, Pontiac, Michigan 48055 U.S.A., November 1975, 27 pages, price 60 cents.

UAG-53 "Description and Catalog of Ionospheric F-Region Data, Jicamarca Radar Observatory (November 1966 - April 1969)", by W. L. Clark and T. E. Van Zandt, Aeronomy Laboratory, NOAA, Boulder, Colorado 80302 and J. P. McClure, University of Texas at Dallas, Dallas, Texas 75230, April 1976, 10 pages, price 33 cents.

UAG-54 "Catalog of Ionosphere Vertical Soundings Data", prepared by Environmental Data Service, NOAA, Boulder, Colorado 80302, April 1976, 130 pages, price $2.10.

UAG-55 "Equivalent Ionospheric Current Representations by a New Method, Illustrated for 8-9 November 1969 Magnetic Disturbances", by Y. Kamide, Cooperative Institute for Research in Environmental Sciences, University of Colorado, Boulder, Colorado 80302 and Geophysical Institute, University of Alaska, Fairbanks, Alaska 99701, H. W. Kroehl, Data Studies Division, NOAA/EDS/NGSDC, Boulder, Colorado 80302, M. Kanamitsu, Advanced Study Program, National Center for Atmospheric Research, Boulder, Colorado 80303, J. H. Allen, Data Studies Division, NOAA/EDS/NGSDC, Boulder, Colorado 80302, and S.-I. Akasofu, Geophysical Institute, University of Alaska, Fairbanks, Alaska 99701, April 1976, 91 pages, price $1.60.

UAG-56 "Iso-intensity Contours of Ground Magnetic H Perturbations for the December 16-18, 1971 Geomagnetic Storm", by Y. Kamide, Cooperative Institute for Research in Environmental Sciences, University of Colorado, Boulder, Colorado 80302 and Geophysical Institute, University of Alaska, Fairbanks, Alaska 99701 (currently Guest worker at Data Studies Division, NOAA/EDS/NGSDC, Boulder, Colorado 80302), April 1976, 37 pages, price $1.39.

UAG-57 "Manual on Ionospheric Absorption Measurements", edited by K. Rawer, Institut für Physikalische Weltraumforschung, Freiburg, G.F.R., June 1976, 202 pages, price $4.27.

UAG-58 "ATS6 Radio Beacon Electron Content Measurements at Boulder, July 1974 - May 1975", by R. B. Fritz, Space Environment Laboratory (currently with Wave Propagation Laboratory), NOAA, Boulder, Colorado 80302 USA, September 1976, 61 pages, price $1.04.

UAG-59 "Auroral Electrojet Magnetic Activity Indices AE(11) for 1974", by Joe Haskell Allen, Carl C. Abston and Leslie D. Morris, National Geophysical and Solar-Terrestrial Data Center, Environmental Data Service, December 1976, 144 pages, price $2.16.

UAG-60 "Geomagnetic Data for January 1976 (AE(7) Indices and Stacked Magnetograms)" by J. H. Allen, C. C. Abston and L. D. Morris, NGSDC/EDS/NOAA, July 1977, 57 pages, price $1.07.

UAG-61 "Collected Data Reports for STIP Interval II 20 March - 5 May 1976", edited by Helen E. Coffey and John A. McKinnon, National Geophysical and Solar-Terrestrial Data Center, Environmental Data Service, August 1977, 313 pages, price $2.95.

UAG-62 "Geomagnetic Data For February 1976 (AE(7) Indices and Stacked Magnetograms)" by J. H. Allen, C. C. Abston and L. D. Morris, NGSDC/EDS/NOAA, September 1977, 55 pages, price $1.11.

UAG-63 "Geomagnetic Data for March 1976 (AE(7) Indices and Stacked Magnetograms)" by J. H. Allen, C. C. Abston and L. D. Morris, NGSDC/EDS/NOAA, September 1977, 57 pages, price $1.11.

UAG-64 "Geomagnetic Data for April 1976 (AE(8) Indices and Stacked Magnetograms)" by J. H. Allen, C. C. Abston and L. D. Morris, NGSDC/EDS/NOAA, February 1978, 55 pages, price $1.00.

UAG-65 "The Information Explosion and Its Consequences for Data Acquisition, Documentation, and Processing" by G. K. Hartmann, Max-Planck-Institut für Aeronomie, D-3411 Katlenburg-Lindau 3, GFR, May 1978, 36 pages, price 75 cents.

UAG-66 "Synoptic Radio Maps of the Sun at 3.3mm 1970-1973" by Earle B. Mayfield, Space Science Lab., and Fred I. Shimabukuro Electronics Res. Lab., The Ivan A. Getting Laboratories, The Aerospace Corp., El Segundo, California 90245, May 1978, 30 pages, price 75 cents.

UAG-67 "Ionospheric D-Region Profile Data Base, A Collection of Computer-Accessible Experimental Profiles of the D and Lower E Regions", by L. F. McNamara, Ionospheric Prediction Service, Sydney, Australia, August 1978, 30 pages, price 88 cents.

UAG-68 "A Comparative Study of Methods of Electron Density Profile Analysis", by L. F. McNamara, Ionospheric Prediction Service, Sydney, Australia, September 1978, 56 pages, price $1.41.

UAG-69 "Selected Disturbed D-Region Electron Density Profiles. Their relation to the undisturbed D region", by L. F. McNamara, Ionospheric Prediction Service, Sydney, Australia, October 1978, 50 pages, price $1.29.

UAG-70 "Annotated Atlas of Hα Synoptic Charts for Solar Cycle 20 (1964-1974) Carrington Solar Rotations 1487-1616", by Patrick S. McIntosh, Space Environment Laboratory, ERL/NOAA, February 1979, 327 pages, price $3.50.

UAG-71 "Magnetic Potential Plots Over the Northern Hemisphere for 26-28 March 1976", by A.D. Richmond, SEL/ERL/NOAA, H.W. Kroehl, NGSDC/EDIS/NOAA, M.A. Henning, Lockheed Missiles and Space Co., Aurora, CO, and Y. Kamide, Kyoto Sangyo Univ., Kyoto, Japan, April 1979, 115 pages, price $1.50.